Intestinal Lymphatic Transport of Cannabinoids: Implications for People with Autoimmune Diseases and Immunocompromised Individuals

Atheer Khalaf Zgair

Bsc (pharmacy), Msc (pharmacology)

SCHOOL OF PHARMACY
UNIVERSITY OF NOTTINGHAM
NOTTINGHAM
UNITED KINGDOM

Thesis submitted to The University of Nottingham for the degree of

Doctor in Philosophy

July 2017

To my parents, wife, and children

To the memory of my teacher Dr Majid A. K. Lafi

ABSTRACT

There has been an escalating interest in the medicinal use of *Cannabis sativa* in recent years. Cannabidiol (CBD) and Δ^9-tetrahydrocannabinol (THC), the main constituents of *Cannabis sativa*, have well documented immunomodulatory effects *in vitro* and following administration of high doses to animals. However, these effects have not been clearly evident in humans following oral administration of cannabinoids, probably due to low systemic bioavailability. To note, cannabis and cannabis-containing medicines are currently used for symptomatic relief in autoimmune diseases, such as multiple sclerosis (MS), and in cases of immunodeficiency, such as in cancer patients on chemotherapy regimens. In this thesis, we aimed to elucidate the impact of enhancing the transport of orally administered cannabinoids to the intestinal lymphatic system, the major host of immune cells, on the immunomodulatory effects of cannabinoids.

Oral administration of lipophilic cannabinoids with long-chain triglycerides (LCT) was investigated as a simple approach to enhance the intestinal lymphatic transport. The effect of LCT on the intraluminal processing of orally administered cannabinoids was assessed by means of *in vitro* lipolysis model. The results of *in vitro* lipolysis demonstrated that at least one-third of CBD dose would be solubilised and readily available for absorption to the enterocytes when orally administered in LCT-formulation. The association of CBD with chylomicrons (CM) in the enterocytes and subsequent intestinal lymphatic transport was estimated using an *in silico* model, *in vitro* association by artificial CM-like lipid particles, and *ex vivo* uptake by plasma-derived CM from rats and humans. The results of CM association studies revealed high intestinal lymphatic transport potential for CBD in rats and humans. Similar high lymphatic transport

potential was also reported for THC in our laboratory. Oral co-administration of CBD and THC with LCT to rats increased the systemic exposure by 3-fold and 2.5-fold, respectively, compared to lipid-free formulations. The underlying mechanism of increased bioavailability is likely to enhanced intestinal lymphatic transport and decreased pre-systemic metabolism in the liver. The results of biodistribution experiments indicated that the intestinal lymphatic transport of CBD and THC was, indeed, enhanced following oral co-administration of lipids as denoted by the dramatic increase in the concentrations recovered in MLN and intestinal lymph. The concentrations of CBD and THC in intestinal lymph fluid were in the range of 120 and 60 µg/mL compared to 0.5 and 0.6 µg/mL in plasma, respectively. Moreover, CBD and THC showed dose-dependent immunosuppressive effect on lymphocytes isolated from rats and peripheral blood mononuclear cells (PBMC) isolated from humans as assessed by lymphocyte proliferation assay and flow cytometry analysis of inflammatory cytokines. These effects were only significant at concentrations achieved in the intestinal lymphatic system, but not in plasma, following oral co-administration of cannabinoids with LCT. CBD showed more immunosuppressive effects on lymphocyte proliferation and the expression of inflammatory cytokines comparing to THC. Also, PBMC from MS patients were more susceptible to the immunomodulatory effects of cannabinoids than PBMC from healthy volunteers and cancer patients on chemotherapy.

In conclusion, oral administration of cannabinoids with lipids can enhance the intestinal micellar solubilisation and augment the systemic exposure to cannabinoids by enhancing intestinal lymphatic transport. The concentrations of lipophilic cannabinoids recovered in the intestinal lymphatic system were extremely high and exceeded the immunosuppressive threshold of CBD and THC. The increase in systemic exposure to cannabinoids in humans is of

potentially high clinical importance as it could turn a barely effective dose of orally administered cannabis into highly effective one, or indeed a therapeutic dose into a toxic one. In addition, administering cannabinoids, in particular CBD, with a high-fat meal, as cannabis-containing food, or in lipid-based formulations could represent a valid therapeutic approach to improve the treatment of MS, or other T cell-mediated autoimmune disorders. However, in immunocompromised patients, administration of cannabinoids in this way may deepen the immunosuppressive effects.

ACKNOWLEDGEMENTS

First and foremost, all the praises and thanks be to Allah Almighty, Who has bestowed upon me the strength, guidance, and perseverance to carry on this work.

I would like to express my deep sense of gratitude to my supervisor, Dr Pavel Gershkovich, for the continuous support, encouragement, and motivation, but also for the constructive criticism which extended my understanding to the research from various perspectives. His inspiring guidance, immense knowledge, and invaluable suggestions helped me to overcome all the difficulties I faced throughout the time of research.

I am also very grateful to the expert and knowledgeable co-supervisors, Prof Peter Fischer, Prof Cris Constantinescu, and Prof David Barrett, who have given their valuable time and efforts to support me in every step of this work. It has been a great honour for me to learn from scientists like you.

My deep appreciation goes to the internal assessor, Dr Maria Marlow, for her invaluable advice and feedback throughout the journey of my research. I also appreciate the external assessor, Dr Zubair Ahmed, for kindly giving his valuable time to evaluate this work.

I would like to thank the staff and technicians at Boots Science Building and the Centre for Biomolecular Sciences (CBS) where most of my laboratory work was conducted. Special thanks go to Paul Cooling and Dr Cath Ortori for their help to set up the work on the HPLC and LC-MS/MS systems.

I am indebted to Jehan Aram and Nanci Frakich from Prof Cris Constantinescu's laboratory in the Queen's Medical Centre for providing training and sharing their expertise to conduct the cell work in their laboratory as well as helping the collection of blood samples from multiple sclerosis patients.

My sincere thanks also goes to the friendly staff of the Bio Support Unit (BSU) for the great help they provided to conduct animal experiments, special mention goes to Mark Trussell, Sally-anne Wilford, Ewan Mcneill, Neil Yates, Helen Richards, and Ian Devonshire.

I am thankful to Dr Ivo Hennig and his research team at Nottingham City Hospital for recruiting cancer patients to donate blood samples for the cell work. I am also hugely appreciative to the staff of Nottingham Health Sciences Biobank for being so nice to arrange the delivery of blood samples from Nottingham City Hospital to the Queen's Medical Centre where cell work was conducted.

I am also indebted to the members of Gershkovich group, Dhiaa Taha, Jonathan Wong, Jong Bong (JB) Lee, Joseph Ali, Paloma Benito-Gallo, and Sally Gitting, who have contributed hugely to my personal and professional time at The University of Nottingham. Thanks for all the good times we spend together in and out of the lab. JB, my friend, I will miss all the creative thoughts-generating discussions we used to have. Thank you for being supportive not only for me, but for all other lab mates, hope you and other members the best in your future. Also, I would like to thank Chaolong Qin, Wanshan Feng, and Carlos Sanders-Velez who have recently joined Gershkovich group for the refreshing breaks we had at the time of writing this thesis. My thanks also go to all the undergraduate and postgraduate students I have mentored throughout the last four years.

I would like to convey sincere appreciation to GW Research Ltd (Cambridge, UK) for the generous donation of cannabidiol (CBD) and Δ^9-tetrahydrocannabinol (THC).

I am happy to acknowledge the financial support from the Iraqi Ministry of Higher Education and Scientific Research (MOHESR) as well as acknowledging

my colleagues and the administrative staff at the College of Pharmacy/ University of Anbar for making this scholarship available to me.

Many thanks to all my friends who have made my time at Nottingham unforgettable.

Last but not least, I would like to thank my family for all their love and support. My wonderful parents, my beloved wife, my lovely children: Mohammed, Maryam, Rawan, and Janah, my sister and her family, and my parents-in-law. Thanks for the unconditional love and encouragement you provided, I would not have made it this far without you.

Atheer Zgair

University of Nottingham

April 2017

TABLE OF CONTENTS

LIST OF PUBLICATIONS

Original research papers

Zgair, A., Wong, J. C., Sabri, A., Fischer, P. M., Barrett, D. A., Constantinescu, C. S., & Gershkovich, P. (2015). Development of a simple and sensitive HPLC-UV method for the simultaneous determination of cannabidiol and Delta(9)-tetrahydrocannabinol in rat plasma. *J Pharm Biomed Anal, 114*, 145-151.

Zgair, A., Wong, J. C., Lee, J. B., Mistry, J., Sivak, O., Wasan, K. M., Hennig, I. M., Barrett, D. A., Constantinescu, C. S., Fischer, P. M., & Gershkovich, P. (2016). Dietary fats and pharmaceutical lipid excipients increase systemic exposure to orally administered cannabis and cannabis-based medicines. *Am J Transl Res, 8*(8), 3448-3459.

Zgair, A., Lee, J. B., Wong, J. C., Taha, D. A., Aram, J., Virgilio, D. D., McArthur, J. W., Cheng, Y., Hennig, I. M., Barrett, D. A., Fischer, P. M., Constantinescu, C. S., & Gershkovich, P. (2017). Oral co-administration of cannabis with lipids leads to high levels of cannabinoids in the intestinal lymphatic system and prominent immunomodulatory effects. *Submitted to Scientific Reports*.

Book chapter

Zgair, A., Wong, J. C. M., & Gershkovich, P. (2016). Targeting Immunomodulatory Agents to the Gut-Associated Lymphoid Tissue. In C. Constantinescu, R. Arsenescu & V. Arsenescu (Eds.), *Neuro-Immuno-Gastroenterology* (pp. 237-261). Cham: Springer International Publishing.

Abstracts for poster and oral presentations

Zgair, A., Wong, J. C., Fischer, P. M., Barrett, D. A., Constantinescu, C. S., & Gershkovich, P. (2014). Evaluation of the intestinal lymphatic transport potential of cannabidiol using *in vitro* lipolysis model and *in silico* prediction of affinity to chylomicrons. *APS UK PharmSci 2014.* University of Hertfordshire, Hatfield, UK.

Zgair, A., Wong, J. C., Fischer, P. M., Barrett, D. A., Constantinescu, C. S., & Gershkovich, P. (2015). Targeting cannabinoids to the mesenteric lymph nodes for enhanced immunomodulatory effects in the treatment of multiple sclerosis: In vitro and ex vivo studies. *MS Frontiers 2015.* London, UK.

Zgair, A., Lee, J. B., Wong, J. C., Fischer, P. M., Barrett, D. A., Constantinescu, C. S., & Gershkovich, P. (2015). Effect of Long-Chain Triglyceride Formulation on the Oral Bioavailability of Cannabidiol.

American Association of Pharmaceutical Scientists: Annual Meeting and Exposition 2015 (AAPS 2015). Orlando, Florida, USA.

Zgair, A., Wong, J. C., Sabri, A., Fischer, P. M., Barrett, D. A., Constantinescu, C. S., & Gershkovich, P. (2015). Simultaneous Determination of Cannabidiol and Δ^9-Tetrahydrocannabinol in Rat Plasma Using HPLC. *American Association of Pharmaceutical Scientists: Annual Meeting and Exposition 2015 (AAPS 2015)*. Orlando, Florida, USA.

Zgair, A., Lee, J. B., Wong, J. C., Fischer, P. M., Barrett, D. A., Constantinescu, C. S., & Gershkovich, P. (2016). Long-Chain Triglyceride Formulation Enhances Oral Bioavailability of Cannabidiol by Facilitating Intestinal Lymphatic Transport. *10th World Meeting on Pharmaceutics, Biopharmaceutics and Pharmaceutical Technology*. Glasgow, UK

Zgair, A., Lee, J. B., Wong, J. C., Aram, J., Fischer, P. M., Barrett, D. A., Constantinescu, C. S., & Gershkovich, P. (2016). Targeting Cannabidiol to the Intestinal Lymphatic System for Enhanced Immunomodulatory Effects in the Treatment of Autoimmune Diseases. *American Association of Pharmaceutical Scientists: Annual Meeting and Exposition 2016 (AAPS 2016)*. Colorado, Denver, USA.

LIST OF ABBREVIATIONS

Δ^8-THC	Δ^8-tetrahydrocannabinol
2-AG	2-arachidonoylglycerol
5-FU	5-fluorouracil
AIC	Akaike Information Criterion
ANC	Absolute neutrophil count
ANOVA	One-way analysis of variance
AOIC	Assessment of inflammatory cytokines
Apo B	Apolipoprotein B
$AUC_{0-\infty}$	Area under the curve to infinite time
AUC_{0-t}	Area under the curve from 0 to time of last measurable concentration
BALT	Bronchus-associated lymphoid tissue
BBB	Blood brain barrier
BCS	Biopharmaceutics Classification System
BIC	Bayesian information criterion
BrdU	Bromo-2'-deoxyuridine
CALT	Conjunctiva-associated lymphoid tissue
CB_1	Cannabinoid receptors 1
CB_2	Cannabinoid receptors 2
CBC	Cannabichromene
CBD	Cannabidiol
CBE	Cannabielsoin
CBG	Cannabigerol
CBL	Cannabicyclol
CBN	Cannabinol
CBND	Cannabinodiol
CBT	Cannabitriol
CFA	Complete Freund's adjuvant
Cl	Clearance
CM	Chylomicrons
C_{max}	Maximum concentration in plasma
CNS	Central nervous system
DALT	Salivary gland duct-associated lymphoid tissue
DC	Dendritic cells
DDT	4,4-Dichlorodiphenyltrichloroethane
D-PBS	Dulbecco's phosphate buffered saline
EAE	Experimental autoimmune encephalomyelitis
EBV	Epstein-Barr virus
EDSS	Kurtzke Expanded Disability Status Score
ELISA	Enzyme-linked immunosorbent assay
F	Absolute oral bioavailability
FAE	Follicle-associated epithelium
FBS	Fetal bovine serum
FRB	Freely rotatable bonds
GALT	Gut-associated lymphoid tissue
GM-CSF	Granulocyte-macrophage colony-stimulating factor
HBA	Hydrogen bond acceptors
HBD	Number of hydrogen bond donors
HIV	Human immunodeficiency virus

HPLC	High-performance liquid chromatography
HQC	High quality control
I	Ionomycin calcium
ILF	Isolated lymphoid follicles
IS	Internal standard
ITP	Idiopathic thrombocytopenic purpura
IV	Intravenous
KBr	Potassium bromide
LBDDS	Lipid-based drug delivery systems
LC-MS/MS	Liquid chromatography tandem-mass spectrometry
LCT	Long-chain triglycerides
LDALT	Lacrimal duct-associated lymphoid tissue
LLOQ	Lower limit of quantification
LP	Lamina propria
LPA	Lymphocyte proliferation assay
LQC	Low quality control
Ly	Lymphocyte
MALT	Mucosa-associated lymph tissues
MBP	Myelin basic protein
MHC	Major histocompatibility complex
MLN	Mesenteric lymph nodes
MQC	Medium quality control
MS	Multiple sclerosis
NALT	Nasal-associated lymphoid tissue
NO	Nitric oxide
NSGCT	Non-seminomatous germ cell tumours
PBMC	Peripheral blood mononuclear cells
PE	Polyethylene
PHA	Phytohaemagglutinin
PLP	Proteolipid protein
PMA	Phorbol myristate
PP	Peyer's patches
PPARγ	Peroxisome proliferator-activated receptors
PPL	Project licence
PPMS	Primary-progressive multiple sclerosis
PRMS	Progressive-relapsing multiple sclerosis
PSA	Polar surface area
PTSD	Posttraumatic stress disorder
QC	Quality control
r^2	Correlation coefficient
RE	Relative error
RPC	Reversed phase chromatography
RRMS	Relapsing-remitting multiple sclerosis
RSD	Relative standard deviation
SARS	Severe acute respiratory syndrome
SD	Sprague Dawley
SEDDS	Self-emulsifying drug delivery systems
SEM	Standard error of the mean
SLE	Systemic lupus erythematosus
SLE	Systemic lupus erythematosus
SMEDDS	Self-microemulsifying delivery systems
SNEDDS	Self-nanoemulsifying delivery systems
SPMS	Secondary-progressive multiple sclerosis

$t_{1/2}$	Terminal half-life
TG	Triglycerides
THC	Δ^9-tetrahydrocannabinol
t_{max}	Time to maximum concentration in plasma
TRP	Transient receptor potential
TU	Testosterone undecanoate
UV	Ultraviolet
$V_{d\ ss}$	Apparent volume of distribution at steady state
WBC	White blood cell count

LIST OF FIGURES

LIST OF TABLES

1. INTRODUCTION

1.1. Medical cannabis

1.1.1. Historical preview

The medical use of *Cannabis sativa*, commonly called hemp, has a very long history. The first known use of cannabis as a remedy was dated back to the times of the Chinese emperor Shen Nung around the 28th century B.C. He was acknowledged for writing what is so called the Pen Ts'ao, the first written pharmacopeia in the history of mankind. In this pharmacopeia, Shen Nung recommended the use of cannabis for the treatment of malaria, constipation, menstrual disorders, and other conditions [1]. The medical value of cannabis was also documented by Indians, Assyrians, and Persians centuries before the Christian era. Thereafter, the medical use of cannabis spread to the Middle East and Africa [2].

It was not until the 19th century when cannabis was introduced to Europe as a potential remedy. This was accredited to the Irish physician William O'Shaughnessy who served with the East India Company. O'Shaughnessy noticed the use of cannabis as an important part of Indian medicine. He conducted some animal experiments to elucidate cannabis safety, followed by clinical trials in patients suffering from rheumatism, seizure, cholera, and tetanus [3, 4]. Cannabis extracts were then widely used in Europe and North America for their therapeutic value as sedative, hypnotic, analgesic, muscle relaxant, and anticonvulsant agents [3, 5, 6]. By 1854, cannabis extract and tincture were adopted in the British Pharmacopeia and the United States Dispensary [7].

The removal of cannabis from British Pharmacopeia in 1932 and 10 years later from American Pharmacopeia was, in part, due to the variability in composition, short shelf-life, unpredictable outcomes of oral administration, and development of more acceptable alternatives, as well as political bias [2, 4, 7]. Nevertheless, many patients were self-medicating to obtain therapeutic benefits from cannabis for various conditions, including AIDS wasting syndrome, multiple sclerosis (MS) and spinal injuries [3, 8]. There has been an escalating interest in the therapeutic benefits of cannabinoids over recent decades. Such benefits are supported by evidence-based studies and testimony from patients who benefited from the use of medical cannabis [9, 10]. Subsequently, increasing public and political pressures supported the legalisation of cannabis for medical use. At present, cannabis is legalized for medical use in 23 states of the US, as well as in Canada, the Netherlands, and Israel. In addition, there are other states and countries which are currently considering the legalization of medical cannabis, including Australia and New Zealand [11].

1.1.2. Cannabinoids and cannabinoid receptors

Although used for centuries, the chemical constituents of cannabis extracts were not identified until the end of the 19th century [12]. Cannabis is a unique source of more than 100 naturally-occurring chemical compounds collectively known as cannabinoids [13]. At present, the term cannabinoids is used for both plant-derived and synthetic compounds that mimic the action or structurally related to the naturally-occurring cannabinoids. Plant-derived cannabinoids are currently termed phytocannabinoids [14, 15]. In general, cannabinoids are classified based on chemical structure into 11 categories. These are derivatives of Δ^9-tetrahydrocannabinol (THC), cannabidiol (CBD), Δ^8-tetrahydrocannabinol (Δ^8-THC), cannabigerol (CBG), cannabichromene

(CBC), cannabinodiol (CBND), cannabielsoin (CBE), cannabicyclol (CBL), cannabinol (CBN), and cannabitriol (CBT) as well as other miscellaneous-type cannabinoids [13]. The two main active phytocannabinoids, the non-psychoactive CBD (**Figure 1.1 A**) and the psychoactive THC (**Figure 1.1 B**), were isolated from the oil extract of hemp in 1940 and 1942, respectively [12]. Two decades later, Raphael Mechoulam and colleagues successfully achieved the chemical synthesis of CBD and THC [12, 16]. In addition, the discovery of endogenously-occurring cannabinoids (endocannabinoids) and their cognate cannabinoid receptors 1 and 2 (CB_1 and CB_2) have renewed the interest in cannabinoids as pharmacologically active compounds [17, 18].

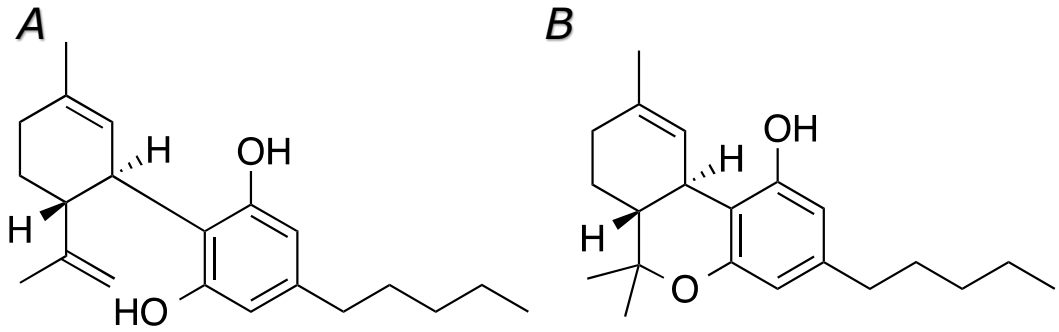

Figure 1.1. Chemical structures of cannabidiol (CBD, **Panel A**) and Δ^9-tetrahydrocannabinol (THC, **Panel B**).

To date, CB_1 and CB_2 are the only cannabinoid receptors that have been identified in animal species, including humans [19]. Both receptors are G-protein coupled receptors, particularly through $G_{i/o}$ proteins [15]. CB_1 receptors are mainly distributed in the central and peripheral nervous system. In contrast, CB_2 receptors are found on different immune cells like lymphocytes, macrophages, natural killer cells, and microglia as well as on some lymphoid tissues like tonsils and spleen [15, 19].

1.1.2.1. Cannabidiol (CBD) and Δ^9-tetrahydrocannabinol (THC)

CBD and THC are among the most abundant cannabinoids in C*annabis sativa*. Over the last few decades, a greater research attention was paid to THC compared to other cannabinoids. This could be due to the fact that THC is the principal compound responsible for the typical psychotropic effects of cannabis [20]. More recently, CBD gained considerable attention as a promising agent with multiple therapeutic effects [21].

1.1.2.1.1.Pharmacokinetics

1.1.2.1.1.1. Absorption

Cannabis is commonly consumed by smoking. This route of administration allows rapid onset of action and self-adjustment of the effect [3, 22]. The bioavailability following smoking varies based on smoking pattern in term of the volume and duration of holding the breath [23]. Ohlsson *et al* [24] reported that the systemic bioavailability of CBD after smoking of an average dose of 19 mg was 31 ± 13% with a peak plasma concentration in the range of 50 ng/mL. In another study, Lindgren *et al* [25] demonstrated that the bioavailability of THC following the smoking of an average dose of 13 mg was 23 ± 16%. The peak plasma concentration reported in that study was 98 ± 44 ng/mL.

Oral administration is another popular method for the consumption of cannabinoids [3, 26]. More often, when patients are self-medicate, cannabis is added to cookies or cakes [22]. The oral absorption of CBD and THC was described to be low and erratic [23]. The oral administration of cannabis extract containing 5.4 mg CBD and 10 mg THC to human volunteers resulted in mean maximum plasma concentration of 0.93 and 4.05 ng/mL, respectively [27]. In a study by Consroe *et al* [28], high doses of CBD (700 mg/day divided in 4 capsules) were administered to 14 Huntington's disease patients for 6 weeks.

Yet, mean plasma levels were in the range of 5.9 - 11.2 ng/ml. Similarly, low systemic bioavailability (6 ± 3%) and plasma levels (4.4 – 11 ng/mL) were achieved following the oral administration of 20 mg THC in chocolate cookies to healthy men [29].

Both cannabinoids are currently available as pharmaceutical formulations. Epidiolex® (an oral solution of CBD) was recently approved by the FDA as an orphan antiepileptic drug in the treatment of Dravet and Lennox-Gastaut syndromes [30, 31]. To the best of our knowledge, the systemic bioavailability was not reported following oral administration of Epidiolex®, or at least not available in public domain. However, in a clinical trial by Geffrey *et al* [32], plasma levels of CBD were reported in the range of 82 – 1000 ng/mL following 4 weeks oral administration of Epidiolex® (CBD dose of 20 mg/kg/day). Dronabinol (Marinol®) is an oral preparation of synthetic THC currently approved to treat nausea and vomiting associated with cancer chemotherapy and to enhance appetite in AIDS patients suffering from weight loss [33]. Oral administration of Marinol® capsules containing 10 mg THC to human volunteers resulted in low peak plasma levels and systemic bioavailability, 3.8 ng/mL and 7 ± 3%, respectively [34, 35]. Namisol® is another oral THC-based formulation recently developed in a novel drug emulsifying system by Echo Pharmaceuticals B.V. (Nijmegen, the Netherlands) [36]. The peak plasma concentration of THC following oral administration of Namisol® tablets containing 8 mg THC to human volunteers was 4.69 ng/mL [36]. The low oral bioavailabilities reported for CBD and THC after oral administration were primarily attributed to the extensive first-pass metabolism in the liver [37, 38]. Therefore, administration by routes that avoid the first-pass effect in the liver such as oromucosal and rectal administrations were applied in an attempt to enhance the systemic bioavailability of cannabinoids [35]. Nabiximols (Sativex®) is a commercially

available oromucosal spray which contains a mixture of CBD and THC. It is used to alleviate spasticity in MS patients [39]. In a controlled double-blind study, similar doses of THC were administered to 9 healthy human volunteers in oral capsules (Marinol®) and oromucosal spray (Sativex®) [40]. Sativex® was not superior to Marinol® in regards to peak plasma levels and systemic exposure to THC. In addition, the authors reported peak plasma levels of CBD following the administration of Sativex® (two actuations to deliver 5 mg CBD), which were in the range of 0.6 – 3.9 ng/mL [40]. These levels were in the same range as those reported after the oral administration of comparable dose of CBD (5.4 mg) [27]. In contrast, rectal administration was demonstrated to markedly enhance the systemic exposure to THC in humans compared to equivalent oral doses [37]. However, considerable inter-individual variability was reported in that study following rectal administrations.

1.1.2.1.1.2. Distribution

CBD and THC are highly lipophilic compounds, thereby rapidly distributing to highly perfused tissues such as lung, liver, kidney, spleen, heart, and brain [31, 41]. In a study by Alozie *el al* [42], the authors reported that CBD and THC are rapidly distributed to the brain following IV administration to rats. In addition, both cannabinoids were found to accumulate in fatty tissues following repeated administrations as a result of their high lipophilic nature, suggesting the formation of fatty acids conjugates in fatty tissues [23, 31, 43]. It was also demonstrated that both cannabinoids are highly bound to plasma proteins (> 90%) [23, 31].

1.1.2.1.1.3. Metabolism

CBD and THC are extensively metabolised by hepatic enzymes. Both cannabinoids undergo phase I oxidation reactions, leading to the formation of

hydroxy-metabolites, particularly 7-OH-CBD and 11-OH-THC, respectively. Hydroxy-metabolites can be further oxidised to carboxylic acid-metabolites [35, 44]. Phase II metabolism is predominantly glucuronide conjugation for both cannabinoids [45, 46]. Little is known about the pharmacological activity of CBD metabolites in humans [45]. In contrast, 11-OH-THC, the hydroxy-metabolite of THC, has equipotent pharmacological activity as THC [46]. To date, there has been little discussion about the extrahepatic metabolism of CBD. It has been suggested, however, that intestine, lung, and brain contribute, at least partially, to the metabolism of THC [35].

Unlike THC, data from *in vitro* studies have demonstrated that CBD has potent inhibitory effects on multiple hepatic enzymes, raising concerns about potential drug-drug interactions with drugs metabolised by the same enzymes [47]. In fact, in a clinical trial by Geffrey *et al* [32], CBD was concomitantly administered with the antiepileptic drug clobazam to 13 subjects with refractory epilepsy. CBD caused significant increase in the plasma concentrations of clobazam and its active metabolite norclobazam, demonstrating an inhibitory effect of CBD on the hepatic enzymes (cytochrome P450 isoforms; CYP 2C19 and CYP 3A4) responsible for the metabolism of clobazam and norclobazam. Clobazam-related side effects were thereby reported in 10 out of the 13 subjects, which resolved upon decreasing the dose of clobazam [32]. Similar pharmacokinetic interaction was also reported with hexobarbital [48].

1.1.2.1.1.4. Elimination

In general, CBD and THC are primarily excreted in faeces and, to a lesser extent, in urine. In faeces, hydroxy- and carboxylic acid-metabolites of CBD and THC are predominant, while glucuronide conjugates are the most abundant metabolites recovered in urine [35, 45].

1.1.2.1.2.Pharmacodynamics

1.1.2.1.2.1. Mechanism of action

The pharmacodynamic effects of CBD and THC are governed by diverse activity through multiple receptors, including CB_1 and CB_2 receptors. The current understanding of cannabinoid-cannabinoid receptors interaction has developed over the last two decades, particularly after the discovery endocannabinoids. To date, it is believed that there are at least 15 endocannabinoids that can interact with cannabinoid receptors, of which N-arachidonoylethanolamine (anandamide) and 2-arachidonoylglycerol (2-AG) are well recognised [49]. Endocannabinoids modulate the activity of cannabinoid receptors (CB_1 and CB_2) by targeting orthosteric sites (interaction of a ligand at these sites directly enhances or inhibits the activity of the receptor). In addition, CB_1 receptor has allosteric sites (interaction of a ligand at these sites modulates the activity of an orthosteric ligand) [49].

Until recently, there was controversy about the affinity and the mode of action of CBD on cannabinoid receptors. Some reports suggested lack of affinity whereas others proposed weak antagonistic activity [50-52]. However, in a study by Laprairie *et al* [53], CBD was suggested to act as a negative allosteric modulator of CB_1 receptors, which means that it can negatively attenuate the agonistic activity of orthosteric ligands such as THC and the endocannabinoid 2-AG. This might explain the ability of CBD to decrease some of the psychotropic side effects induced by the action of THC on CB_1 receptors *in vivo* [54]. Another proposed mechanism involves inhibiting the cellular uptake of the endocannabinoid anandamide [54]. CBD also acts on other G-protein coupled receptors, such as GPR55 and GPR18. These receptors are commonly called putative cannabinoid receptors [49]. CBD was suggested to behave as an antagonist of GPR55 and GPR18 receptors [54]. Nevertheless, the majority of

therapeutic effects of CBD are proposed to be mediated by modulating non-cannabinoid receptors, such as serotonin receptors, adenosine receptors, opioid receptors, the nuclear peroxisome proliferator-activated receptors (PPARγ), glycine receptors, gabaergic receptors, and the transient receptor potential (TRP) channels [54].

Unlike CBD, THC has a well-defined affinity to CB_1 and, to a lesser extent, to CB_2 as a partial agonist, thereby acting as a mixed agonist-antagonist based on the state of activity of the receptor [15]. The characteristic psychotropic effects of THC are mediated by its action on CB_1 receptors [55]. It is worth noting that some *in vitro* studies demonstrated that chronic treatment with THC caused desensitisation of cannabinoid receptors [56]. This suggests tolerance to cannabinoid receptor-mediated effects of THC upon continuous administration [57]. Similar to CBD, THC also mediates some of its pharmacological effects by modulating multiple non-cannabinoid receptors, including GPR55, GPR18, serotonin receptors, adenosine receptors, opioid receptors, PPARγ receptors, glycine receptors, and TRP channels [55]. The mode of pharmacological effects of CBD and THC on different receptors are summarised in **Table 1.1**.

1.1.2.1.2.2. Selected pharmacological effects of CBD and THC

1.1.2.1.2.2.1. Actions on immune cells

Data from *in vitro* and *in vivo* studies demonstrated that CBD has dose-dependent immunomodulatory effects on immune cells (usually immunosuppression) [58]. THC has also shown dose-dependent effects. Yet, these effects were described as biphasic, having stimulatory effects at nanomolar concentrations and inhibitory effects at macromolar concentrations (around ten-fold the concentrations observed in the plasma of cannabis

smokers) [59, 60]. The immunosuppressive effects of CBD and THC involve different mechanisms such as suppression of proliferation, maturation, migration, and cytokine expression of immune cells [58]. An example of the immunosuppressive effects of CBD and THC was demonstrated in a study by Jenny *et al* [61]. In that study, CBD and THC significantly inhibited the proliferation of mitogen-stimulated peripheral blood mononuclear cells (PBMC) at macromolar concentrations, 7.5 and 10 μg/mL, respectively. Similar effects were also demonstrated on murine immune cells [62, 63].

It is still to be clarified what is the exact mechanism by which cannabinoids produce the immunosuppressive effects. Recent reports suggested that the immunosuppressive effects of CBD are mediated by non-cannabinoid receptor mechanisms that involve the activation of adenosine receptors [64, 65]. In contrast, the immunosuppressive effects of THC are apparently mediated by multiple targets which include cannabinoid and non-cannabinoid receptors [59].

Table 1.1. Pharmacological targets of cannabidiol (CBD) and Δ^9-tetrahydrocannabinol (THC) [54].

	Target		Functionality
CBD	Cannabinoid receptors	CB_1	Negative allosteric modulator
		CB_2	Antagonist (weak affinity)
		anandamide uptake	Inhibitor
	Putative cannabinoid receptors	GPR55	Antagonist
		GPR18	Antagonist
	Serotonin receptors	$5\text{-}HT_{1A}$	Agonist
		$5\text{-}HT_{2A}$	Partial agonist (weak affinity)
		$5\text{-}HT_{3A}$	Antagonist
	Adenosine receptors	A_{1A}	Agonist
	Opioid receptors	μ- and δ-OPR	Allosteric modulator
	Peroxisome proliferator-activated receptors (PPAR)	PPARγ	Agonist
	Glycine receptors	α_1	Positive allosteric modulator
		α_3	Positive allosteric modulator
	Gabaergic receptors	$GABA_A$	Positive allosteric modulator
	TRP channels	TRPV1, 2, 3	Agonist
		TRPA1	Agonist
THC	Cannabinoid receptors	CB_1	Partial agonist
		CB_2	Partial agonist
	Putative cannabinoid receptors	GPR55	Agonist
		GPR18	Agonist
	Serotonin receptors	$5HT_{3A}$	Antagonist
	Opioid receptors	μ- and δ-OPR	Allosteric modulator
	Peroxisome proliferator-activated receptors (PPAR)	PPARγ	Agonist
	Glycine receptors	α_1	Positive allosteric modulator
		α_3	Positive allosteric modulator
	TRP channels	TRPV2, 3, 4	Agonist
		TRPM8	Antagonist
		TRPA1	Agonist

1.1.2.1.2.2.2. Pain

A number of clinical studies have showed that cannabis administration significantly improves pain associated to MS, rheumatoid arthritis, cancer, as well as human immunodeficiency virus (HIV)-associated neuropathic pain [66-68]. It was suggested that the control of pain induced by CBD and THC is mediated, at least in part, by antagonistic activity at 5-HT_{3A} receptors [55]. Other mechanisms might include modulation of glycine receptors by CBD [69] and THC [55], and CB_1 receptors by THC [70].

1.1.2.1.2.2.3. Anti-emetic

The mechanism by which CBD induces the anti-emetic effect is thought to be through the activation of 5-HT_{1A} receptors in the dorsal raphe nucleus. This was demonstrated in a rat model of nausea-like behaviour, in which the anti-emetic effect of CBD was abolished by the specific 5-HT_{1A} receptor antagonist WAY100635 [71]. The anti-emetic effect of THC seems to be mediated by the activation of presynaptic CB_1 receptors on the serotoninergic neurons, thereby suppressing 5-HT release and inhibiting emesis [72].

1.1.2.1.2.2.4. Neuroprotection

There is a growing body of literature that recognises the neuroprotective effects of cannabinoids as a promising therapeutic approach in the treatment of neurodegenerative diseases like MS [73]. Early studies demonstrated that the neuroprotective effects of cannabinoids, including THC, *in vivo* are mainly CB_1-mediated. This might be mediated through attenuating glutamate-induced and calcium influxes-mediated neuronal toxicity [74, 75]. However, recently, CBD significantly improved the neurological disability in an animal model of MS, indicating neuroprotective effects. This was attributed to the remarkable ability of CBD to inhibit the neurotoxic activity of sodium channels [73]. Moreover, the

inhibition of oxidative stress could be another mechanism by which CBD and THC exhibit neuroprotection [76].

1.1.2.1.2.2.5. Other pharmacological effects

In addition to the pharmacological effects listed above, other pharmacological effects of potential therapeutic values are listed in **Table 1.2**. In fact, there are much more pharmacological effects of CBD and THC that are broadly reviewed elsewhere [20, 77].

Table 1.2. Some pharmacological effects of potential therapeutic value of cannabidiol (CBD) and Δ^9-tetrahydrocannabinol (THC) [57].

CBD
Anxiolytic
Anticonvulsant
Inhibitory effect on L-DOPA-induced dystonia
Antipsychotic
Sleep-promoting effect
Inhibitory effect on cancer cell proliferation
Reduction of intra-ocular pressured

THC
Inhibitory effects on gastro-intestinal tract motility
Reduction of intra-ocular pressure
Facilitation of sleep
Appetite stimulation
Inhibitory effect on cancer cell proliferation

1.1.2.1.3.Current Therapeutic applications

The current therapeutic applications, including those in clinical trials, of medical cannabis (crude pant materials) and pharmaceutical formulations containing CBD and/or THC are listed in **Table 1.3**.

Table 1.3. Common therapeutic applications of cannabis and cannabis-derived medicines that contain cannabidiol (CBD) and/or Δ^9-tetrahydrocannabinol (THC) [78-81].

Therapeutic use	Cannabis and cannabis-based medicines
Nausea and vomiting associated with chemotherapy	Plant materials Marinol® capsules (dronabinol, synthetic THC) Cesamet® capsules (nabilone, synthetic analogue of THC)
Appetite stimulation in HIV/AIDS	Plant materials Marinol®
Relief of spasm in multiple sclerosis	Plant materials Sativex® oromucosal spray (nabiximols, mixture of natural CBD and THC)
Pain associated with cancer and neuropathic pain	Plant materials Sativex®
Treatment of Dravet and Lennox-Gastaut syndromes	Epidiolex® oral solution (natural CBD)
Adjuvant treatment of severe chronic painful conditions like in rheumatoid arthritis and Parkinson's disease-related pain	Plant materials
Tourette disease	Plant materials
Posttraumatic stress disorder (PTSD)	Plant materials

Plant materials are more often administered by vaporisers, smoking joints, and orally with food.

1.2. The immune system

The immune system is a collection of cells, tissues, and molecules that provide a fundamental defence barrier against harmful mediators such as infectious microbes, toxins, and cancer cells [82]. The responses of the immune system against microbes protect the body from a wide range of life-threating infections. In fact, enhancing immune responses by vaccination is a commonly

used approach to prevent and eradicate infections [83]. The immune system has the ability, at normal conditions, to initiate responses against a wide variety of harmful antigens but not against the body's own antigens. This ability is generally known as tolerance [82]. However, immunological tolerance might be overwhelmed by over-active immune responses to self-antigens causing what is called autoimmunity. Autoimmunity could progress to autoimmune diseases, in which immune responses cause inflammation and tissue damage, thereby interfering with normal physiological functions [84]. On the other hand, disorders that attenuate and interfere with normal immunological responses result in increased susceptibility to infections. This condition is commonly known as immunodeficiency [82].

1.2.1. Autoimmune diseases

As mentioned above, autoimmune disease is defined as a tissue damage induced by immune responses against self-antigens. These responses could be organ specific or systemic (**Figure 1.2**) [84]. The mechanisms of tissue damage by autoimmune diseases are similar to three of the classical hypersensitivity reactions (type II, III, and IV). First, antibody-mediated autoimmune diseases (type II), in which antibodies directed against cell surface antigens to cause cell/ tissue destruction like in autoimmune haemolytic anaemia, or modulate cell surface receptors like in Graves' disease. Second, immune complex-mediated autoimmune diseases (type III). In this class, antigens bind to soluble antibodies to from a complex which can accumulate in the vascular bed of various tissues to cause injury and inflammation. Systemic lupus erythematosus (SLE) is a typical autoimmune disease of this class. Third, T cell-mediated autoimmune diseases (type IV), in which T cells, particularly T_H1, recognise antigens displayed on the surface of class II major histocompatibility complex

(MHC). This initiates the release of inflammatory cytokines such as TNF-α, TNF-β, IFN-γ, IL-3, and granulocyte-macrophage colony-stimulating factor (GM-CSF), which eventually cause inflammation and tissue damage. A well-known example of this class is multiple sclerosis (MS) [82, 83]. **Table 1.4** contains examples of autoimmune diseases categorised according to the predominant mechanism of hypersensitivity involved.

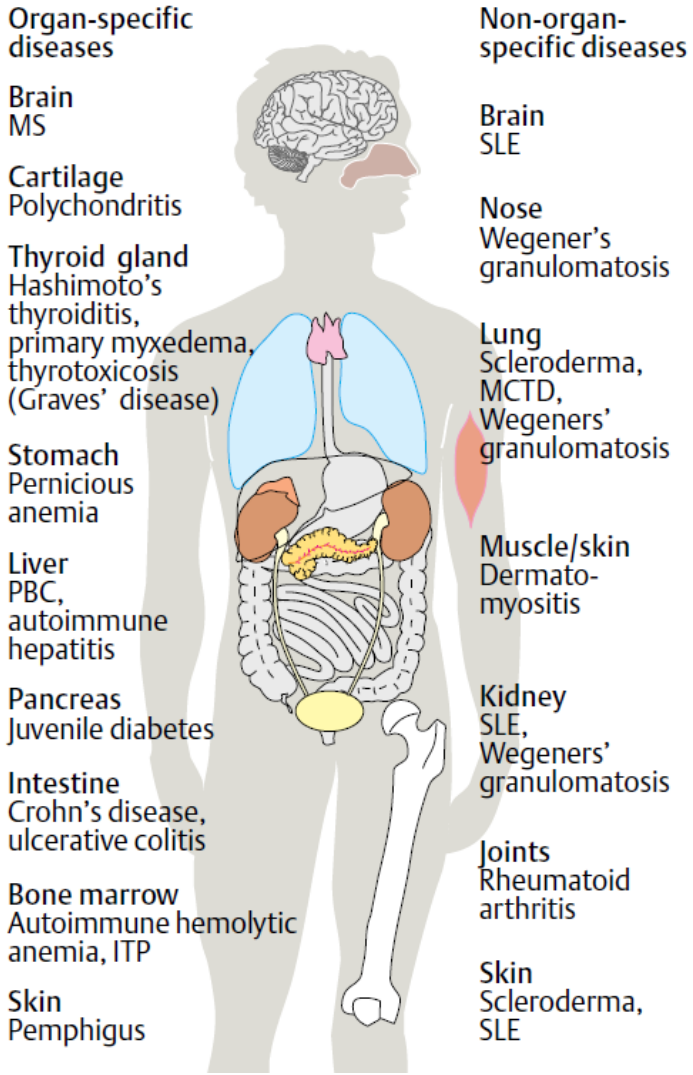

Figure 1.2. Organ-specific and systemic autoimmune diseases. MS, multiple sclerosis; SLE, systemic lupus erythematosus; MCTD, mixed connective tissue disease; PBC, primary biliary cirrhosis; ITP, idiopathic thrombocytopenic purpura [85].

Table 1.4. Classification of common autoimmune diseases based on the predominant mechanism of hypersensitivity involved in tissue injury [82, 84].

Mechanism of autoimmunity	Autoimmune disease
Antibody-mediated	Autoimmune haemolytic anaemia Idiopathic thrombocytopenic purpura (ITP) Myasthenia gravis Graves' disease
Immune complex-mediated	Systemic lupus erythematosus (SLE) Mixed cryoglobulinaemia
T cell-mediated	Multiple sclerosis (MS) Rheumatoid arthritis Type 1 (insulin-dependent) diabetes mellitus Crohn's disease Ulcerative colitis Hashimoto's thyroiditis

T cell-mediated autoimmune diseases have recently gained much of the research interest. Therefore, in the next few sections of this thesis, we will be focusing on T cell-mediated autoimmune diseases, with an emphasis on MS.

1.2.1.1. Multiple sclerosis (MS)

MS is a chronic inflammatory demyelinating disease of the central nervous system (CNS), and the second cause of neurological disabilities in young adulthoods. It affects more than 2.5 million people worldwide [86, 87]. The course of disease can be relapsing-remitting or progressive. More often, the disease starts as relapses followed by complete or partial retrieval of neurological functions in the relapsing-remitting course, and eventually progresses to irreversible neurological dysfunctions in the progressive course of the disease [88]. The clinical symptoms of the diseases vary according to the affected area of the CNS. Most common symptoms include: weakness of the limbs, spasticity, optic neuritis, ataxia, bladder dysfunction, depression, and fatigue [86].

1.2.1.1.1.Clinical types of MS

The course of MS disease can be classified, based on clinical assessment, to 4 types [86]. These are:

A. Relapsing-remitting MS (RRMS). The majority (85%) of MS cases start as RRMS. The course of disease includes recurrent neurological attacks, which develop over days to weeks, followed by complete or partial retrieval of neurological functions. Stable neurological functions could continue for months or years before the patient could experience another attack (**Figure 1.3 A**).

B. Secondary-progressive MS (SPMS). This course of the disease starts as RRMS, which evolves to more steady neurological dysfunctions unrelated to acute attacks (**Figure 1.3 B**).

C. Primary-progressive MS (PPMS). PPMS patients show steady decline in neurological functions from the onset of the disease without experiencing attacks (**Figure 1.3 C**).

D. Progressive-relapsing MS (PRMS). The course of disease is more similar to PPMS, in which there is a steady decline in neurological functions. However, patients could experience short attacks which further intensify disability (**Figure 1.3 D**).

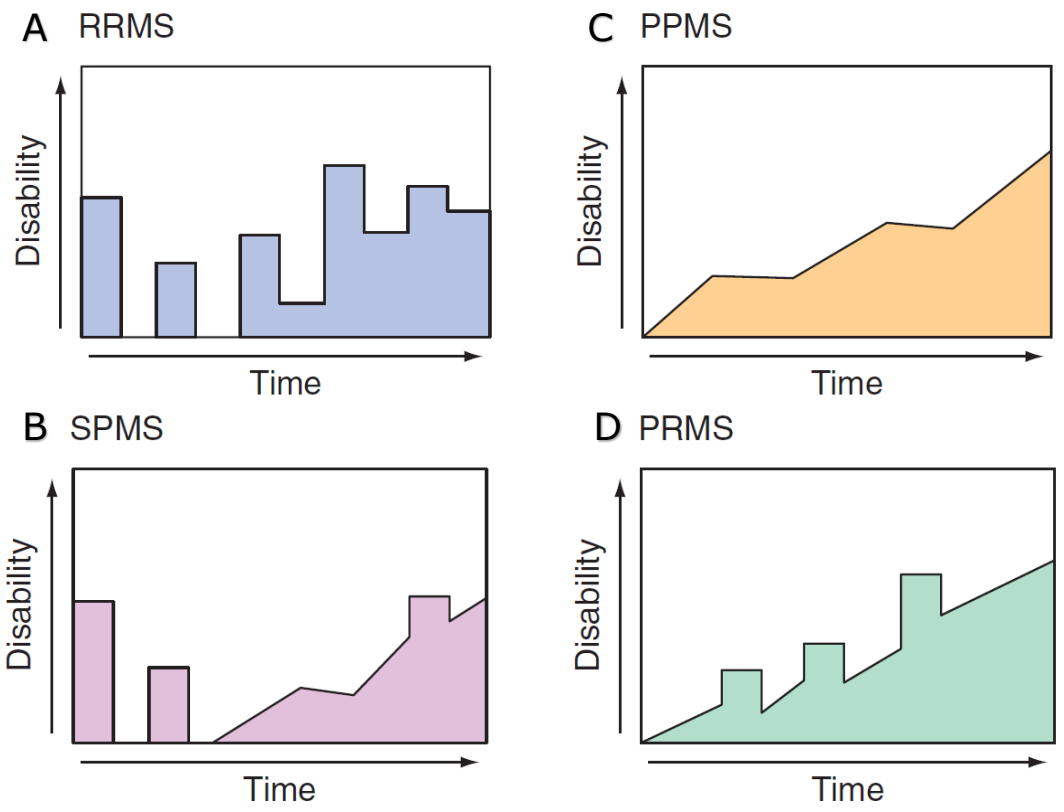

Figure 1.3. The clinical course of neurological disability in multiple sclerosis (MS). **Panel A**: relapsing-remitting MS (RRMS). **Panel B**: secondary-progresive MS (SPMS). **Panel C**: primary-progressive MS (PPMS). **Panel D**: primary-relapsing MS (PRMS) [86].

1.2.1.1.2.Epidemiology of MS

Epidemiological studies have shown that MS has geographical gradient being of higher prevalence in temperate-zone areas such as North America and northern Europe relative to tropical areas [89]. The prevalence of MS in women was described to be as much as three-fold higher than in men [86]. As for environmental risk factors, vitamin D deficiency, infection with Epstein-Barr virus (EBV) after childhood, and cigarette smoking are well correlated with MS [90]. Genetic factors are an additional risk for MS. Studies in the US demonstrated that African American men are 40% less susceptible to MS than

white men. In addition, first-degree relatives to an MS patient are apparently at higher risk of developing MS [89, 91].

1.2.1.1.3.Pathophysiology of MS

The aetiology of MS is not yet completely understood, however, pitfalls in the immune system as a result of genetic and/ or environmental factors have been suggested [88, 92]. Common pathophysiological features of MS lesions include inflammation, demyelination, and scarring [93]. However, symptom expression is primarily due to disturbances of axonal conduction in the relevant pathway, for instance, conduction block in the optic nerve causes the visual symptoms of MS. Although the exact mechanism of conduction block is still to be clarified, demyelination seems to be the predominant cause [94]. Demyelination occurs when myelin-specific auto-reactive T cells are activated in the peripheral tissues, particularly in the draining lymph nodes [87]. This enhances the ability of T cells to penetrate the blood-brain barrier (BBB) [95]. BBB penetration is facilitated by some inflammatory mediators, such as TNF-α and IFN-γ, which are released from T cells [96]. Once in the CNS, T lymphocytes are reactivated by interaction with MHC presented by local antigen-presenting cells, particularly macrophages and microglia (the resident macrophages of the CNS). This promotes T cell transition to the pro-inflammatory phenotype T_H1 [92]. More recently, T_H17 cells have also emerged as a major factor in the pathogenesis of MS [97]. Activated T cells can then secrete inflammatory cytokines such as TNF-α and IFN-γ. These cytokines cause myelin sheath destruction. Additional myelin damage can be produced by plasma cell derived antibodies (**Figure 1.4**). More inflammatory cells are recruited to the area including the myelin antibody secreting B cells. Microglial cells also migrate toward the site of injury where they produce cytotoxic mediators and pro-inflammatory cytokines, which can further intensify cell damage [58]. All

together, these effects subsequently cause neuronal demyelination [92]. Axons can initially retrieve conduction by redistribution of ion channels over the demyelinated area or even by complete remyelination. These adaptive processes can explain the recovery of neurological functions in the remission phase of the relapsing-remitting MS [88, 98]. More often, irreversible disabilities are developed as a consequence of neuronal and axonal loss. The irreversible injuries are usually caused by (a) free radical-mediated oxidative stress due to nitric oxide (NO) and oxygen radicals and (b) excitotoxicity due to over-exposure to excitatory amino acids such as glutamate. These two mechanisms ultimately give rise to the irreversible progressive course of MS [99].

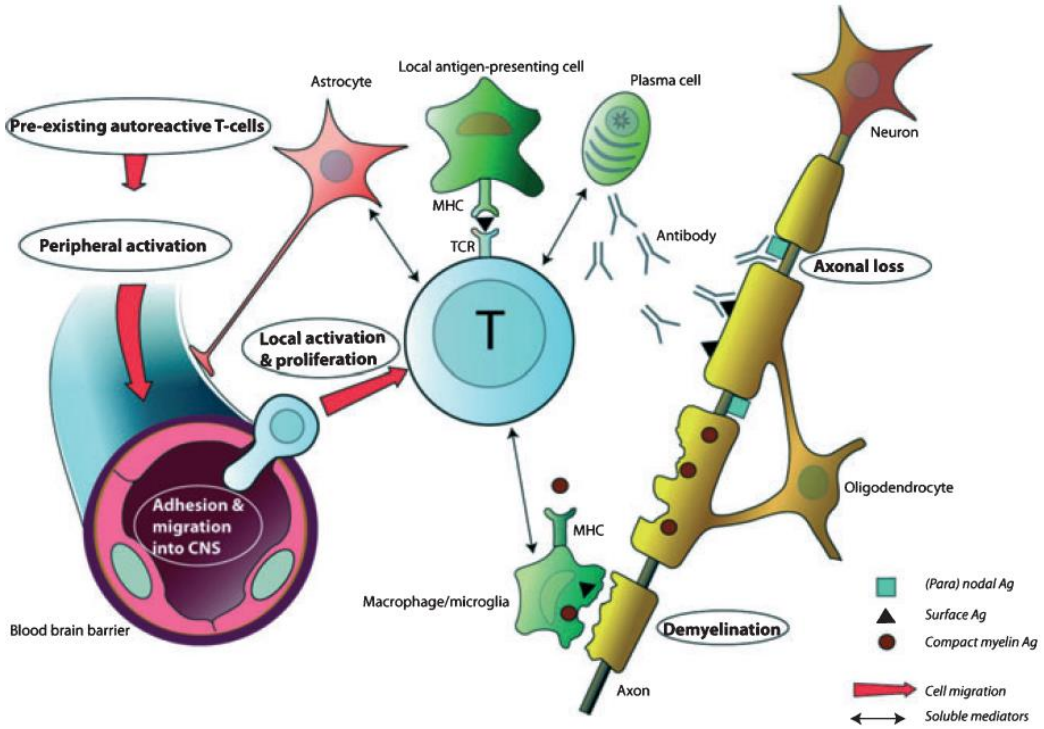

Figure 1.4. Schematic representation of the pathogenesis of multiple sclerosis lesion, which shows the peripheral priming of auto-reactive T cells and subsequent invasion and inflammation to the central nervous system [92].

1.2.1.1.4.Treatment strategies

Current treatment strategies of MS include two main approaches: treatment with disease-modifying agents and symptomatic treatment [100].

1.2.1.1.4.1. Disease-modifying agents

The current understanding of MS as an autoimmune disease has supported the use of immunomodulatory agents to decrease the extent of neuroinflammation accompanying relapses and postpone disease progression toward the irreversible disability. As such, disease-modifying agents are of therapeutic value in MS patients who still experience neurological attacks, particularly RRMS and SPMS patients [86, 100]. Disease-modifying approach can be further divided to two strategies: short-term management intended to reduce the severity of acute attacks and long-term treatment aimed to control the disease and prevent new attacks. More often, high doses of corticosteroids are used for short period to treat acute attacks [100]. For the long-term disease-modifying, ten drugs are currently approved for clinical use (**Table 1.5**) [101]. These drugs act by different immunomodulatory mechanisms, such as suppressing the proliferation of lymphocytes, decreasing the production of inflammatory cytokines, increasing anti-inflammatory cytokines production, preventing the migration of inflammatory cells across the BBB, and/or interfering the circulation of pro-activated T cells from lymphoid tissues to the systemic circulation [102]. In addition to these drugs, other therapeutic options are currently available as off-label therapies for RRMS and SPMS, such as azathioprine, methotrexate, cyclophosphamide, and methylprednisolone [86].

Table 1.5. Main mechanisms of action of disease-modifying therapies that are currently in use for the treatment of multiple sclerosis (MS) [102].

Treatment	Mechanism of action
Interferon b-1a/b	Ameliorate the production of pro-inflammatory cytokines (TNF-α, IFN-γ and IL-17) and enhance the release of anti-inflammatory cytokines (IL-10 and IL-4)
Glatiramer acetate	Ameliorates the production of pro-inflammatory cytokines (TNF-α and IL-12) and enhances the release of anti-inflammatory cytokines (IL-10 and IL-4)
Mitoxantrone	Suppresses the proliferation of lymphocytes (T and B cells) and macrophages. Also, it decreases the production of pro-inflammatory cytokines (TNF-α, IFN-γ and IL-2)
Natalizumab	Interferes with the migration of inflammatory cells across the BBB
Fingolimod	Prevents the circulation of pro-activated T cells from lymphoid tissues to the systemic circulation, including the CNS
Teriflunomide	Suppresses the proliferation of T and B lymphocytes
Dimethyl fumarate	Activates a nuclear factor pathway that promotes anti-inflammatory effects, as well as processing a neuroprotective effect by interfering oxidative stress mechanisms
Alemtuzumab	Leads to the formation of new pattern of lymphocytes population

1.2.1.1.4.2. Symptomatic treatment

Symptomatic treatment is aimed to decrease the impact of disability on the quality of life of MS patients. Common symptoms that are targeted by symptomatic therapies include spasticity, pain, ataxia and tremor, fatigue, bladder dysfunction, bowel dysfunction, and sexual dysfunction [103]. Pharmacological and non-pharmacological treatment strategies are used to relieve symptoms in MS patients, which are reviewed in details elsewhere [104]. Noteworthy, clinical trials in MS patients have demonstrated that cannabinoids

have beneficial effect in the treatment of spasticity [105, 106], pain [106-109], and bladder dysfunction [110].

1.2.1.1.5.Experimental models of MS

The animal models of MS were developed to better understand the pathogenesis of the disease. In fact, animal models of MS have greatly enriched the existing knowledge of MS pathogenesis and supported the development of therapeutic agents that are currently in clinical use [111]. To date, the available animal models of MS include experimental autoimmune encephalomyelitis (EAE), virally-induced demyelinating, and toxin-induced demyelinating models [112]. EAE model in rodents is used to simulate the inflammatory components of MS and it is the most commonly used model of MS in preclinical research [113]. EAE is induced by immunising the animal with a CNS antigen or passive transfer of inflammatory cells from immunised animal to a naïve recipient. This initiates inflammatory process that eventually overcomes immunological tolerance and induces neurological disability [114]. The course of disease in EAE could be relapsing or chronic based on the species of the animals used and the immunisation protocol [114, 115].

Kozela *et al* [116] have demonstrated that parenteral administration of CBD has therapeutic effects on the clinical signs of EAE in C57BL/6 mice. The therapeutic effects of CBD involved suppressing the proliferation of T lymphocytes and the activity of microglial cells, as well as neuroprotective effects. In contrast, no therapeutic immunomodulatory effects were evident in EAE in ABH mice [117, 118]. Worth noting that EAE in ABH mice is widely used to explore the neurodegenerative pathogenesis of MS [119, 120]. However, to our knowledge, the suitability of ABH mice model to demonstrate the therapeutic effects of immunomodulatory drugs has not been validated. In regards to THC, it was demonstrated to alleviate the clinical signs of EAE in

Lewis rats and guinea pigs by immunosuppressive effects on lymphocyte function and migration [121].

1.2.2. Immunodeficiency

The critical function of the immune system is to protect the body against infections. Immunodeficiency can be defined as an impairment in the function [116]of the immune system that might lead to a life-threating illness. Immunodeficiency could be primary (inherited) or secondary (acquired) to other disease [83]. Common causes of secondary immunodeficiency are summarised in **Table 1.6**.

Table 1.6. Common causes of secondary immunodeficiency [82, 83].

Causes of secondary immunodeficiency	Examples
Virus infection	Human immunodeficiency virus (HIV) infection
Chemotherapy treatments for cancer	Alkylating agents, cytotoxic antibiotics, antimetabolites, vinca alkaloids and others
Immunosuppression for graft rejection and inflammatory diseases	Corticosteroids, calcineurin inhibitors, antiproliferative immunosuppressants (azathioprine, mycophenelate)
Nutritional deficiencies	Protein-calorie malnutrition

Immunocompromised individuals are at high risk of infections. Two sources of infections are common in immunocompromised state: (1) common pathogens like S. aureus, E. coli, and Proteus, which could affect healthy individuals as well, or (2) opportunistic pathogens like S. epidermidis, H. simplex, Candida spp., and cytomegalovirus that affect immunologically-weak individuals. The latter pathogens account for higher mortality than common pathogens [84].

1.3. The lymphatic system

The current understanding of the lymphatic system and lymphoid tissues has developed over the centuries. Until recently, the lymphatic system was thought to be merely a drainage system for fluids and proteins from interstitial space back to the blood [122]. Currently, however, the lymphatic system is considered to have a central role in the pathogenesis of several diseases such as cancers, viral infections, some parasitic infections, and autoimmune disorders. In fact, it is the main pathway for the metastases of some epithelial-origin solid tumours, such as those of the colon, breasts, lungs, and prostate [123]. In addition, the lymphatic system is now recognized as a crucial part of the immune system. It is here where invader antigens are trapped, processed, presented to immune cells and consequently where immune responses are evoked [124]. These responses are important for the protection of the body from bacterial, viral, parasitic, and fungal threats, as well as the growth of tumour cells [125].

1.3.1. Functions of the lymphatic system

The main functions of the lymphatic system include fluid recovery, dietary lipid absorption, and immunity.

1.3.1.1. Fluid recovery

Fluids continuously escape from blood capillaries to the surrounding tissues. However, a significant proportion of these fluids cannot be reabsorbed by venous capillaries. Indeed, up to four litres of fluids and half of all plasma proteins can extravasate each day. This in turn could lead to circulatory failure and increased tissue pressure if unrecovered. The lymphatic system, therefore, maintains the body's fluid balance by reabsorption of the extravasated fluids and proteins back to the systemic circulation [126-128].

1.3.1.2. Lipid absorption

The intestinal lymphatic system has an essential physiological role in the absorption of dietary lipids and lipid-soluble vitamins [126, 127]. The first step in the absorption of dietary lipids is their digestion and micellar solubilisation in the gastrointestinal lumen. This happens mainly by the action of pancreatic lipase/co-lipase complex and bile salts in the small intestine. Once digested, the products of lipid hydrolysis are then incorporated into mixed micelles, which promote the diffusion of digested lipids to the apical membrane of enterocytes [129]. Inside enterocytes, most of the long-chain triglycerides (LCT) are re-synthesized from long-chain fatty acids and monoglycerides, mainly by the action of acyltransferases. LCT are then assembled with apolipoprotein B (Apo B), phospholipids, cholesterol, and cholesterol esters to form large lipoproteins with a lipid core (chylomicrons, CM). Mature CM are then secreted by exocytosis through the basolateral membrane of enterocytes. Being large particles, CM cannot pass the walls of vascular capillaries, but are absorbed to the lymph lacteals instead [130-133]. Due to the presence of lipids in the form of CM, lymph fluid following high-fat meal looks like a turbid emulsion, which is commonly called 'chyle' [123].

1.3.1.3. Immunity

The immune system is not a definite organ system *per se*, but rather a population of cells distributed in most organs to defend the body against any potential invaders. The most important immune cells involved in immune responses are lymphocytes. Over 90% of lymphocytes are localised in the lymphatic system [134, 135].

When collecting fluid and plasma proteins, the lymphatic system also picks up foreign bodies from tissues. These bodies are drained along the lymph to the regional lymph nodes where immune cells can initiate an immune response.

Therefore, lymph nodes stand as checkpoints that examine lymph fluid before it is being drained to the bloodstream [135].

1.3.2. Components of the lymphatic system

1.3.2.1. Lymph

Lymph is usually a clear and colourless fluid, which is drained from the interstitium. In addition to the recovered fluids and plasma proteins, lymph may also contain lipids, immune cells, hormones, bacteria, viruses, cellular debris, or even cancer cells. Substantial differences in lymph composition arise from physiological and/or pathological conditions of the tissue from which lymph is drained, as well as its location along the lymphatic vessels [127, 136].

1.3.2.2. Lymphatic vessels

The lymphatic system is the body's second circulatory system. However, unlike the closed structure of the cardiovascular vessels, the lymphatic system consists of unidirectional, blind-ended, and thin-walled capillary vessels where lymph is driven without a central pump [122, 137, 138]. Lymphatic capillaries drain in the afferent collecting vessels, which then pass through one or more gatherings of lymph nodes. Lymph fluid then passes through the efferent collecting vessels, larger trunks, and finally the lymphatic ducts. Subsequently, ducts drain lymph to the systemic circulation [123, 139].

1.3.2.3. Lymphatic organs

The lymphatic organs can be classified as primary or secondary. Primary lymphatic organs include the thymus gland and bone marrow, which produce mature lymphocytes (that can identify and respond to antigens). Secondary lymphatic organs include lymph nodes, spleen, and mucosa-associated lymph tissues (MALT) [140-142]. It is within the secondary lymphatic organs where lymphocytes initiate immune responses. MALT are distributed throughout

mucous membranes and provide a defence mechanism against a wide variety of inhaled or ingested antigens. MALT can be categorized according to their anatomical location to bronchus-associated lymphoid tissue (BALT), nasal-associated lymphoid tissue (NALT), salivary gland duct-associated lymphoid tissue (DALT), conjunctiva-associated lymphoid tissue (CALT), lacrimal duct-associated lymphoid tissue (LDALT), and gut-associated lymphoid tissue (GALT, the intestinal lymphatic system) [140, 143].

1.3.2.3.1.The intestinal lymphatic system

The intestinal lymphatic system consists of effector and immune induction sites. The former is represented by lymphocytes distributed throughout the lamina propria (LP) and intestinal epithelium, while the latter involves organized tissues such as mesenteric lymph nodes (MLN), Peyer's patches (PP), and smaller isolated lymphoid follicles (ILF) [144-147].

1.3.2.3.1.1. Mesenteric lymph nodes (MLN)

MLN are the largest gatherings of lymph nodes in the body, found in the base of the mesentery. The structure of MLN is similar to that of peripheral lymph nodes, and can be divided into two regions: the medulla and cortex. The cortex is mainly composed of T cells areas and B cell follicles (**Figure 1.5**). It is within the T cells area where circulating lymphocytes enter the lymph node and dendritic cells (DC) present antigens to T cells [133, 148, 149]. Lymph (containing cells, antigens, and CM) is collected from the intestinal mucosa and reaches MLN via the afferent lymphatics. Lymph fluid subsequently leaves MLN through efferent lymphatics to reach the thoracic duct that drains to the blood [144, 149].

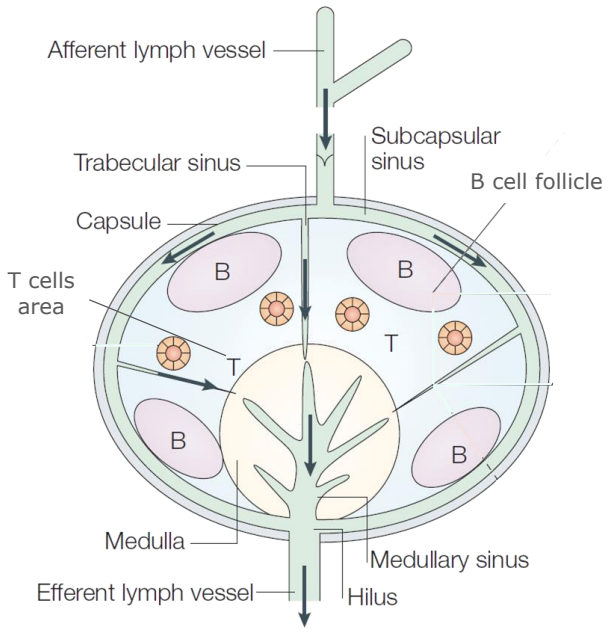

Figure 1.5. Schematic representation of the main structural components of a lymph node. Modified from von Andrian *et al* [133].

1.3.2.3.1.2. Peyer's patches (PP)

These are lymphoid nodules distributed in the mucosa and submucosa of the intestine. They consist of a subepithelial dome area and B cell follicles dispersed in a T cells area. A single layer of epithelial cells, called follicle-associated epithelium (FAE), separates lymphoid areas of PP from the intestinal lumen. FAE is permeated by specialized enterocytes called microfold (M) cells. These cells are considered as a gate for the transport of luminal antigens to PP (**Figure 1.6**) [144, 147].

1.3.2.3.1.3. Isolated lymphoid follicles (ILF)

ILF are a combination of lymphoid cells in the intestinal LP. ILF are structurally similar to PP in the sense that they are composed of germinal centre covered by FAE containing M cells. However, unlike PP, ILF lack a discrete T cells area. Although its function is not completely understood, FAE is thought to

be a complementary system to PP for the induction of intestinal immunity (**Figure 1.6**) [150, 151].

It is noteworthy that the intestinal lymphatic system is the largest lymphatic organ in the human body and contains more than half of the body's lymphocytes [152, 153]. The intestinal lymphatic system is also exposed to more antigens than any other part of the body, in the form of commensal bacteria and alimentary antigens, in addition to those from invasive pathogens. The intestinal immune system must therefore be able to distinguish antigens that require a protective immune response and to develop a state of immune hypo-responsiveness (oral tolerance) for those antigens that are harmless to the body [144, 147, 151]. The mechanism governing this process involves sampling of luminal antigens in the intestinal epithelium by DC. Antigens can cross the epithelium through M cells that are found in the FAE of PP. The antigens can then interact with DC in the underlying subepithelial dome region. Antigens are then presented to local T cells in PP by DC. DC can also migrate to the draining MLN where they present antigens to local lymphocytes [140, 144, 147, 154]. Alternative pathways for antigen transport across the intestinal epithelial cells involve receptor-mediated transport and direct sampling from the lumen by DC's projections. Antigen-loaded DC migrate to the MLN through afferent lymphatics where they present antigens to T cells. Subsequently, differentiated lymphocytes migrate from MLN through the thoracic duct and blood stream, and eventually accumulate in the mucosa for an appropriate immune response (**Figure 1.6**) [144, 155].

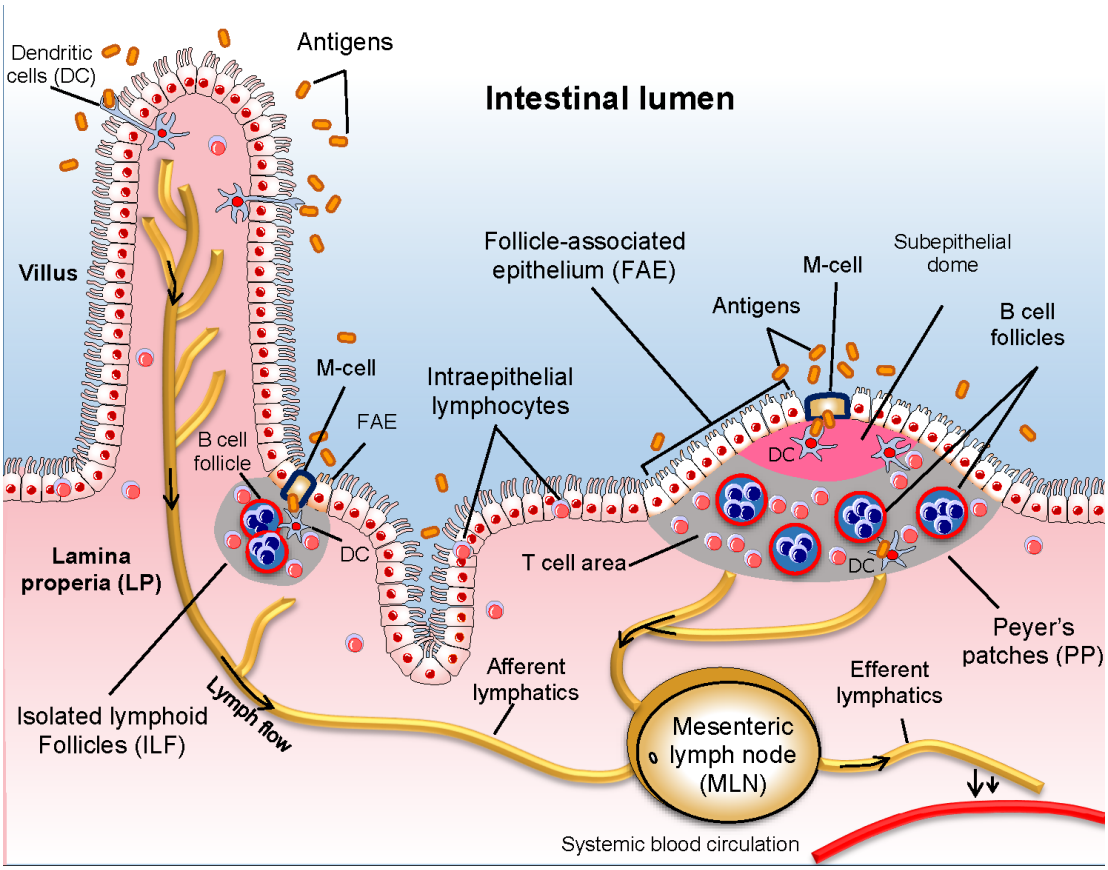

Figure 1.6. Schematic representation of the intestinal lymphatic system. Dendritic cells (DC) can sample luminal antigens that (1) cross M cells of Peyer's patches (PP) and isolated lymphoid follicles (ILF), and (2) transported to lamina properia (LP) by receptor-mediated mechanisms. In addition, DC can use trans-epithelial projections to sample antigens directly from the lumen. DC then present antigens to local lymphocytes or migrate to mesenteric lymph nodes (MLN) for lymphocyte priming.

1.3.3. Intestinal lymphatic transport

In general, the intestinal lymphatic system could be a target (effective compartment) and/or a route through which therapeutic agents are delivered to the systemic circulation.

1.3.3.1. Advantages of intestinal lymphatic transport

The advantages of intestinal lymphatic transport can be summarised as follows:

1. Increasing the bioavailability of lipophilic drugs when orally co-administered with lipid vehicles. This primarily occurs as a result of enhancing micellar solubilisation of the drug in the small intestine and drug-CM association in enterocytes [156]. Intestinal lymphatic transport avoids hepatic first-pass metabolic loss by diverting the absorption of lipophilic drugs toward intestinal lymphatics rather than the portal vein, which is extremely important for drugs exhibiting significant first-pass metabolism [132].
2. Achieving high local concentration in the intestinal lymphatic system could be a novel approach to enhance the therapeutic effects of particular pharmacological agents such as immunomodulators, chemotherapeutic, and anti-infective agents [123, 134]. Targeting immunomodulatory drugs to the intestinal lymphatic system, which is the major host of immune cells [127, 133], could be a unique strategy to enhance the pharmacological effects of immunomodulators. This approach is central in the hypothesis of this PhD project as will be discussed later. In addition, the lymphatic system is a main pathway of intestinal tumour metastases. Therefore, targeting cytotoxic drugs to the intestinal lymphatics could decrease dose-related systemic side effects and systemic dilution, thereby provides advantages in the treatment of tumour metastases [157, 158]. Being the largest lymphatic organ, the intestinal lymphatic system is a valid delivery target for antiviral agents, as some viruses spread and develop within the lymphatic system. Those of particular importance are HIV [159], morbillivirus, canine distemper virus, severe acute respiratory syndrome associated coronavirus (SARS), hepatitis B, and hepatitis C [160].

3. Intestinal lymphatic transport of lipophilic drugs results in delivery of the drug to the systemic circulation in CM-associated form, which might attenuate the pharmacokinetic and/or pharmacodynamics properties [158, 161].

1.3.3.2. Common approaches for enhancing intestinal lymphatic transport

1.3.3.2.1.Lipid-based drug delivery systems (LBDDS)

1.3.3.2.1.1. Co-administration with lipids

One of the simplest methods for enhancing the intestinal lymphatic transport of lipophilic drugs is the oral co-administration with LCT [162, 163]. It was believed before that the lymphatic system has insignificant contribution in drug absorption compared to the vascular system. Indeed, it is true for hydrophilic and some moderately lipophilic molecules. However, recent advances in the field led to the conclusion that intestinal lymphatic system is the primary route for the absorption of highly lipophilic drugs that possess certain physicochemical properties and co-administered with LCT or long-chain fatty acids. In such circumstances, more than 70% of the absorbed dose could be delivered to the systemic circulation via the intestinal lymphatic system [164, 165].

The mechanism governing intestinal lymphatic transport of drugs involves the association of the drug with CM in enterocytes. CM serve as carriers that transport drug to the intestinal lymphatic system. However, to achieve such association specific physicochemical properties, particularly log D7.4 ≥ 5 and high lipid solubility, are essential [132, 166]. The digestion of LCT can enhance micellar solubilisation of lipophilic compounds in intestinal lumen, as well as CM synthesis in enterocytes and, eventually, promotes lymphatic transport [167].

Many researchers have demonstrated that oral co-administration of lipids can effectively enhance the bioavailability of lipophilic drugs by promoting intestinal lymphatic transport. Caliph *et al* [162] showed that the oral co-administration of halofantrine with LCT can significantly enhance the intestinal lymphatic transport and therefore the systemic exposure to halofantrine in rats. Another example was in a work by Gershkovich *et al* [165] who demonstrated that the oral bioavailability of PRS-211,220, a synthetic lipophilic cannabinoid, was enhanced following oral co-administration with LCT. Worth mentioning that the aforementioned drugs i.e. halofantrine and PRS-211,220 were shown to be highly associated with CM [165, 166, 168]. Therefore, when orally administered in conditions facilitating intestinal lymphatic transport these drugs avoided the hepatic first-pass metabolism and achieved high bioavailability. On the other hand, drugs that have low association with CM, like testosterone, showed very low intestinal lymphatic transport and low oral bioavailability due to extensive first-pass metabolism [169].

1.3.3.2.1.2. Other lipid based drug delivery systems

1.3.3.2.1.2.1. Emulsions

In general, emulsions are composed of three components: oil, surfactant, and water. The ratio of each component can determine if the resulted emulsion is oil-in-water, water-in-oil, micelles, oily dispersions, or self-emulsifying drug delivery systems (SEDDS, solutions that are emulsified upon contact with water). SEDDS can protect the drug from chemical and/or enzymatic degradation in the small intestine (the drug is basically protected in stabilised oil droplets), it can also enhance dissolution rate and the solubility of the drug in the intestinal lumen. In addition, the lipid component can promote intestinal lymphatic transport (by increasing lipoprotein synthesis in the enterocytes)

[170]. Self-microemulsifying and self-nanoemulsifying drug delivery systems (SMEDDS and SNEDDS, respectively) are types of self-emulsifying systems which are classified based on droplet size of the resulted emulsion [171]. In a study by Holm *et al* [172], halofantrine was formulated in SEDDS using LCT as a lipid component in the formulation. The authors demonstrated that oral administration of this formulation to canines has enhanced the extent of intestinal lymphatic transport.

1.3.3.2.1.2.2. Liposomes

Liposomes are closed spherical structures consisting of at least one phospholipid bilayer, ranging from 100 to 5000 nm. The amphiphilic nature of phospholipids allows the incorporation of both hydrophilic and hydrophobic drugs [173]. Similar to SEDDS, liposomes can also protect the drug form intestinal degradation and increase systemic uptake [174]. Some authors have suggested that liposomes can enhance intestinal lymphatic transport [175, 176]. However, the mechanism by which liposomes enhanced the lymphatic transport was not clearly identified.

1.3.3.2.2.Nanoparticles

Nanoparticle formulation has been suggested as an approach to increase the bioavailability of orally administered drugs by enhancing intestinal lymphatic transport. One type of nanoparticles that has been demonstrated to enhance the intestinal lymphatic transport is solid lipid nanoparticles (SLN) [177]. Clozapine [178] and nimodipine [179] are examples of drugs formulated as SLN and delivered, to some extent, to the systemic circulation via the intestinal lymphatic system. However, similar to liposomes, the mechanism of SLN intestinal lymphatic transport is still to be clarified.

1.3.3.2.3.Prodrugs

Prodrug approach can be used to modify a drug's physicochemical properties in such a way that would improve its intestinal lymphatic transport. The prodrug can be designed to have log D7.4 ≥ 5 and high lipid solubility [132, 166] (enhanced potential of uptake by CM), so that it's intestinal lymphatic transport is enhanced when the prodrug is co-administered orally with LCT. Prodrugs can also be designed to be structurally similar to TG or phospholipids and thereby can be involved in lipid digestion processes and incorporated with CM during lipoproteins assembly process in the enterocytes [180].

Testosterone undecanoate (TU) is an example of produrg that has been synthesised to enhance the bioavailability of orally administered testosterone. TU is a lipophilic ester that can liberate free testosterone upon hydrolysis by esterases. Unlike testosterone, oral administration of TU can produce androgenic activity in rats [181] and humans [182]. However, Coert *et al* [181] have demonstrated that the majority of the orally administered TU is metabolised in the intestinal lumen and the non-metabolised TU is absorbed exclusively by the intestinal lymphatic system. Shackleford *et al* [183] have also shown that the bioavailability of testosterone has increased as a result of enhanced intestinal lymphatic transport of TU. Yet, the bioavailability of testosterone was in the range of 3% following oral administration of TU. Apparently, intestinal degradation has decreased the amount of TU achieved in enterocytes and available for incorporation with CM.

1.4. Project hypothesis

Recent years have witnessed the re-emergence of cannabinoids as a promising therapeutic agents. Compared with other cannabinoids, CBD and THC received most of the research interest. Researchers demonstrated multiple pharmacological effects of CBD and THC, of which immunomodulation has received considerable attention [57, 184]. *In vitro* studies have demonstrated that the immunomodulatory effects of CBD and THC are evident only at relatively high concentrations (≥ 7.5 and 10 µg/mL, respectively [61]) which were not reported in human plasma following the administration of cannabinoids by conventional routs (inhaled, oromucosal, and oral) [24, 25, 27, 61, 62].

Therefore, the main hypothesis of this PhD project is that enhancing the intestinal lymphatic transport of lipophilic cannabinoids by oral co-administration with dietary lipids could deliver cannabinoids to lymphatics at concentrations that exceed their immunomodulatory threshold. As the intestinal lymphatic system is the major host of immune cells, the intestinal lymphatic transport of cannabinoids could be a novel therapeutic approach for autoimmune diseases or might have detrimental effects in immunocompromised states. This hypothesis was translated to the following research questions:

- Are CBD and THC good candidates for intestinal lymphatic transport?
- How enhancing the intestinal lymphatic transport of CBD and THC could affect their plasma pharmacokinetics and tissue distribution?
- Would the concentrations of CBD and THC achieved in the intestinal lymphatic system indeed exceed their immunomodulatory threshold?
- What are the therapeutic, or perhaps the detrimental, effects of enhancing the intestinal lymphatic transport of CBD and THC?

1.5. Project aim

The overall aim of this PhD project is to assess the impact of enhancing the intestinal lymphatic transport on the immunomodulatory effects of lipophilic cannabinoids, and the subsequent implications for people with autoimmune diseases and immunocompromised individuals.

The specific objectives of this work are therefore:

1. Development and validation of sensitive and robust bio-analytical methods for the determination of cannabinoids in biological matrices, such as lipolysis medium, lymph, and plasma (chapter 3).
2. Assessment of intraluminal processing of orally administered cannabinoids in LCT-based formulations (**Figure 1.7 A**; chapter 4).
3. Evaluating intestinal lymphatic transport potential of orally administered cannabinoids (**Figure 1.7 B**; chapter 4).
4. Assessment of the effect of LCT co-administration on plasma pharmacokinetics and biodistribution of orally administered cannabinoids (**Figure 1.7 C**; chapter 5).
5. Assessment of the immunomodulatory effects of cannabinoids on PBMC of healthy donors, autoimmune disease patients (MS patients), and immunocompromised individuals (cancer patients on chemotherapy), as well as on murine lymphocytes using concentrations similar to those achieved in the intestinal lymphatic system (**Figure 1.7 D**; chapter 6).

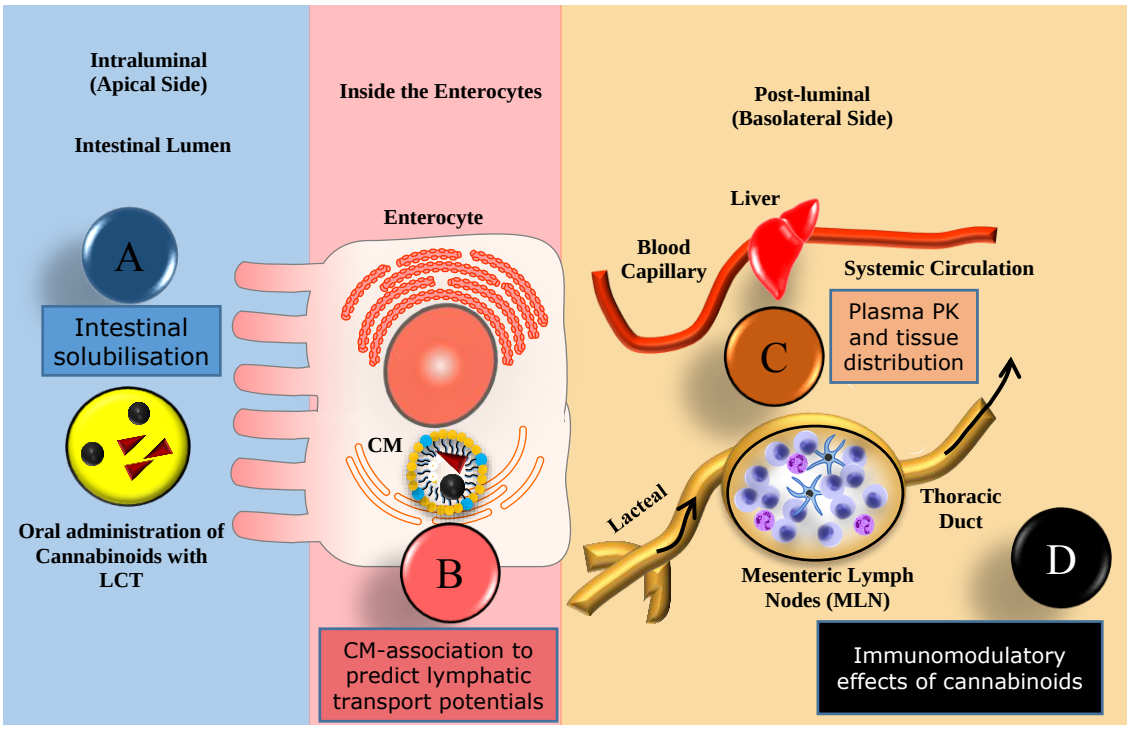

Figure 1.7. Schematic diagram represents the objectives of assessing the implications of intestinal lymphatic transport of orally administered cannabinoids. LCT, long-chain triglycerides; CM, chylomicrons; PK, pharmacokinetics.

2. MATERIALS AND METHODS

2.1. Materials

Cannabidiol (CBD; CAS: 13956-29-1) and Δ^9-tetrahydrocannabinol (THC; CAS: 1972-08-3) were donated by GW Pharmaceuticals (Cambridge, UK). 4,4-Dichlorodiphenyltrichloroethane (DDT, CAS: 50-29-3), probucol (CAS: 23288-49-5), Trizma® maleate, porcine pancreatin powder (8 × USP specifications), L-α-phosphatidylcholine, sodium hydroxide, potassium bromide (KBr), tetrahydrofuran, Intralipid®, RMPI-1640 culture medium with L-glutamine, Histopaque®-1077, fetal bovine serum (FBS), penicillin-streptomycin (Pen-Strep), Dulbecco's phosphate buffered saline (D-PBS), phytohaemagglutinin (PHA), phorbol myristate (PMA), ionomycin calcium (I), and brefeldin A were purchased from Sigma Aldrich (Dorset, UK). Sesame oil, peanut oil, sodium taurocholate hydrate, sodium chloride, acetonitrile, n-hexane, and water were purchased from Fisher Scientific (Leicestershire, UK). Vitamin D_3 (CAS: 67-97-0) and calcium chloride were purchased from Alfa Aesar (Lancashire, UK). BD Pharm Lyse™ was purchased from BD Biosciences (Oxford, UK). APC anti-rat CD3, PE anti-mouse / rat TNF-α, FITC anti-rat IFN-γ, BV421 anti-human TNF-α and PerCP/Cy5.5 anti-human IL-2 antibodies were bought from Biolegend UK Ltd (London, UK). ECD anti-human CD3, PE-Cy7 anti-human CD8, FITC anti-human IFN-γ antibodies were obtained from Beckman Coulter (London, UK). PE anti-human IL-17A and APC anti-human GM-CSF antibodies were obtained from eBioscience (Ireland, UK). All other reagents were of analytical grade or higher and used without further purification.

2.2. Bio-analytical assay for the determination of cannabidiol (CBD) in lipolysis fractions

2.2.1. Method description

2.2.1.1. Preparation of standard solutions and quality control (QC) samples

CBD and probucol (used as internal standard; IS) were accurately weighed and dissolved in acetonitrile to prepare stock solutions of 64 and 0.5 mg/mL concentrations, respectively. CBD stocks were then diluted to a series of working standard solutions for the preparation of calibration curve points. In addition, separately weighed CBD was used to prepare the low quality control (LQC), medium quality control (MQC), and high quality control (HQC) samples (**Table 2.1**).

2.2.1.2. Sample preparation

Lipolysis samples (from lipid, micellar, and sediment fractions) were prepared for high performance liquid chromatography coupled with ultraviolet detector (HPLC-UV) analysis by liquid-liquid extraction method. This method was a modification of previously reported method for the detection of synthetic lipophilic cannabinoids in rat plasma [165]. Briefly, thirty microliters of the IS probucol (0.5 mg/mL for the lipid fraction and 50 µg/mL for the micellar and sediment fraction samples) were added to 200 µL of sample in a 16 × 150 mm glass tube. Tetrahydrofuran (600 µL), or de-ionized water to the sediment fraction samples, was added and vortex-mixed for 2 min. n-Hexane (3 mL) was added to each tube and mixed for 5 min. The tubes were centrifuged (2800 *g*, 7 min, at 10°C) and the upper organic layer was then carefully decanted by 1 mL clear pipette tip to a clean glass tube. The organic layer was evaporated to

dryness under a stream of nitrogen gas at 35°C (Techne DRI-Block evaporation device, type DB-3D, Cambridge, UK) and finally reconstituted with acetonitrile (1.5 mL for the lipid and 200 µL for the micellar and sediment fractions) for analysis. Ten microliters of the sample were injected into the HPLC system.

2.2.1.3. Chromatographic conditions

The chromatographic system was Waters Alliance 2695 Separation Module coupled with Waters 996 photodiode array detector. Samples and column temperatures were controlled by the fitted chiller and heater at 4 and 43°C, respectively. Separation was achieved using ACE Excel Super C18 100 × 4.6 mm, 5 µm particle size column (Hichrom Ltd., Reading, UK), which was protected by ACE Super C18 5 µm guard cartridge. Isocratic type of elution was used where the mobile phase composed of acetonitrile and water (92:08, v/v). Flow rate was set at 0.6 mL/min for 18 min. Absorbance was monitored at 210 nm as both CBD and the IS probucol have apparent absorbance at this wavelength (**Figure 2.1**). Data processing was carried out using Empower™ 2 software.

Table 2.1. Quality control concentrations used for the validation of HPLC-UV method for the determination of cannabidiol (CBD) in lipid, micellar, and sediment lipolysis fractions.

Lipolysis fraction	Level	Concentration of CBD (µg/mL)
Lipid	LQC	40
	MQC	800
	HQC	6400
Micellar	LQC	2
	MQC	20
	HQC	100
Sediment	LQC	1
	MQC	40
	HQC	200

LQC, MQC, and HQC; lower, medium, and high quality controls, respectively.

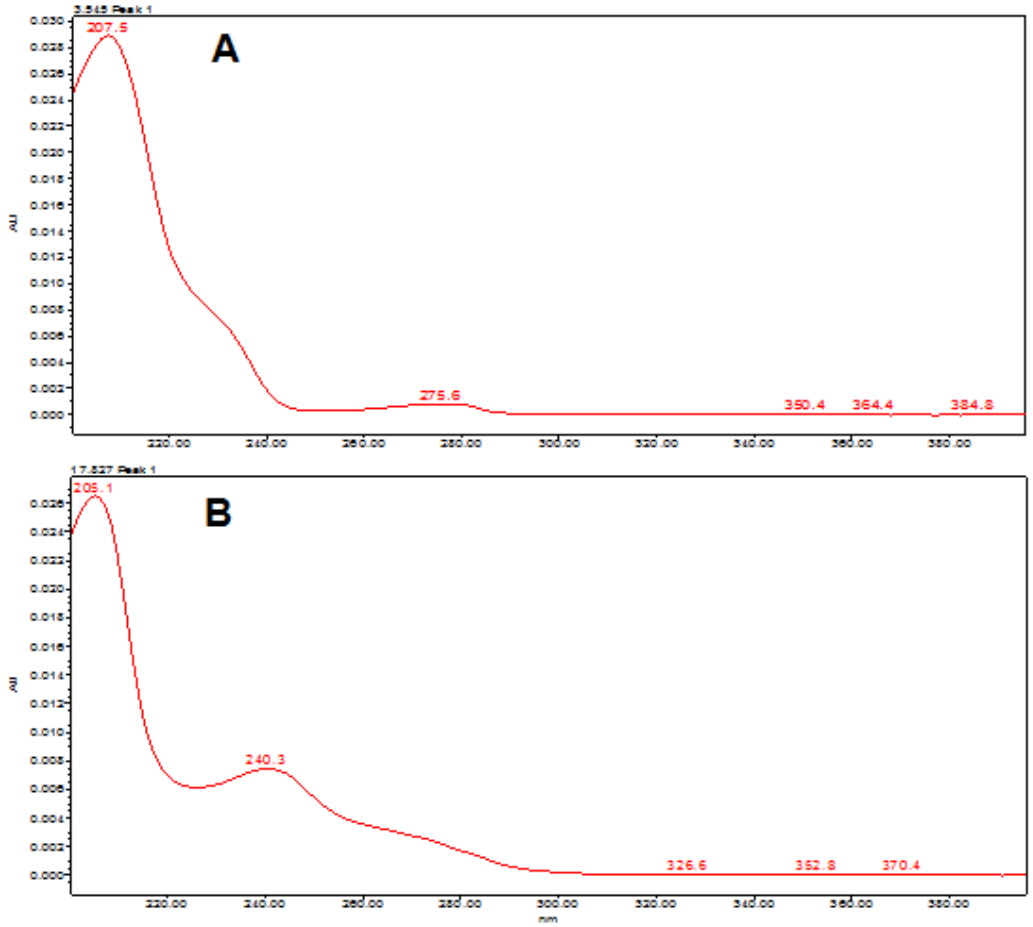

Figure 2.1. Ultraviolet (UV)-spectra of cannabidiol (CBD, **Panel A**) and the internal standard probucol (**Panel B**).

2.2.2. Method validation

The validation of the current method was performed in accordance with the FDA Guidance for Bioanalytical Method Validation in term of selectivity, linearity, precision, and accuracy [185].

2.2.2.1. Selectivity

The selectivity of the developed method was investigated by comparing chromatography of extracted lipid, micellar, and sediment blank samples with samples spiked with CBD at the lower limit of quantification (LLOQ) (n = 6, for each fraction).

2.2.2.2. Sensitivity and linearity

The LLOQ for the current method was defined as the lowest concentration of the injected samples that has acceptable relative standard deviation (RSD; **Equation 2.1**) and relative error (RE; **Equation 2.2**) values according to FDA guidelines i.e. RSD ≤ 20% and RE within ± 20% for intra-day analyses [185, 186]. The linearity was evaluated over the concentration range of calibration curves. Graphical plots of peak area ratio (peak area of CBD/ peak area of IS) against CBD concentration of the calibration standards were constructed. Linear regression parameters were used to evaluate linearity [187].

$$\text{Relative standard deviation (RSD)} = \frac{\text{SD}}{\mu} \times 100\% \quad (2.1)$$

Where SD is the standard deviation and μ is the mean of values.

$$\text{Relative error (RE)} = \frac{\text{calculated concentration} - \text{nominated concentration}}{\text{nominated concentration}} \times 100\% \quad (2.2)$$

2.2.2.3. Intra- and inter-day precision and accuracy

RSD and RD values were used to assess intra-and inter-day precision and accuracy, respectively. Six replicates of each QC sample (**Table 2.1**) were injected within one day to evaluate intra-day precision and accuracy. While inter-day precision and accuracy were determined by injecting the QC samples at four separate days. The method was considered precise and accurate when RSD ≤ 15% and RE within ± 15% for both intra- and inter-day runs of QC samples [185].

2.3. Bio-analytical assay for the determination of CBD in lipid-particles, rat chylomicrons (CM), and human CM emulsions

2.3.1. Method description

2.3.1.1. Preparation of standard solutions and QC samples

CBD and DDT (used as IS) were accurately weighed and dissolved in acetonitrile to prepare stock solutions of 1 and 0.5 mg/mL concentrations, respectively. CBD stocks were then diluted to prepare working standard solutions of 1, 2, 5, 10, 25, 50, and 100 µg/mL concentrations for the preparation of calibration curve points: 50, 100, 200, 500, 1000, 2500, 5000, and 10000 ng/mL. In addition, separately weighed CBD was used to prepare LLOQ, LQC, MQC, and HQC samples at concentrations of 100, 200, 1000, and 10000 ng/mL, respectively.

2.3.1.2. Sample preparation

Artificial lipid-particles, rat chylomicrons (CM), and human CM association samples were prepared for HPLC-UV analysis by liquid-liquid extraction method. Briefly, DDT (IS, 20 µL of 50 µg/mL solution) was added to 200 µL of sample in a 16 × 150 mm glass tube. A volume of 600 µL of tetrahydrofuran was then added and vortex-mixed for 2 min. n-Hexane (3 mL) was added to each tube and mixed for 5 min. The tubes are centrifuged (2800 *g*, 10 min, at room temperature) and the upper organic layer was then carefully decanted by 1 mL clear pipette tip to a clean glass tube. The organic layer was evaporated to dryness under a stream of nitrogen gas at 35°C (Techne DRI-Block evaporation device, type DB-3D, Cambridge, UK), reconstituted in 200 µL of acetonitrile, and 10 µL was injected into the HPLC system.

2.3.1.3. Chromatographic conditions

The chromatography system was Waters Alliance 2695 Separation Module coupled with Waters 996 photodiode array detector. Separation was achieved using ACE Excel Super C18 100 × 4.6 mm, 5 µm particle size column (Hichrom Ltd., Reading, UK), protected by ACE Super C18, 5 µm guard cartridge. Isocratic elution was used where the mobile phase composed of acetonitrile and water (75:25, v/v). Flow rate was set at 0.8 mL/min for 15 min. Column and samples temperatures were controlled at 43 and 5°C, respectively. Absorbance was monitored at 210 nm and data processing was carried out using Empower™ 2 software.

2.3.2. Method validation

The validation of this method was performed as described in section 2.2.2.

2.4. HPLC-UV method for the determination of CBD in rat plasma

2.4.1. Method description

2.4.1.1. Preparation of standard solutions and QC samples

Stock standard solutions of CBD and DDT (used as IS) were prepared in acetonitrile at concentrations of 1.92 and 0.5 mg/mL, respectively, and stored at –20°C. Working standard solutions of 200 and 50 µg/mL, respectively, were prepared by dilution of stocks in acetonitrile and were also stored at –20°C. The working solutions of CBD were diluted in acetonitrile immediately before preparation of calibration curves to concentrations of 0.15, 0.2, 0.3, 0.4, 1, 2, 4, 10, 20, 100 and 200 µg/mL. Plasma calibration curves were prepared at concentrations of 7.5, 10, 15, 20, 50, 100, 200, 500, 1000, 5000, and 10000 ng/mL. Independently prepared CBD stock solutions of 0.2, 0.4, 2 and 20 µg/mL

were used for the preparation of LLOQ (10 ng/mL), LQC (20 ng/mL), MQC (100 ng/mL), and HQC (1000 ng/mL) samples, respectively. These samples were then processed as described below.

2.4.1.2. Sample preparation

Samples were prepared for HPLC-UV analysis by a combination of protein precipitation and liquid-liquid extraction steps. Fifteen microliters of the IS (50 µg/mL, DDT) was added to 150 µL of rat plasma sample in a 16 × 150 mm glass tube. Plasma proteins were precipitated by the addition of 600 µL of cold acetonitrile (stored at –20°C for 5 min), and the sample was then vortex-mixed for 1 min. Water (600 µL) was added and the sample was vortex-mixed again for 1 min. n-Hexane (3 mL) was added to each tube and vortex-mixed for 5 min. The tubes were centrifuged (1160 *g*, 15 min, at 10°C) and the upper organic layer was then carefully decanted by glass pipette to a new glass tube. The organic layer was evaporated to dryness under a stream of nitrogen gas at 35°C (Techne DRI-Block type DB-3D, Cambridge, UK), reconstituted in 150 µL of acetonitrile, and 30 µL was injected into the HPLC system.

2.4.1.3. Chromatographic conditions

A Waters Alliance 2695 separations module equipped with Waters 996 photodiode array detector was used for the analysis. Samples and column temperatures were controlled by the fitted chiller and heater at 4 and 55°C, respectively. Separation was achieved using an ACE C18-PFP 150 × 4.6 mm, 3 µm particle size column (Hichrom Ltd., Reading, UK), protected by an ACE C18-PFP 3 µm guard cartridge. The mobile phase was a mixture of acetonitrile and water in a ratio of 62:38 (v/v). The flow rate was set at 1 mL/min for 20 min. The absorbance of all compounds of interest (CBD and DDT) was monitored at 220 nm. Data processing was carried out using Empower™ 2 software.

This method was also used for the determination of CBD and THC in intestinal lymph fluid as well as the determination of THC in rat plasma and brain tissue homogenates.

2.4.2. Method validation

In addition to the validation parameters described in section 2.2.2, recovery and stability were also assessed for this method in accordance with the FDA Guidance for Bioanalytical Method Validation [185].

2.4.2.1. Recovery

To assess the extraction efficiency of the assay, the recovery of CBD was determined by comparing the peak areas from extracted samples at three concentrations (LQC, MQC, and HQC) with non-extracted acetonitrile solutions of equivalent concentrations (n = 5 for each level) [185]. The recovery of the IS was determined in the same way (at one concentration level).

2.4.2.2. Stability

Storage stability of CBD in rat plasma was evaluated under different conditions: freeze-thaw stability (3 cycles from –80°C to room temperature), room temperature stability (6 h at room temperature), short-term stability (24 h at –80°C), and long term stabilities (30 and 60 days at –80°C) were performed at LQC, MQC, and HQC (n = 6 for each level). In addition, autosampler stability of the processed samples (16 h at 4°C) was performed at LQC, MQC and HQC (n = 6 for each level). Samples were considered stable if precision and accuracy values were within the acceptable limits (RSD ≤ 15% and RE within ± 15%, respectively).

2.5. Bio-analytical assay for the determination of CBD in mesenteric lymph nodes, spleen, and brain tissues of rat

2.5.1. Preparation of tissue homogenate

Mesenteric lymph nodes (MLN), spleen, and brain tissues were collected from naïve male Sprague Dawley (SD) rats (Charles River Laboratories, UK) weighing 300 – 349 g (n = 6). The protocol for this study was approved by The University of Nottingham Ethical Review Committee in accordance with the Animals [Scientific Procedures] Act 1986 under the project licence (PPL) number 40/3698. The procedure of tissue collection was performed as described later in this chapter, sections 2.8.4.1 and 2.8.4.3. Tissues were accurately weighed and homogenized with saline (1:3 w/v) in ice bath at 18000 rpm for 3 min (POLYTRON® PT 10-35 GT, Kinematica AG, Luzern, Switzerland). Homogenates were then processed as described below for sample preparation, section 2.5.2.2.

2.5.2. Method description

2.5.2.1. Preparation of standard solutions and QC samples

CBD and DDT (used as IS) were accurately weighed and dissolved in acetonitrile to prepare stock solutions of 1 and 0.5 mg/mL concentrations, respectively. CBD stocks were then diluted to prepare working standard solutions of 0.2, 0.5, 1, 2, 5, and 10 µg/mL concentrations. Calibration curve points were prepared at concentrations of 20, 50, 100, 200, 500, and 1000 ng/mL. In addition, separately weighed CBD was used to prepare LLOQ, LQC, MQC, and HQC samples at concentrations of 50, 100, 200, and 1000 ng/mL, respectively.

2.5.2.2. Sample preparation

Samples were prepared for HPLC-UV analysis by a combination of protein precipitation and liquid-liquid extraction steps as described above in section 2.4.1.2 for the preparation of plasma samples with minor modifications. Briefly, ten microliters of the IS (50 µg/mL, DDT) were added to 100 µL of tissue homogenate sample in a 16 × 150 mm glass tube. A volume of 450 µL of cold acetonitrile was added to precipitate proteins, and the sample was then vortex-mixed for 1 min. Water (450 µL) was added and the sample was vortex-mixed again for 1 min. n-Hexane (3 mL) was added to each tube and vortex-mixed for 10 min. The tubes were centrifuged (1160 *g*, 10 min, at room temperature) and the upper organic layer was then carefully decanted by a clear 1 mL pipette tip to a clean glass tube. The organic layer was evaporated to dryness under a stream of nitrogen gas at 35°C (Techne DRI-Block type DB-3D, Cambridge, UK), reconstituted in 100 µL of acetonitrile, and 30 µL was injected into the HPLC system.

2.5.2.3. Chromatographic conditions

The chromatographic conditions used for the separation of CBD in MLN, spleen, and brain tissue homogenates were similar to those described in section 2.4.1.3 for the determination of CBD in artificial lipid-particles emulsion. Exception is that the absorbance of the compounds of interest, CBD and DDT, was monitored at 230 nm.

2.5.3. Method validation

The validation of this method was performed as described in section 2.2.2.

2.6. Determination of THC in MLN and spleen tissues of rat

MLN and spleen tissues were homogenised as described above in section 2.5.1 and prepared for analysis as described in section 2.5.2.2 (vitamin D_3 was used as IS instead of DDT). Concentrations of THC in MLN and spleen homogenates were determined by liquid chromatography tandem-mass spectrometry (LC-MS/MS) system consisted of Quattro Ultima triple-quadrupole mass spectrometer (Waters) coupled with Agilent HPLC system (1100 Series, Agilent Technologies) as previously described for the determination of THC in microsomal samples [188]. Briefly, separation was achieved using Waters XBridge C18 75 × 2.1 mm, 2.5 µm particle size column (Waters Corp., MA, USA), protected by Waters XBridge 2.5 µm guard cartridge. The mobile phase was a mixture of acetonitrile and water in a ratio of 90:10 (v/v) containing 0.1% formic acid (v/v). The flow rate was set at 0.3 mL/min at 60°C for 8 min. The mass spectrometric system was operated in the positive ionisation mode to trace ions as follows (*m/z* precursor ion/ product ion): THC (315.2/ 193.0) and Vitamin D_3 (385.3/ 259.3). Nitrogen was used for nebulization and as a dissolution gas at follow rates of 650 L/h and 150 L/h, respectively. Source temperature and desolvation temperature were set at 125 and 350°C, respectively. The capillary and cone voltages were 3.6 kV and 35 V, respectively. Data acquisitions and processing was performed using Masslynx software packages (version 4.1, Waters Corp., MA, USA).

2.7. Techniques for the assessment of intraluminal processing and intestinal lymphatic transport of orally administered CBD

2.7.1. Assessment of intraluminal processing

2.7.1.1. Preparation of simulated digestion buffers

Intestinal digestion buffer simulating the content of jejunum was prepared as previously described by Benito-Gallo *et al* [189]. Briefly, Trizma® maleate, sodium chloride, and calicium chloride were mixed with water to achieve final concentrations of 50, 150, and 5 mM, respectively. In addition, sodium taurocholate and L-α-phosphatidylcholine (act as bile salt and phospholipid, respectively) were added to the buffer at concentrations of 5 and 1.25 mM, respectively, to mimic fasting gastrointestinal state. The pH of the buffer was then adjusted to 6.8 using 1 M sodium hydroxide solution. The complete buffer was kept protected from light at 4°C until time of use.

2.7.1.2. Preparation of pancreatin extract solution

Fresh pancreatin extract solution was prepared before each experiment as previously described [189]. Briefly, one gram of porcine pancreatin powder (containing pancreatic lipase and co-lipase) was added to 5 mL of the incomplete buffer (digestion buffer without bile salt and phospholipid). The mixture was vortex-mixed for 15 min and centrifuged at 1200 *g* and 4°C for 15 min. The supernatant was then collected and kept in ice until use.

2.7.1.3. Preparation of lipid-based formulations of CBD

The lipid-based formulations of CBD were freshly prepared before each experiment. CBD was accurately weighed and dissolved in an appropriate volume of sesame oil to prepare 2.5, 5, 10, 20, 40, 80 and 160 mg/mL solutions.

2.7.1.4. *In vitro* lipolysis

The *in vitro* lipolysis experiments used in this study were based on previously used and validated conditions (**Table 2.2**) [189]. The reaction vessel contained 35.5 mL of the digestion buffer. A volume of 160 µL of freshly prepared lipid-based formulation of CBD was dispersed in the reaction vessel and mixed for 15 min. Lipolysis was then initiated by the addition of 3.5 mL of pancreatin extract. Sodium hydroxide solution (1 M) was used as a titrant to maintain the pH of the reaction medium at 6.8 (Electrode, DG111-SC pH). Titration was set to stop when the pH of the medium equilibrates at the control band (pH 6.8 ± 0.05) for at least 1 min. The electrode was controlled by a computer software (LabX light v3.1, Mettler Toledo Inc.) (**Figure 2.2**).

Table 2.2. Setting parameters of the pH−stat titrator unit (T50 Graphix, Mettler Toledo Inc., Leicester, UK) used for *in vitro* lipolysis experiments [189].

Parameter	Setting
Tendency	Positive
Maximum dosing rate	1 mL/min
Minimum dosing rate	3 µL/min
Maximum volume	30 mL
Minimum volume	0.003 mL/min
Stir speed	35%
Set potential	6.8 pH
Control band	0.05 pH

After completion of the lipolysis process, the resulting reaction medium was ultracentrifuged at 268350 *g* (SORVALL® TH-641 Rotor, Thermo Fisher Scientific, UK) for 90 min at 37°C. Upper lipid, middle micellar, and lower sediment fractions were separated after centrifugation and stored at –80°C until analysis.

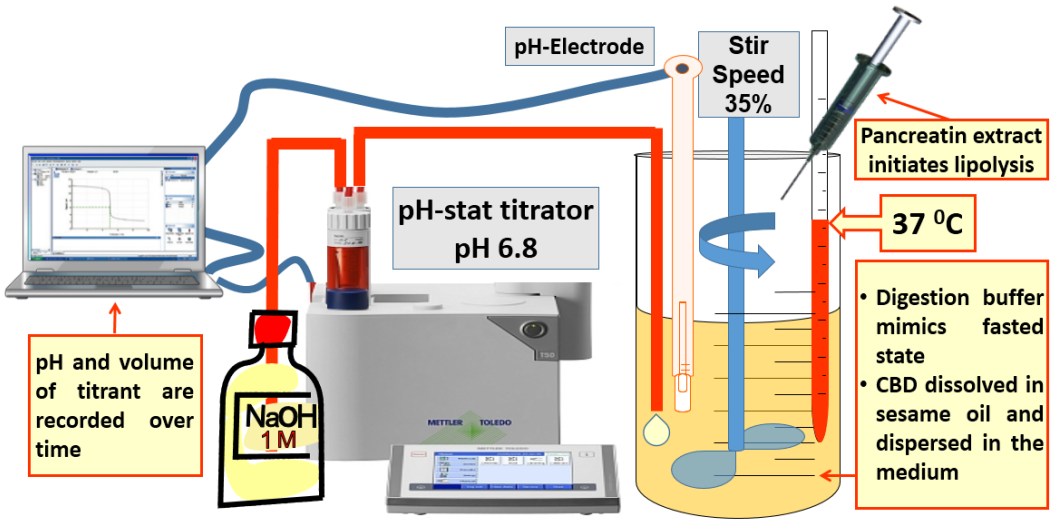

Figure 2.2. Schematic representation of the *in vitro* lipolysis model.

2.7.2. Assessment of CBD association with CM

2.7.2.1. *In silico* prediction of CBD association with CM

Previously developed multiple regression *in silico* model was applied to predict the affinity of CBD to CM in the enterocyte [190]. This model depends on a combination of physicochemical properties of the tested compound, which (in the order of importance) are: Log $D_{7.4}$, the degree of ionization (Log *P* – Log $D_{7.4}$), polar surface area (PSA), number of hydrogen bond acceptors (HBA), freely rotatable bonds (FRB), density, molar volume, and number of hydrogen bond donors (HBD). These properties were predicted by ACD/I-Lab software (online interface, http://ilab.cds.rsc.org/). The values for the physicochemical properties were then adjusted with their unscaled regression coefficients (**Table 2.3**) to yield LOGIT values. Subsequently, the degree of association of CBD with CM was mathematically calculated from LOGIT values using **Equations 2.3-2.5**.

Table 2.3. Physicochemical properties and their unscaled regression coefficients used in the *in silico* prediction for the association with chylomicrons (CM) [190].

Physicochemical property	Unscaled regression coefficient
Log $D_{7.4}$	0.299879
Log *P* - Log $D_{7.4}$	-0.238127
PSA	-0.00855215
HBA	-0.184359
FRB	0.0805226
Density	1.45337
Molar Volume	0.00545912
HBD	0.0823094
Constant	-5.24138

PSA, polar surface area; HBA, number of hydrogen bond acceptors; FRB, freely rotatable bonds; HBD, number of hydrogen bond donors.

$$\text{Toatal LOGIT values} = \sum(\text{physicochemical propertie} \times \text{unscaled regression coefficient}) \quad (2.3)$$

$$\text{Degree of association (X)} = \text{total LOGIT values} + \text{model constant} \quad (2.4)$$

$$\%\ \text{Association with CM} = \frac{10^x}{1+10^x} \quad (2.5)$$

2.7.2.2. Association of CBD with artificial CM-like lipid particles and natural rat and human CM

2.7.2.2.1.Preparation of artificial lipid particle emulsion

Intralipid® 20% was used as a source of lipid particles as previously described [190]. Intralipid® is an emulsion of lipid particles, which are composed of lecithin, soybean triglycerides and glycerin. Although natural CM have more complex structure, the uptake of lipophilic compounds by artificial emulsions has been shown to provide a reasonably close estimate for the degree of association with CM before proceeding with experiments that require materials from animals or humans [190, 191].

Intralipid® was diluted with phosphate-buffered saline with a density of 1.006 g/mL and pH of 7.4 to achieve triglyceride (TG) concentration of 100 mg/dL. A TG enzymatic kit was used to assess TG concentration according to the manufacturer's protocol (Sigma Aldrich, Dorset, UK) using a BIO-TEK FL600™ plate reader (BIO-TEK INSTRUMENTS, INC. Vermont, USA). The lipid particle emulsion was then used to assess the uptake of CBD as described below in section 2.7.2.2.4.

2.7.2.2.2.Preparation of rat plasma-derived CM emulsion

The protocol for this study was approved by the Home Office in accordance with the Animals [Scientific Procedures] Act 1986 under the project licence (PPL) number 40/3698. Two male SD rats (Charles River Laboratories, UK) weighing 275 – 300 g were used in this experiment. The rats were housed in the University of Nottingham Bio Support Unit, and kept in a temperature controlled, 12 hours light-dark cycle environment with free access to water and food.

CM separation from rat blood was performed as previously described [166]. Briefly, animals were fasted overnight with free access to water. Next morning, animals were administered 0.5 mL peanut oil by oral gavage. Two more doses of peanut oil (0.3 mL each) were administered 1 and 2 hours after the first administration. One hour after the last dose, animals were anaesthetised with 2% isoflurane and a total blood volume of 10-12 mL was collected from the posterior vena cava of each animal. Plasma was separated from blood by centrifugation (800 *g*, 5 min, at 15°C). KBr (0.57 g) was then added to 4 mL of plasma aliquots to adjust the density to 1.1 g/mL. Standard solutions of phosphate buffer saline with densities of 1.006, 1.019, and 1.063 g/mL were prepared and layered on top of plasma aliquots to build a density gradient in polyallomer ultracentrifuge tubes. Samples were ultracentrifuged at

268350 *g* (SORVALL® TH-641 Rotor, Thermo Fisher Scientific, UK) for 35 min at 15°C. Following ultracentrifugation, the top 1 mL layer containing CM was collected using a glass pipette. TG concentration of the CM emulsion was determined using a TG enzymatic kit (Sigma Aldrich, Dorset, UK) and BIO-TEK FL600™ plate reader (BIO-TEK INSTRUMENTS, INC. Vermont, USA). TG concentration was adjusted to 100 mg/dL by dilution with standard solution of 1.006 g/mL density. CM emulsion was kept at 4°C waiting the uptake experiments (< 24 hours).

2.7.2.2.3.Preparation of human plasma-derived CM emulsion

The protocol for this experiment was approved by the Faculty of Medicine and Health Sciences Research Ethics Committee, Queens Medical Centre, Nottingham University Hospitals, Nottingham, UK (BT12102015 CBS SoP). An exclusion criterion was the use of any medication within one week prior to the study. Three male healthy human volunteers (25-35 years old) were recruited for this study. After 12 hours overnight fasting, participants had a high-fat breakfast. Three to four hours following the meal (expected time of peak plasma-CM level [192, 193]) blood samples (30 mL) were collected in heparinised tubes (Vacutainer® Blood Collection Tubes). Plasma was separated from blood by centrifugation (800 *g*, 10 min, at 15°C). CM separation was performed as described above for rat CM. The CM emulsion was kept at 4°C pending uptake experiments (< 24 hours).

2.7.2.2.4.Uptake experiment

The uptake of CBD by artificial lipid particles emulsion, rat CM emulsion, and human CM emulsion was performed as previously described [166]. Briefly, stock solutions of CBD (110.39 µg/mL) were freshly prepared in propylene glycol–ethanol (99:1, v/v) before each experiment. A volume of 10 µL of CBD

stock solution was added to 2 mL of the emulsion (100 mg/dL TG content) to achieve a molar concentration of 1.75×10^{-6} M. The emulsion, spiked with CBD, was then incubated at 37°C for 1 hour with continuous mixing. Following incubation, the density of the emulsion was adjusted to 1.1 g/mL using KBr. Artificial lipid particles or natural CM were then separated by density gradient ultracentrifugation (SORVALL® TH-641 Rotor, Thermo Fisher Scientific, 268350 *g*, 35 min, 15°C). The top 1 mL layer was collected following ultracentrifugation using a glass pipette and kept at –80°C for analysis. CBD content of this layer represents the fraction of the spiked dose associated with lipid artificial particles, rat CM, or human CM (**Figure 2.3**).

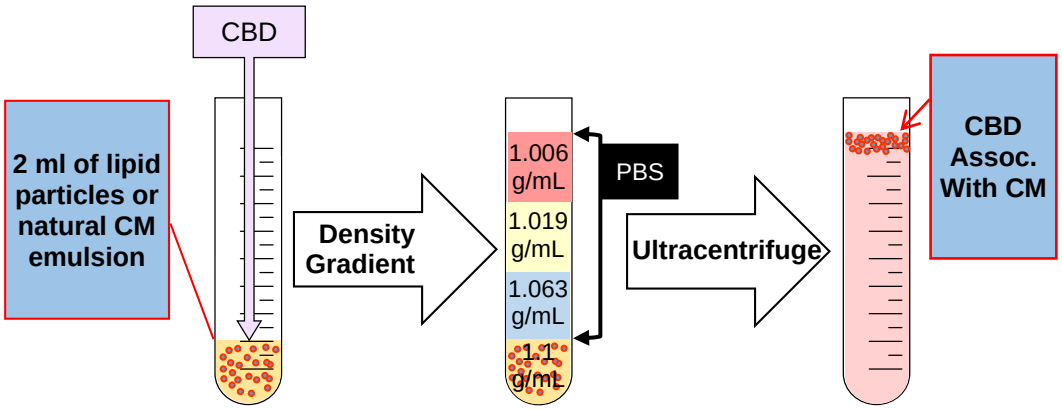

Figure 2.3. Experimental design for the uptake of cannabidiol (CBD) by artificial lipid particles, natural chylomicrons (CM) from rats, and natural CM from humans.

2.8. Techniques for the assessment of plasma pharmacokinetics and biodistribution of CBD and THC in rats

2.8.1. Animals and ethical approval

All experiments and procedures were approved by the UK Home Office in accordance with the Animals [Scientific Procedures] Act 1986 under the project

licence (PPL) number 40/3698. Experiments were performed using male SD rats (Charles River Laboratories) weighing 300 – 349 g. The rats were housed in the University of Nottingham Bio Support Unit, and kept in a temperature-controlled, 12 hours light-dark cycle environment with free access to water and food.

2.8.2. Cannulation of jugular vein

2.8.2.1. Preparation of intravenous catheters

Two-part catheter consisting of polyethylene tubing (PE-50) connected to silastic tubing was used for the cannulation of the right jugular vein. For the preparation of catheters, Tygon tubing (~ 2 mm length) was slide 25 mm to each end of a 180 mm length PE-50 tubing. Silastic tubing (~ 10 mm length) was cut into a V shape at one end and then fitted to one end of the PE-50 segment. Finally, blunt needle (23 G) was attached to the other end of the PE-50 segment (**Figure 2.4**). Catheters were washed with double distilled water and sterilized by ethylene oxide gas to be used in surgery.

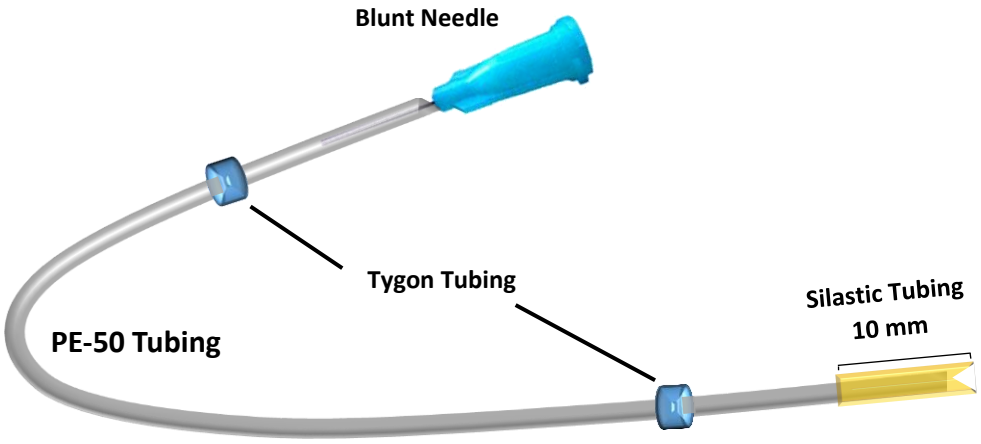

Figure 2.4. Schematic representation for the catheter used in the cannulation of the right jugular vein of rats.

2.8.2.2. Preparation of the animals for surgery and anaesthetic protocol

Rats were acclimatized in the University of Nottingham Bio Support Unit for at least 4 days before surgery. On the day of surgery, anaesthesia was induced by IP injection of Ketamine and xylazine (90 mg/kg and 9 mg/kg, respectively). Once the rat was sedated (~ 5 min after injection), the fur in the dorsal neck and the area of right ventral neck toward the upper part of the thorax was shaved. Shaved areas were sterilised with alcohol 2% chlorhexidine skin wipes (Clinell®, GAMA Healthcare Ltd., London, UK). Protection ointment was applied to the eyes to prevent corneal dryness. Pedal withdrawal reflex was used as a guide to assess the depth of surgical anaesthesia, surgery could only proceed in the absence of pedal withdrawal reflex. The anaesthetised rat was wrapped with a transparent and self-adhesive drape (GLAD® Press'n Seal) and placed over a heating pad ready for the surgery.

2.8.2.3. Surgical procedure

The rat was laid on back with the head positioned toward the surgeon. The anatomical position of the right jugular vein was identified as the pulsatile position on the skin surface of the ventral neck. Over this position, blunt dissection was performed until the jugular vein could be clearly seen. About 1 cm of the jugular vein was then isolated from the surrounding tissue by method of blunt dissection. Small skin incision (~ 0.5 cm) was made on the dorsal neck. The cannula was then tunnelled subcutaneously from the dorsal neck incision toward the ventral neck with the silastic end close to the jugular vein. The vein was grasped by a forceps ~ 0.4 cm away from the end closer to the chest of the animal and small incision was made in the vein using iris scissors. The cannula inserted into the vein for 2.5 cm and promptly secured by a silk suture. Heparinised sterile saline (0.1 mL, 100 IU/mL) was injected and withdrawn to

check if the cannula is properly installed. The muscle layer above the vein and the skin in the ventral neck were sutured by 4-0 absorbable polyglactine suture (MEDSORB PLGA, MEDEKS®). The cannula was also secured from the dorsal neck side, and skin sutured by the 4-0 absorbable polyglactine suture. Finally, cannula was cut 3-4 cm away from the dorsal neck and plugged with a sterile metal pin. Animals were administered subcutaneous injection of meloxicam (1 mg/kg) and separately housed in single cages. Rats were allowed to recover for an average period of 36 hours before the conduction of pharmacokinetic experiments.

2.8.3. Plasma pharmacokinetic experiments

2.8.3.1. Intravenous administration of CBD

Preliminary pharmacokinetic experiment was performed to demonstrate the application of the bioanalytical method developed for the determination of CBD in rat plasma. In this experiment, two male SD rats (Charles River Laboratories, UK) weighing 330 – 350 g were used. Animals were administered an IV bolus of 5 mg/kg CBD (10 mg/mL solution in propylene glycol–ethanol–sterile water (80:10:10, v/v/v)). Blood samples of 0.35 mL were withdrawn from the cannula before dosing, and at 5, 15, 30, 120, and 420 min following IV administration. Plasma was separated by centrifugation (3000 *g*, 10 min, at 15°C) and stored at –80°C until analysis.

To explore the pharmacokinetic profile of CBD, four male SD rats (Charles River Laboratories, UK) weighing 300 – 349 g were administered an IV bolus of CBD at a dose of 4 mg/kg (8 mg/mL solution in propylene glycol–ethanol–sterile water (80:10:10, v/v/v)). Blood samples (0.25 mL) were then withdrawn from the cannula at 5, 15, 30, 60, 120, 240, 360, 480, and 720 min. Plasma was

separated by centrifugation (3000 *g*, 10 min, 15°C) and stored at –80°C until analysis.

Similar to the protocol described above for CBD, pharmacokinetic experiment of IV bolus administration of THC to 5 male SD rats was performed together with my colleague Jonathan Wong [194].

2.8.3.2. Oral administration of CBD and THC

CBD and THC were administered orally in lipid-free and lipid-based formulations. Male SD rats (Charles River Laboratories, UK) weighing 300 – 349 g were used in this experiment. CBD or THC were administered by oral gavage at a dose of 12 mg/kg in lipid-free formulation (12 mg/mL solution in propylene glycol–ethanol–sterile water (80:10:10, v/v/v)) to 4 and 6 rats, respectively, and oral gavage of CBD or THC in long-chain triglycerides (LCT)-based formulation at a dose of 12 mg/kg (12 mg/mL solution in sesame oil) were administered to 4 and 5 rats, respectively. Following the administration of CBD and THC doses, animals were administered water (1mL) by oral gave. Blood samples (0.25 mL) were then withdrawn from the cannula at 30, 60, 120, 180, 240, 300, 360, 480, and 720 min after oral administrations. Plasma was separated by centrifugation (3000 *g*, 10 min, at 15°C) and stored at –80°C until analysis.

2.8.3.3. Pharmacokinetic analysis

Phoenix WinNonlin 6.3 software (Pharsight, Mountain View, CA, USA) was used for pharmacokinetic analysis of the plasma concentration-time data using non-compartmental and compartmental approaches.

2.8.3.3.1.Non-compartmental approach

The pharmacokinetic variables estimated for the IV bolus plasma cocentration-time data are: the terminal half-life ($t_{1/2}$), the area under the

plasma concentration-time curve from 0 to time of last measurable concentration ($AUC_{0\text{-}t}$), AUC from time 0 to infinite time ($AUC_{0\text{-}\infty}$), apparent volume of distribution at steady state ($V_{d\ ss}$), and clearance (Cl). For oral data, in addition to $AUC_{0\text{-}t}$ and $AUC_{0\text{-}\infty}$, maximum concentration in plasma (C_{max}) and time to C_{max} (t_{max}) were directly determined from the plasma concentration-time data. The software was set to calculate AUC parameters using the linear up/log down method. The absolute oral bioavailability (F) for oral administrations was calculated by **Equation 2.6**.

$$\mathrm{F} = \frac{\mathrm{AUC}_{0-t}\mathrm{PO}}{\mathrm{AUC}_{0-t}\mathrm{IV}} \times \frac{\text{Dose IV}}{\text{Dose PO}} \times 100\% \qquad (2.6)$$

2.8.3.3.2.Compartmental approach

Different compartmental models were applied to explore the pharmacokinetic models that best describe the time course of the input and disposition (distribution and elimination) of CBD and THC following IV bolus and oral administrations. For IV bolus administration, three models were applied. These are one-, two-, and three-compartment models, all assume first-order kinetic elimination from the central compartment. For oral administration data, four models were applied. These are one-compartment, one-compartment with lag time for absorption, two-compartments, and two-compartments with lag time for absorption models. All models assume first-order kinetic input and elimination. Akaike Information Criterion (AIC), Bayesian information criterion (BIC), and plots of observed and predicted concentrations vs time were used to describe the model that best fit the data.

2.8.4. Biodistribution experiments

2.8.4.1. Localization, collection, and dissection of mesenteric lymph nodes (MLN)

Rats were euthanized at the pre-determined time points of t_{max} and one-hour prior to t_{max} (t_{max} – 1 h). These time points were obtained from oral bioavailability studies described in section 2.8.3.2. MLN were then collected as previously described [195]. Briefly, immediately following euthanization, animal carcass was laid on back and the ventral abdominal wall was incised to expose the intestine (**Figure 2.5 A**). MLN were identified as a chain of small yellowish nodules running alongside the colon (**Figure 2.5 B**). MLN were then gently removed from the mesenteric tissue in the abdominal cavity using small scissor and forceps. Pair of small round-end spatulas were used to separate the MLN from the surrounding connective tissue (MLN have more firm structure than the surrounding tissue). MLN were weighed and homogenized with normal saline (1:3 w/v) on ice at 18000 rpm for 3 min (POLYTRON® PT 10-35 GT, Kinematica AG, Luzern, Switzerland). Homogenates were then assessed for CBD and THC content as described in sections 2.5 and 2.6, respectively.

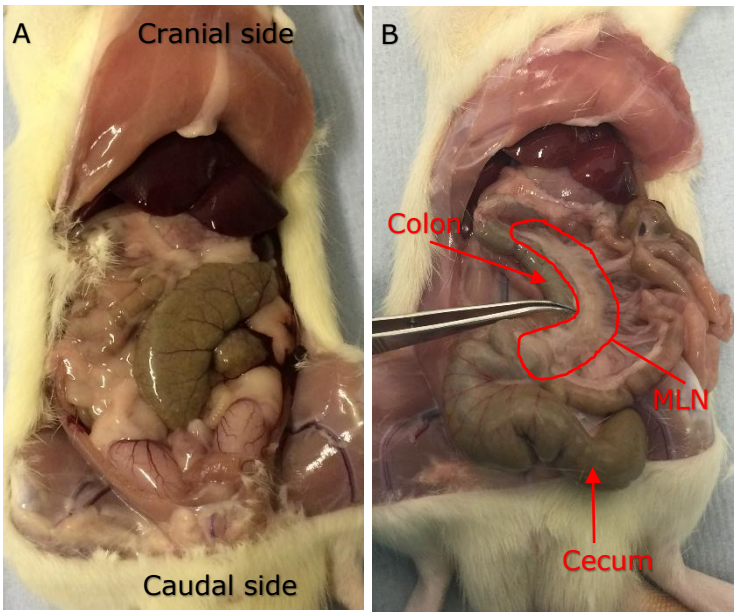

Figure 2.5. Anatomical localisation and collection of mesenteric lymph nodes (MLN) from rats. **Panel A**: incision of the ventral abdominal wall to expose the intestine. **Panel B**: identification and collection of MLN.

2.8.4.2. Localization of mesenteric lymph duct and collection of lymph

Rats were euthanized one-hour prior to the time of maximum concentration in plasma (t_{max} – 1 h). Immediately following euthanization, animal carcass was laid on back and a U shape incision was made in the ventral abdominal wall to expose the intestine (**Figure 2.5 A**). The mesenteric lymph duct was localized as described previously [196]. Briefly, the intestine was moved to the right side of the abdomen. This exposes the left kidney and the left renal vein. A ten-millilitre empty syringe was placed horizontally under the animal. The mesenteric lymph duct can be identified as a white duct running alongside the left renal vein. The duct was ligated using 3-0 silk suture. A 25 G needle connected to 1 mL syringe was used to collect lymph form the duct (~ 50 µL of lymph was collected form each animal). Blood (0.35 mL) was also sampled from the posterior vena cava.

2.8.4.3. Collection of spleen and brain tissues

The abdominal cavity was exposed as described above in section 2.8.4.1 (**Figure 2.5 A**). The spleen is located attached to and below the stomach. The spleen was collected using forceps. For the collection of the brain, the head of the rat was completely removed. The bottom blade of a small scissors was inserted into the opening where the skull opens into the spinal canal. The skull was cut through the midline. The brain was then exposed and gently removed to a collection tube [195].

2.9. Techniques for the assessment of the immunomodulatory effects of CBD and THC

2.9.1. Ethical approvals

2.9.1.1. Animals

All experiments and procedures were approved by the UK Home Office in accordance with the Animals [Scientific Procedures] Act 1986 under the project licence (PPL) number 40/3698. Experiments were performed using male SD rats (Charles River Laboratories) weighing 300 – 349 g. The rats were housed in the University of Nottingham Bio Support Unit, and kept in a temperature-controlled and 12 hours light-dark cycle environment with free access to water and food.

2.9.1.2. Human samples

The protocol for the preparation of human plasma-derived CM emulsion was approved by the Faculty of Medicine and Health Sciences Research Ethics Committee, Queens Medical Centre, Nottingham University Hospitals, Nottingham, UK (BT12102015 CBS SoP). Lymphocyte proliferation and flow cytometry experiments conducted on peripheral blood mononuclear cells (PBMC) isolated from healthy volunteers and multiple sclerosis (MS) patients

(**Table 2.4**) were approved by the Research Ethics Committee East Midlands – Nottingham 2, Nottingham, UK (08/H0408/167/AM05). Lymphocyte proliferation and flow cytometry experiments conducted on PBMC isolated from patients on chemotherapy to treat non-seminomatous germ cell tumours (NSGCT, **Table 2.5**) were approved by Nottingham Health Sciences Biobank at Nottingham University Hospitals, Nottingham, UK (ACP162). Informed written consent was obtained from all participants.

Table 2.4. List of multiple sclerosis (MS) patients whose blood samples were used for the assessment of immunomodulatory effects of cannabidiol (CBD) and Δ^9-tetrahydrocannabinol (THC). All patients were not on disease-modifying drugs or known to have cannabinoids.

Patient code	Age (Y)	Gender	Type of MS	EDSS	Experiment
CMS-01	35	F	RRMS	1.5	LPA
CMS-02	55	F	RRMS	2.5	LPA
CMS-03	33	F	RRMS	1.5	LPA
CMS-04	51	F	RRMS	3	LPA
CMS-05	30	M	RRMS	3	LPA
CMS-06	55	F	RRMS	4	LPA
CMS-07	26	F	RRMS	2.5	LPA
CMS-08	69	F	SPMS	6.5	AOIC
CMS-09	55	F	RRMS	2.5	AOIC
CMS-10	33	F	RRMS	2.5	AOIC
CMS-11	53	F	RRMS	4.5	AOIC
CMS-12	74	F	SPMS	5.5	AOIC
CMS-13	30	F	RRMS	2	AOIC

RRMS, relapsing-remitting MS; secondary-progressive MS; EDSS, Expanded Disability Status Scale; LPA, lymphocyte proliferation assay; AOIC, assessment of inflammatory cytokines.

Table 2.5. List of non-seminomatous germ cell tumour (NSGCT) patients whose blood samples were used for the assessment of the immunomodulatory effects of cannabidiol (CBD) and Δ^9-tetrahydrocannabinol (THC). Bloods were taken after a minimum of one cycle of chemotherapy at time of expected total white blood cell and neutrophil count recovery.

Patient code	Age (y)	WBC (10^9/l)	ANC (10^9/l)	Ly (10^9/l)
CTC-01	35	1.1	0.1	0.8
CTC-02	59	2.2	0.5	1.4
CTC-03	21	2	0.5	1.2
CTC-04	21	6.4	3.8	1.7
CTC-05	36	2.9	0.4	1.2
CTC-06	43	4.3	1.5	2.2
CTC-07	29	6.1	3.6	1.7
CTC-08	46	11	9.7	0.9
CTC-09	18	2.4	1.1	0.9
CTC-10	38	10.3	6.3	2.7

WBC, white blood cell count; ANC, absolute neutrophil count; Ly, lymphocyte.

2.9.2. Preparation of complete cell culture medium

The complete cell culture medium used in the experiments for the assessment of the immunomodulatory effects of CBD and THC was prepared by mixing RMPI-1640 culture medium containing L-glutamine with FBS and Pen-Strep to get final concentrations of 10 and 1% (v/v), respectively.

2.9.3. Preparation of single-cell suspension from MLN and spleen of rats

Following 5 days of acclimatisation, animals were euthanized. The ventral abdominal wall was wiped with 70% ethanol solution and incised to expose the intestine. MLN and spleen were aseptically collected. MLN placed in a sterile petri dish and gently dissected from surrounding tissue. The spleen was scored with a clean scalpel. MLN and spleen were then mashed on a cell strainer (70 µm Nylon, Corning Falcon™) with continuous addition of D-PBS. Red blood cells in the cell suspension of the splenocytes were lysed by lysing buffer (BD

Bioscience). Immune cells from MLN and splenocytes were then washed twice with D-PBS. Viability was assessed using trypan blue exclusion. Cell suspension was centrifuged (400 *g*, 5 min, at room temperature) and resuspended in complete RMPI-1640 culture medium at concentration of 1.2×10^6 to be used for proliferation and flow cytometry experiments.

2.9.4. Isolation of peripheral blood mononuclear cells (PBMC) from human blood

PBMC were obtained from heparinised venous blood of healthy adult volunteers, MS patients (**Table 2.4**), and NSGCT patients (**Table 2.5**) by density centrifugation (800 *g*, 30 min, at 20°C) using Histopaque®-1077. Cells were washed twice with D-PBS and centrifuged (400 *g*, 10 min, at room temperature). Cells then resuspended in complete RMPI-1640 culture medium at concentrations of 7.5×10^5 and 1×10^6 cells/mL for lymphocyte proliferation assay and flow cytometry experiments, respectively.

2.9.4.1. Freeze-thawing of PBMC

Cryopreserved PBMC were used for the flow cytometry experiments. For freezing, PBMC were suspended in a freezing solution (DMSO – FBS (10:90, v/v)) at concentrations of $1 \times 10^7 - 1.5 \times 10^7$ cells/mL at room temperature. Soon thereafter, cells were transferred to cryogenic vials (~ 1 mL aliquot/vial, Nalgene® Cryoware, Thermo Fisher Scientific, UK). The vials were placed in a pre-chilled (4°C) CoolCell® controlled-rate freezing container (Fisher Scientific, Leicestershire, UK). The container was placed into a –80°C freezer for 24-48 hours before being transferred to liquid nitrogen.

For cell thawing, the cryovials were placed in 37°C water bath for 30 seconds. A volume of 1 mL complete RMPI-1640 culture medium was pipetted dropwise on top of the cells. The content was then transferred dropwise to a

50-mL Falcon tube which contains 10 mL of pre-heated complete RMPI-1640 culture medium, while gently mixing the tube. The tube was centrifuged to pellet (400 *g*, 7 min, at room temperature). The supernatant was discarded and cell pellet was washed twice with 30 mL complete RMPI-1640 culture medium (400 *g*, 7 min, at room temperature). Cells were then re-suspended in 30 mL complete RMPI-1640 culture medium and incubated overnight in a humidified atmosphere of 5% CO_2 at 37°C. Next morning, viability was assessed using trypan blue exclusion and cells proceeded into flow cytometry experiments.

2.9.5. Preparation of human CM-associated CBD

Human plasma-derived CM emulsion was prepared from three male healthy human volunteers as described in section 2.7.2.2.3. The uptake of CBD by human CM emulsion was performed as previously described with small modifications [166]. Briefly, stock solution of CBD (12 mg/mL) was prepared in propylene glycol–ethanol (90:10, v/v). A volume of 25 µL of the solution was added to 2 mL of the CM emulsion and incubated at 37°C for 1 hour with continuous mixing. Following incubation, the density of the emulsion was adjusted to 1.1 g/mL using KBr. CM were then separated by density gradient ultracentrifugation (SORVALL® TH-641 Rotor, Thermo Fisher Scientific, 268350 *g*, 35 min, at 15°C). The top 1 mL layer was collected following ultracentrifugation using a glass pipette. The concentration of CBD in CM emulsion was assessed as described in section 2.3. CM-associated CBD was kept at 4°C pending proliferation assay experiments (< 24 hours).

2.9.6. Lymphocyte proliferation assay

Immune cells from rats (MLN and spleen cells) and PBMC from human participants were cultured in flat clear-bottom 96-well microplates (Thermo Scientific Nunc®) at concentrations of 8.4×10^4 and 5.2×10^4 cells/well,

respectively. Working stock solutions of CBD and THC in RMPI-1640 culture medium-DMSO (99:1, v/v) were prepared at concentrations of 10, 25, 50, 75, 100, 150, and 200 µg/mL. Working stock solutions of CM-associated CBD were also prepared at the same aforementioned concentrations. Cannabinoids were incubated with cells at final concentrations of 1, 2.5, 5, 7.5, 10, 15, and 20 µg/mL in a humidified atmosphere of 5% CO_2 at 37°C for 30 min, the final concentration of DMSO in cell suspensions was 0.1% (v/v). Cells were then stimulated by Phytohaemagglutinin (PHA, 10 µg/mL) and incubated in a humidified atmosphere of 5% CO_2 at 37°C for 2 days. Cell proliferation was assessed by enzyme-linked immunosorbent assay (ELISA) based on bromo-2'-deoxyuridine (BrdU) incorporation into newly synthesised DNA according to the manufacturer protocol (Roche Applied Science, Roche Diagnostics Ltd, UK). Finally, the absorbance of these wells was observed at 370 nm, with reference wavelength at 492 nm using plate reader (EnVision® Multilabel Plate Reader, PerkinElmer Inc., USA). Absorbance values were normalised to the absorbance of culture medium-treated cells.

2.9.7. Flow cytometry experiments

CBD and THC were accurately weighed and dissolved in DMSO to prepare stock solutions at concentrations of 1, 2.5, 5, 10, and 20 mg/mL. Working stock solutions were freshly prepared before each experiment by diluting the DMSO-dissolved cannabinoids with complete RMPI-1640 culture medium to final concentrations of 50, 125, 250, 500, and 1000 µg/mL. These stocks were used to spike 0.5 mL of freshly isolated immune cells of MLN and splenocytes from rats and thawed PBMC from human participants to get CBD or THC concentrations of 1, 2.5, 5, 10, and 20 µg/mL. Cells were incubated with cannabinoids in a humidified atmosphere of 5% CO_2 at 37°C for 30 min. Cells

were then stimulated with phorbol myristate acetate and ionomycin (PMA & I, 50 and 500 ng/mL, respectively) in the presence of brefeldin A (10 µg/mL) and incubated in a humidified atmosphere of 5% CO_2 at 37°C for 5 hours. After stimulation, cells were washed twice with D-PBS and centrifuged to pellet (290 *g*, 5 min, at 20°C). Cell pellet was resuspended and labelled with Zombie UV™ Fixable Viability kit. Cells were incubated in dark place at room temperature for 20 min. Fixation and permeabilization was performed using BD Cytofix/Cytoperm™ kit according to the manufacturer's protocol (BD Bioscience). Rat immune cells were labelled with APC anti-rat CD3, PE anti-mouse / rat TNF-α, and FITC anti-rat IFN-γ antibodies. Human PBMC were labelled with BV421 anti-human TNF-α, PerCP/Cy5.5 anti-human IL-2, ECD anti-human CD3, PE-Cy7 anti-human CD8, FITC anti-human IFN-γ, PE anti-human IL-17A, and APC anti-human GM-CSF antibodies. Cells were incubated in dark place at 4°C for 30 min. Next, cells were washed with 1 mL of Perm buffer (BD Bioscience) followed by a second wash with 1 mL of FACS buffer (2% of FBS in D-PBS). Finally, cell were resuspended in BD fixation buffer (BD Bioscience) and kept overnight at 4°C. Next day, data were collected on MoFlo® Astrios™ EQ flow cytometer and analysed using Kaluza analysis software V 1.5 (Beckman Coulter, UK).

3. DEVELOPMENT AND VALIDATION OF SENSITIVE AND ROBUST BIO-ANALYTICAL METHODS FOR THE DETERMINATION OF CANNABIDIOL (CBD) IN BIOLOGICAL MATRICES

3.1. Introduction

The development of sensitive and robust analytical methods is a key element to conduct successful and reliable pharmacokinetic and pharmacodynamic experiments. The choice of analytical method depends on many factors including, but not limited to, the characteristics of the analyte and the matrix, the availability of analytical equipment, the complexity of the technique, and other technical issues related to the volume and number of samples to be analysed [197]. Recent years have witnessed a rapid expansion of research-interest in cannabinoids, of which cannabidiol (CBD) has received considerable attention. CBD is a highly lipophilic compound as denoted by its high log *P* value (6.53, http://ilab.cds.rsc.org/). The highly lipophilic nature of CBD supported the use of reversed phase chromatography (RPC, based on hydrophobic stationary phase) as a separation technique in most of the analytical methods previously developed for the determination of CBD [28, 35, 38, 42, 198-206]. Different detection methods, however, were coupled with the RPC for the quantification of the separated CBD. Early analytical methods used radioactivity based detections [35, 38, 42]. Radioactivity based assays are often non-specific in sense of differentiating the analyte from its metabolite in a biological matrix [207]. In addition, environmental concerns of disposing

radioactive materials is another drawback for the use of radioactivity-based assays [208]. Later on, ultraviolet (UV) detection and mass spectrometry (LC-MS) based assays were also developed for the detection of CBD [199, 200, 202, 206, 209-211]. In general, mass spectrometers offer more sensitive and selective analysis than UV detectors. Yet, equipment, maintenance, and sample running costs preclude the use of mass spectrometers in tight budget laboratories [212]. Previously published methods that used UV detectors [199, 200, 211, 213] are limited by the high initial sampling volumes needed for the analysis and/or low sensitivity of detection.

Therefore, the aim of this study was to develop and validate sensitive, simple, and cost-effective analytical methods for the determination of CBD in lipolysis fractions, chylomicrons (CM) emulsions, rat plasma, and tissue homogenates using the available equipment in our own lab, high-performance liquid chromatography (HPLC) machine coupled with UV detector. These methods will help to conduct and improve the quality of quantitative cannabinoids-related research in laboratories where sophisticated LC-MS/MS instrumentation is not available.

3.2. Experimental design

The development and validation of the analytical methods described in this chapter were in accordance with the FDA Guidance for Bioanalytical Method Validation [185]. Experimental details are described in chapter 2, sections 2.2, 2.3, 2.4, and 2.5. In addition, a preliminary pharmacokinetic experiment was performed to demonstrate the application of the bioanalytical method for the determination of CBD in plasma following IV bolus administration to 2 rats. This experiment was performed as described in chapter 2, section 2.8.

3.3. Results

3.3.1. Development and validation of bio-analytical assay for the determination of CBD in lipolysis fractions

3.3.1.1. Method development

The extraction of CBD from lipolysis fractions was performed by a liquid-liquid extraction method, which was a modification of a method reported for the extraction of two synthetic lipophilic cannabinoids from rat plasma [165]. This extraction method provided reasonably clean chromatography (**Figure 3.1, 3.2,** and **3.3**), demonstrating selective extraction of CBD from the matrix of lipolysis fractions. Different mobile phase compositions, flow rates, temperatures, and injectable volumes have been attempted. However, best separation of CBD peak from matrix peaks was achieved at the following chromatographic conditions: mobile phase composed of acetonitrile and water (92:08, v/v), which was set to flow at 0.6 mL/min, column temperature of 43^{o}C, and injectable volume of 10 µL. CBD was found to elute at 3.5 min, while it's IS (probucol) eluted at approximately 16.1 min. Absorbance was monitored at 210 nm for 18 min (**Figure 3.1**, **3.2,** and **3.3**).

3.3.1.2. Method validation

3.3.1.2.1.Selectivity

The developed assay shows good selectivity since neither CBD nor the IS were found to interfere with matrix-related peaks of blank samples from the lipid, micellar, and sediment fractions (**Figure 3.1, 3.2,** and **3.3**).

3.3.1.2.2.Sensitivity and linearity

For the purpose of this assay, the low quality control (LQC) of the lipid, micellar, and sediment fractions was also defined as the lower limit of quantification (LLOQ). Relative standard deviation (RSD) and relative error (RE) values were within the acceptable limits (**Table 3.1**) as defined by the FDA guidelines [185]. LLOQ for the lipid, micellar, and sediment fractions were 40, 2, and 1 µg/mL, respectively. The LLOQ achieved by this method provided sufficient sensitivity to detect CBD following the lipolysis of the lipid-based formulation that has the lowest tested concentration of CBD (2.5 mg/mL). The linearity of the developed assay was confirmed over the concentration range of calibration curves with correlation coefficient (r^2) values over 0.99.

3.3.1.2.3.Intra- and inter-day precision and accuracy

The intra- and inter-day precision and accuracy for CBD were within the acceptable limits for all QC samples as indicated by the values of RSD (< 15%) and RE (within ±15%), respectively (**Table 3.1**).

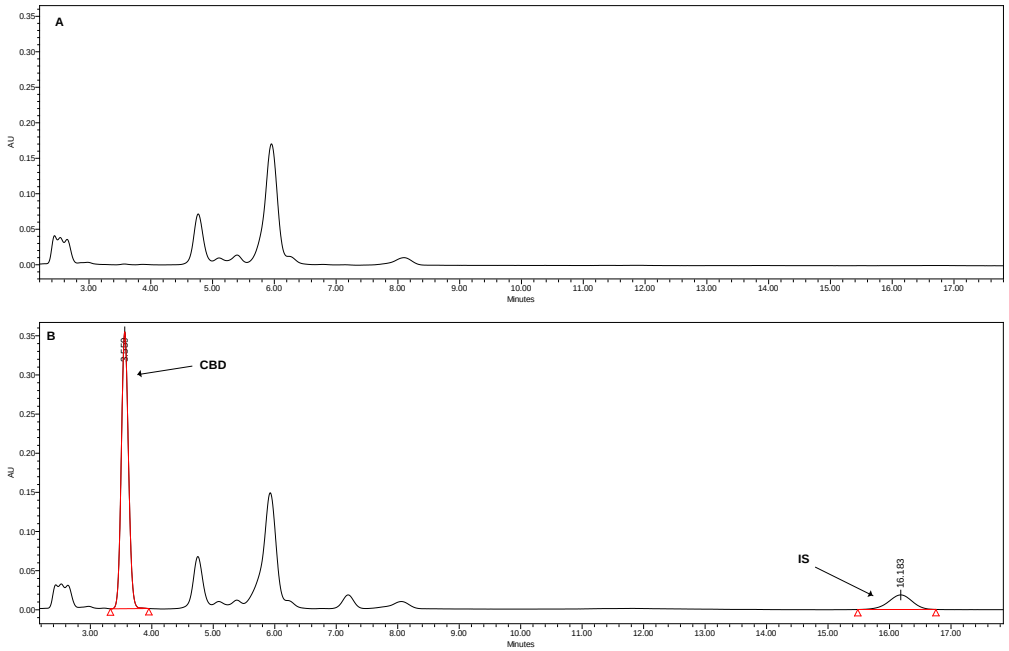

Figure 3.1. Representative chromatography of blank lipid fraction (**Panel A**), blank lipid fraction spiked with cannabidiol (CBD, 100 µg/mL) and probucol (IS) (**Panel B**); all detected at 210 nm.

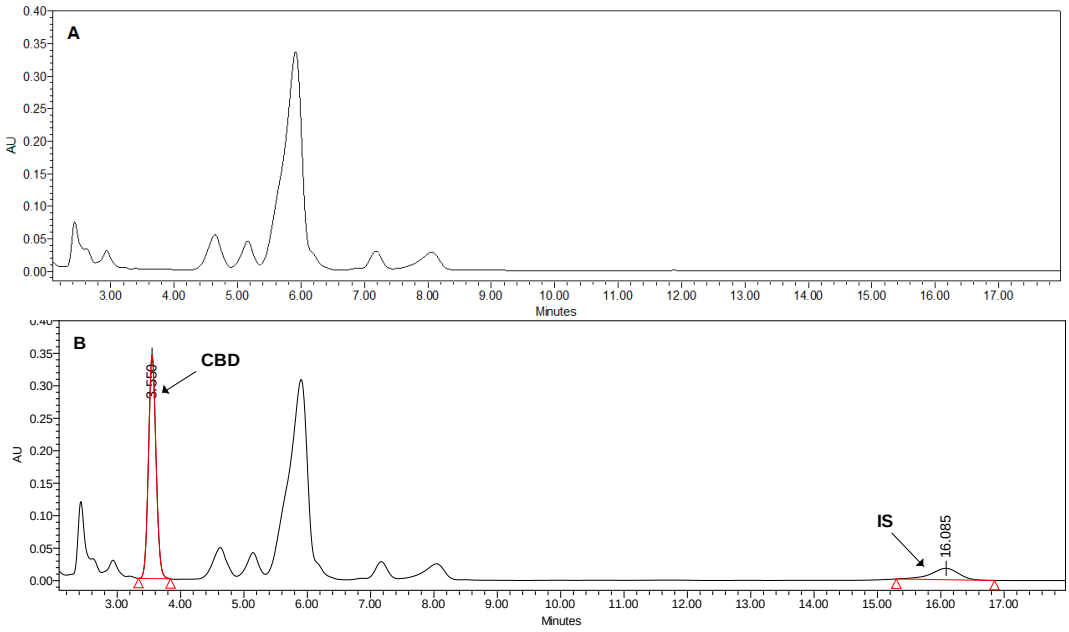

Figure 3.2. Representative chromatography of blank micellar fraction (**Panel A**), blank micellar fraction spiked with cannabidiol (CBD, 20 µg/mL) and probucol (IS) (**Panel B**); all detected at 210 nm.

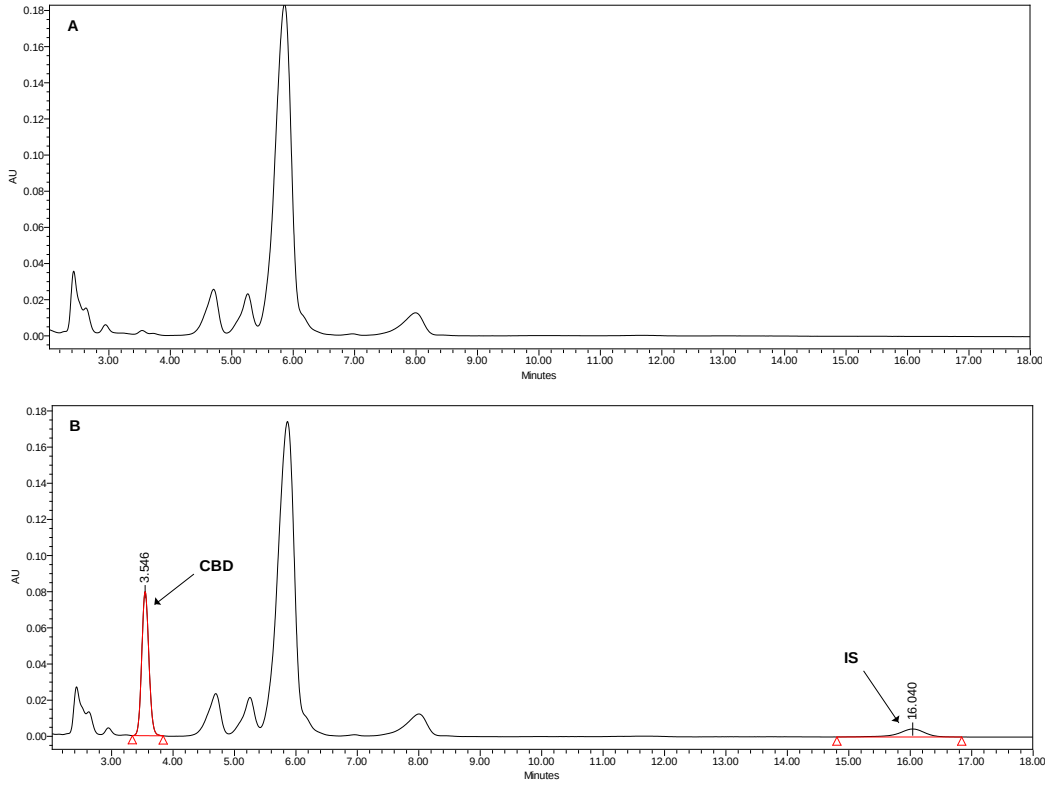

Figure 3.3. Representative chromatography of blank sediment fraction (**Panel A**), blank sediment fraction spiked with cannabidiol (CBD, 5 µg/mL) and probucol (IS) (**Panel B**); all detected at 210 nm.

Table 3.1. Intra- and Inter-day precision and accuracy data for the determination of cannabidiol (CBD) in lipid, micellar, and sediment fractions of the *in vitro* lipolysis medium.

Lipolysis fraction	Level	Concentration of CBD (µg/ml)	Intra-day (n = 6)		Inter-day (n = 4)	
			RSD%	RE%	RSD%	RE%
Lipid	LQC	40	2.7	-14.9	8.9	7.7
	MQC	800	0.1	-6.1	1.3	-7.6
	HQC	6400	2.6	-2	1.5	-0.3
Micellar	LQC	2	0.9	4.6	7	-2.4
	MQC	20	1.1	3	9.3	-0.3
	HQC	100	1.7	6.8	6	1.3
Sediment	LQC	1	2.4	11.3	2.9	8.2
	MQC	40	2	2.3	5.6	4.7
	HQC	200	2	-2.3	3.6	-0.2

RSD, relative standard deviation; RE, relative error; LQC, MQC, and HQC; lower, medium, and high quality controls, respectively.

3.3.2. Development of bio-analytical assay for the determination of CBD in lipid-particles, rat chylomicrons (CM), and human CM emulsions

3.3.2.1. Method development

The preparation of samples in the current method followed the same procedure for the determination of CBD in lipolysis fractions. However, at the conditions of this method, the elution time of probucol (the IS for the determination of CBD in lipolysis fractions) was more than 30 min. Therefore, 4,4-dichlorodiphenyltrichloroethane (DDT, eluted at 12.5 min) was used as an IS instead. Mobile phase compositions containing acetonitrile and water (92:08 to 70:30, v/v) and flow rates in the range of 0.4 – 1 mL/min have been attempted for the optimisation of this assay. The chromatographic conditions which gave best separation of CBD and DDT from matrix-related peaks were isocratic elution of the mobile phase (acetonitrile and water (75:25, v/v)) at 0.8 mL/min for 15 min and column temperature of 43°C. The injectable volume was 10 µL. The absorbance was monitored at 210 nm.

3.3.2.2. Method validation

The validation of the current method was performed using artificial lipid-particles emulsion. The chromatography of blank and CBD-spiked artificial lipid-particles were found to be comparable with chromatography from rat and human CM emulsions.

3.3.2.2.1.Selectivity

The developed assay shows high selectivity since CBD and DDT did not interfere with matrix-related peaks of blank samples (**Figure 3.4**).

3.3.2.2.2.Sensitivity and linearity

RSD and RE values for CBD were within the acceptable limits at the LLOQ (**Table 3.2**), which was found to be 100 ng/mL. The linearity of the method was confirmed over the concentration range of 50 – 10000 ng/mL with r^2 values ≥ 0.99 in all calibration curves.

3.3.2.2.3.Intra- and inter-day precision and accuracy

Table 3.2 shows the intra- and inter-day precision and accuracy for CBD. All values were within the acceptable limits i.e. RSD (< 15%) and RE (within ±15%).

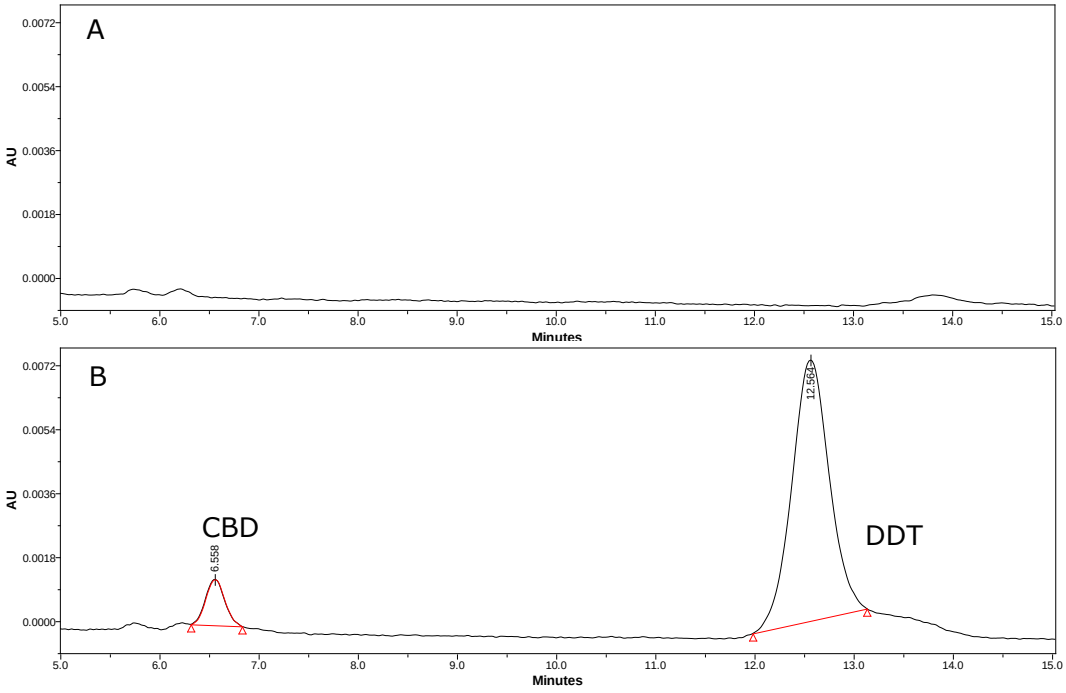

Figure 3.4. Representative chromatography of blank artificial lipid-particles emulsion (**Panel A**), blank artificial lipid-particles emulsion spiked with cannabidiol (CBD, 5 µg/mL) and DDT (IS) (**Panel B**); all detected at 210 nm.

Table 3.2. Intra- and Inter-day precision and accuracy data for the determination of cannabidiol (CBD) in artificial lipid-particles emulsion.

	Intra-day (n = 6)		Inter-day (n = 6)	
Level (concentration of CBD)	RSD%	RE%	RSD%	RE%
LLOQ (100 ng/ml)	9.7	-4		
LQC (200 ng/ml)	5.2	10.8	5.6	3.4
MQC (1000 ng/ml)	1	-2.8	4.8	1.1
HQC (10000 ng/ml)	1.9	-11.1	5.7	-8.6

RSD, relative standard deviation; RE, relative error; LLOQ, lower limit of quantification; LQC, MQC, and HQC; lower, medium, and high quality controls, respectively.

3.3.3. Development of a simple and sensitive HPLC-UV method for the determination of CBD in rat plasma

3.3.3.1. Method development

Initially, a liquid-liquid extraction method using tetrahydrofuran and n-hexane was attempted for sample preparation, similar to the extraction of CBD from lipolysis fractions and CM emulsion samples. However, the chromatography resulting from this method showed significant interference between background plasma peaks and the peak of CBD, and tetrahydrofuran in particular was not efficient in precipitating proteins. Therefore, a different protein precipitation method using acetonitrile was attempted, as it had previously been shown to be an effective solvent for plasma protein precipitation [214], and also for the extraction of lipophilic compounds from plasma samples [215-217]. The use of cold, compared with room temperature, acetonitrile appreciably decreased the size of background plasma peaks, but low-magnitude interfering peaks were still present at the same retention time as CBD. Subsequently, the addition of a liquid-liquid extraction stage using n-hexane significantly improved separation of analytes from the background plasma peaks. In addition, a cleaner baseline was obtained by the dilution of plasma

samples in water. This could possibly be explained by improved retention of hydrophilic contaminants in the water-miscible phase.

Different HPLC columns were tested for the separation of CBD and the IS (DDT) from background peaks. ACE C18-PFP 150 x 4.6 mm, 3 µm column has provided the best separation efficiency. In addition to DDT, other compounds were tested as IS, including dexamethasone, bifonazole, testosterone, benz[a]pyrene, vitamin D_3, vitamin E, and probucol. It was found that the elution times of these compounds under the chromatographic conditions used were either too short (dexamethasone, bifonazole, testosterone, benz[a]pyrene), or too long (probucol, vitamin D, vitamin E). Finally, DDT was chosen as the most appropriate IS, based on its elution being at appropriate time after CBD.

A simple buffer-free acetonitrile-water based mobile phase was used in this method, which is also compatible with LC-MS analysis, if necessary. Column temperature, flow rate and mobile phase composition were all optimised to give the final instrumentation conditions, which are acetonitrile-water mobile face (62:38, v/v) flowing at 1 mL/min and 55°C column temperature.

3.3.3.2. Method validation

3.3.3.2.1.Selectivity

The method showed good selectivity since matrix-related peaks from blank plasma did not interfere with either CBD or DDT (**Figure 3.5 A** and **B**) at the detection wavelength (220 nm). Likewise, no endogenous peaks were observed at the elution times of CBD and DDT in samples obtained from rats before IV bolus administration. Typical chromatography of rat plasma after IV bolus administration of CBD are shown in **Figure 3.5 C**.

3.3.3.2.2.Sensitivity and linearity

RSD and RE values for CBD were within the acceptable limits at the LLOQ (**Table 3.3**), which was found to be 10 ng/mL. The linearity of the method was confirmed over the concentration range of 10 – 10000 ng/mL based on 10 concentration levels with correlation coefficient (r^2) values ≥ 0.999 in all calibration curves.

3.3.3.2.3. Intra- and inter-day precision and accuracy

RSD and RE values are shown in **Table 3.3**. The intra- and inter-day precision and accuracy for CBD were within the acceptable limits for all QC samples as indicated by the values of RSD (< 15%) and RE (within ±15%), respectively [185].

3.3.3.2.4.Recovery

Mean values of absolute recoveries (mean ± SEM, n = 5) of CBD from rat plasma at the LQC, MQC, and HQC concentrations were 90.5 ± 3.1%, 86.2 ± 1.1%, and 91.0 ± 1.3%, respectively. The recovery of the IS, was 74.6 ± 0.7%. The good sensitivity achieved by this method reflects the high efficiency of the extraction method for CBD.

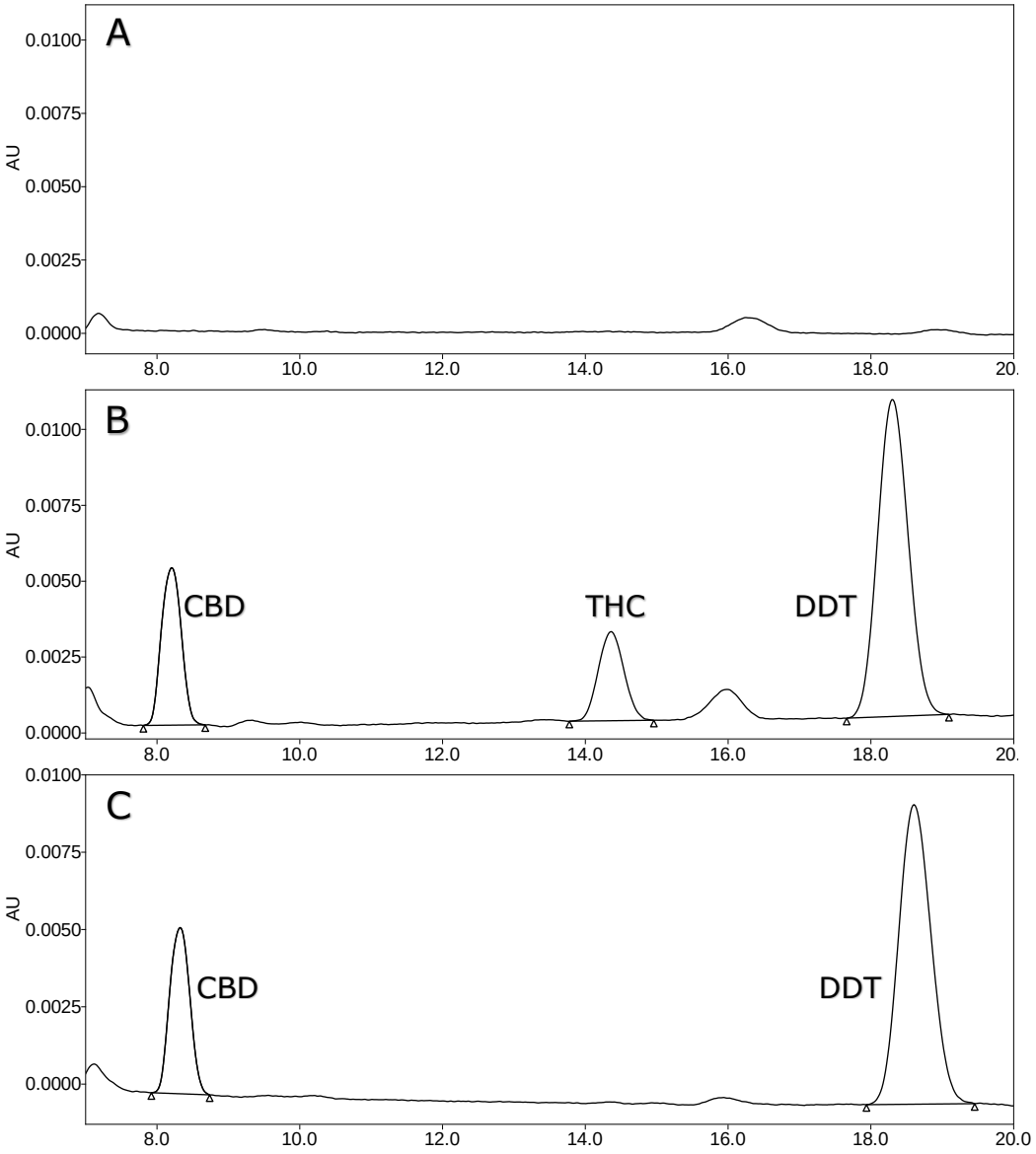

Figure 3.5. Representative chromatography of blank rat plasma (**Panel A**), plasma spiked with cannabidiol (CBD) and Δ^9-tetrahydrocannabinol (THC) at concentrations of 1000 ng/mL in addition to the internal standard 4,4-dichlorodiphenyltrichloroethane (DDT) (**Panel B**), and rat plasma following IV injection of CBD (**Panel C**); all detected at 220 nm.

Table 3.3. Intra- and Inter-day precision and accuracy data for the determination of cannabidiol (CBD) in rat plasma.

Level (concentration of CBD)	Intra-day (n = 6)		Inter-day (n = 6)	
	RSD%	RE%	RSD%	RE%
LLOQ (10 ng/ml)	8.10	6.55	-	-
LQC (20 ng/ml)	8.02	13.6	9.8	0.84
MQC (100 ng/ml)	3.23	-3.00	4.11	-0.82
HQC (1000 ng/ml)	2.60	0.73	5.47	-0.96

RSD, relative standard deviation; RE, relative error; LLOQ, lower limit of quantification; LQC, MQC, and HQC; lower, medium, and high quality controls, respectively.

3.3.3.2.5.Stability

The stability of CBD at LQC, MQC, and HQC under different conditions is presented in

Table 3.4. RSD and RE values indicate that CBD was stable in rat plasma after three cycles of freeze-thawing (-80°C to room temperature), bench -top storage (6 h at room temperature), short term storage (24 h at -80°C), and long term storage (30 and 60 days at -80°C). In addition, CBD was stable in processed samples after 16 h at 4°C (autosampler stability).

Table 3.4. Stability results for cannabidiol (CBD) in rat plasma at different conditions as well as the stability of CBD in processed samples at the autosampler conditions (n = 6 for each level).

Level (concentration of CBD)	Freeze-thaw (3 cycles)		Room temperature (25°C, 6 h)		Short term (-80°C, 24 h)		Long term (-80°C, 30 days)		Long term (-80°C, 60 days)		Autosampler (4 °C, 16 h)	
	RSD%	RE%	RSD%	RE%	RSD%	RE%	RSD%	RE%	RSD%	RE%	RSD%	RE%
LQC (20 ng/ml)	11.7	12.4	9.1	6.3	11.2	-2.4	12.8	10.5	6.4	-15	7.3	14.4
MQC (100 ng/ml)	6.1	-12.4	6	-9.1	2.8	-9.2	7.3	-12.5	3.5	-5.8	3.8	5.6
HQC (1000 ng/ml)	4.9	-14.1	2.9	-4.9	3.9	-7.3	5.9	-9.5	2.2	-6.8	2.1	-0.8

RSD, relative standard deviation; RE, relative error; LQC, MQC, and HQC, lower, medium, and high quality controls, respectively.

3.3.3.3. The application of the developed assay in a pharmacokinetic experiment

To demonstrate the suitability of the developed method for pharmacokinetic studies, the method was applied to a preliminary pharmacokinetic study in rats. The mean plasma concentration-time profile observed following a single IV bolus administration of CBD at a dose of 5 mg/kg is presented in **Figure 3.6**. The pharmacokinetic parameters from the concentration-time profile calculated by non-compartmental analysis are summarised in **Table 3.5**.

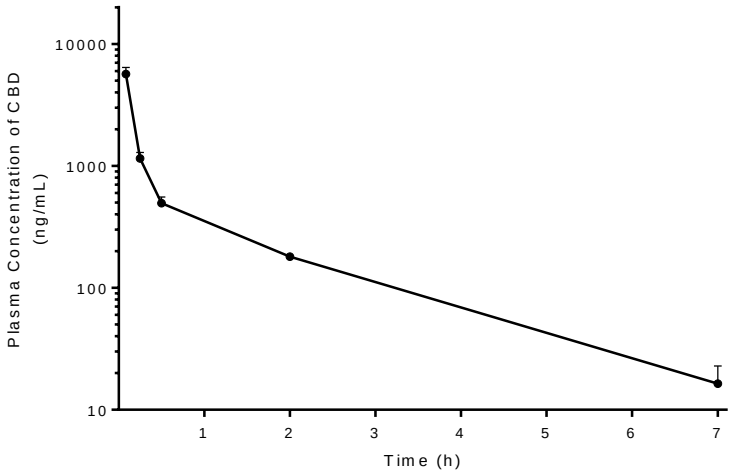

Figure 3.6. Plasma concentration-time profile (mean ± SEM) following single IV bolus administration of cannabidiol (CBD, 5 mg/kg) to rats (n = 2).

Table 3.5. Pharmacokinetic parameters (mean ± SEM) derived from plasma concentration-time profile following single IV bolus administration of cannabidiol (CBD) to rats at a dose of 5 mg/kg (n = 2).

Pharmacokinetic parameter	Value
AUC_{inf} (h.ng/mL)	2581.2 ± 57.9
$AUC_{0\text{-}t}$ (h.ng/mL)	2545.5 ± 70.7
C_0 (ng/ml)	12916.6 ± 2325.3
V_d (mL/kg)	1614.4 ± 273.9
CL (mL/h/kg)	1939.1 ± 43.5
$t_{1/2}$ (h)	1.42 ± 0.15

3.3.4. Development and validation of bio-analytical assay for the determination of CBD in mesenteric lymph nodes, spleen, and brain tissues

3.3.4.1. Method development

The preparation of samples in the current method followed the same procedure described for the determination of CBD in rat plasma. The chromatographic conditions were similar to those used for the determination of CBD in artificial lipid-particles emulsion i.e. mobile phase composed of acetonitrile and water (75:25, v/v), which was set to flow at 0.8 mL/min and 43°C column temperature. The absorbance was monitored at 230 nm, which was found to give the best detection limit.

3.3.4.2. Method validation

The developed assay was validated for the determination of CBD in spleen and brain tissue homogenates. MLN have relatively small mass (~ 170 mg) compared with spleen and brain tissues (~ 650 and 2000 mg, respectively). Therefore, the mass of MLN tissues collected from control animals was only sufficient to prepare the calibration curve samples, but not the validation samples. Nevertheless, the method showed efficient separation of CBD from interfering peaks in MLN samples (**Figure 3.7**), which demonstrates the suitability of the current method for the determination of CBD in MLN homogenates.

3.3.4.2.1.Selectivity

The developed assay shows good selectivity since CBD and DDT were not found to interfere with matrix-related peaks of blank samples (**Figure 3.7**, **3.8**, and **3.9**).

3.3.4.2.2.Sensitivity and linearity

RSD and RE values for CBD were within the acceptable limits at the LLOQ for spleen and brain tissues, which was found to be 50 ng/mL (**Table 3.6**). The linearity of the method was confirmed over the concentration range of 20 – 1000 ng/mL with r^2 values ≥ 0.99 in all calibration curves.

3.3.4.2.3.Intra- and inter-day precision and accuracy

The intra- and inter-day precision and accuracy for CBD were within the acceptable limits for all QC samples as indicated by the values of RSD (< 15%) and RE (within ±15%), respectively (**Table 3.6**).

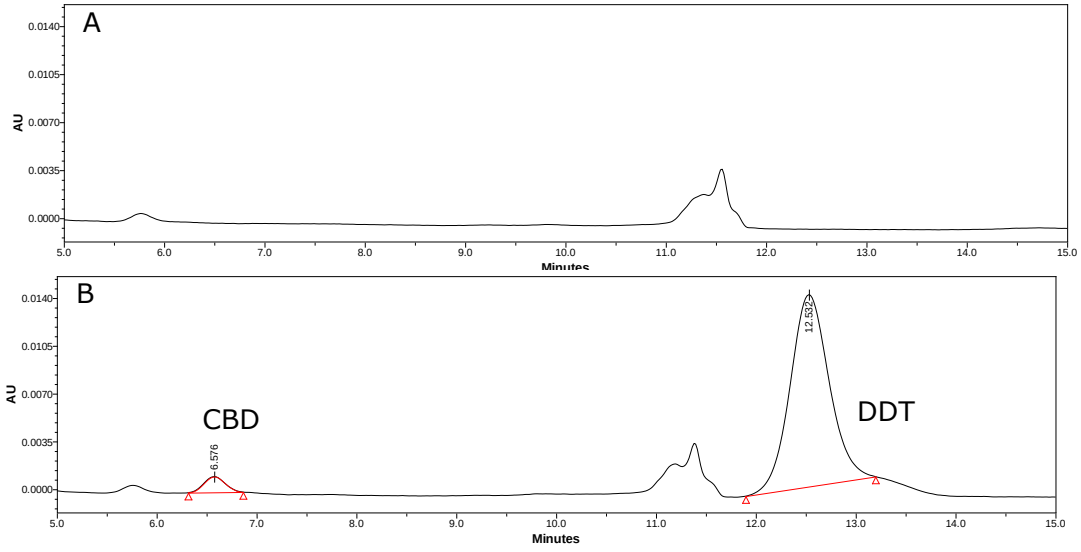

Figure 3.7. Representative chromatography of blank mesenteric lymph nodes (MLN) homogenate (**Panel A**), blank MLN homogenate spiked with cannabidiol (CBD, 500 ng/mL) and DDT (IS) (**Panel B**); all detected at 230 nm.

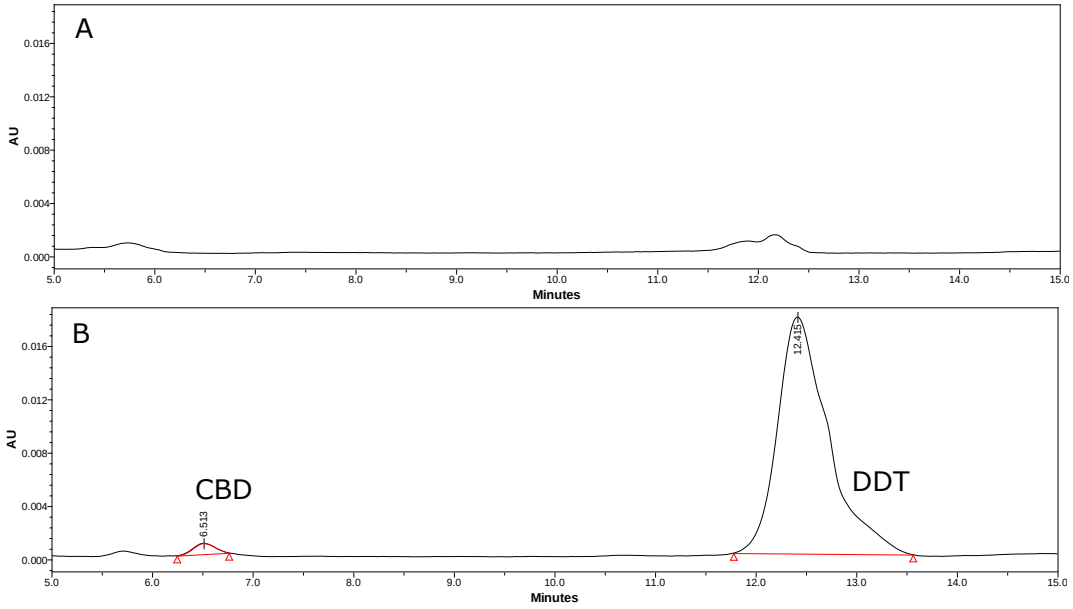

Figure 3.8. Representative chromatography of blank spleen homogenate (**Panel A**), blank spleen homogenate spiked with cannabidiol (CBD, 500 ng/mL) and DDT (IS) (**Panel B**); all detected at 230 nm.

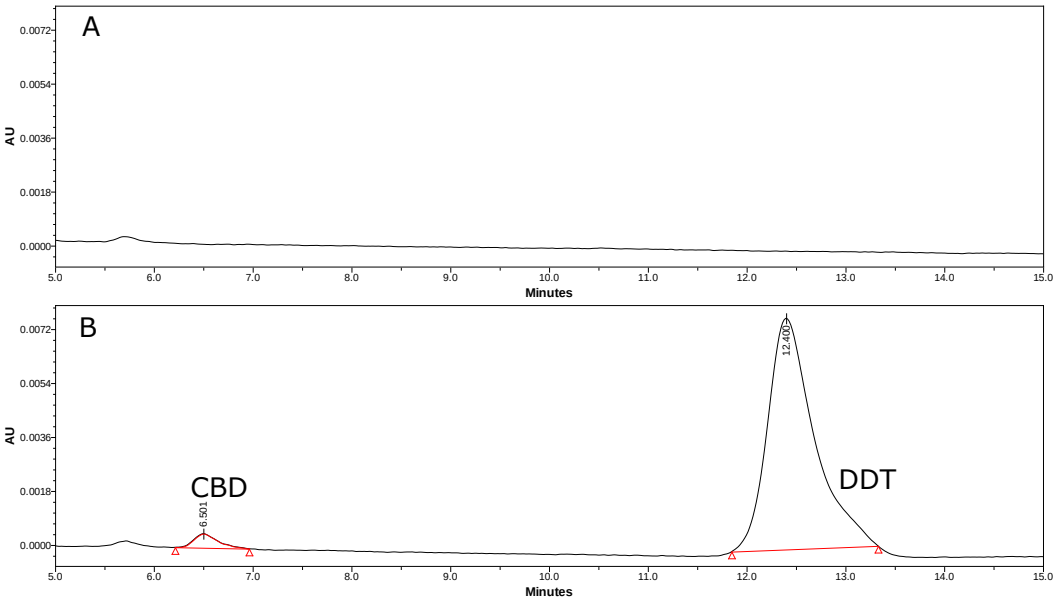

Figure 3.9. Representative chromatography of blank brain homogenate (**Panel A**), blank brain homogenate spiked with cannabidiol (CBD, 500 ng/mL) and DDT (IS) (**Panel B**); all detected at 230 nm.

Table 3.6. Intra- and Inter-day precision and accuracy data for the determination of cannabidiol (CBD) in spleen and brain tissue homogenates.

Level (concentration of CBD)	Intra-day (n = 6)		Inter-day (n = 6)	
	RSD%	RE%	RSD%	RE%
Spleen				
LLOQ (50 ng/ml)	6.2	7.5		
LQC (100 ng/ml)	4.6	12.8	13.1	-5.2
MQC (200 ng/ml)	5.9	4.7	6.3	4
HQC (1000 ng/ml)	6.8	-7.3	9.4	-15
Brain				
LLOQ (50 ng/ml)	3.2	0.9		
LQC (100 ng/ml)	8.8	-0.8	8	-1.1
MQC (200 ng/ml)	7.9	-5.5	8.7	4.3
HQC (1000 ng/ml)	9.8	-7.9	4.5	1.8

RSD, relative standard deviation; RE, relative error; LLOQ, lower limit of quantification; LQC, MQC, and HQC; lower, medium, and high quality controls, respectively.

3.4. Discussion

Cannabis is a unique source of more than 100 cannabinoids [13] of which CBD has a well-documented safety profile following administration of high doses to humans [218]. This safety profile, coupled with the therapeutic activity of CBD, has supported the use of CBD-based formulations to treat Dravet and Lennox-Gastaut syndromes in children [30]. In addition, CBD has a long-list of therapeutic potentials (reviewed in [31, 219]). Therefore, there is a growing body of interest in the preclinical research of CBD in many laboratories to validate more therapeutic applications of CBD. In this study, we aimed to develop simple and cost-effective analytical methods for the determination of CBD in biological matrices. These methods could support quantitative preclinical researches using affordable technique, namely HPLC-UV.

We have successfully developed HPLC-UV methods for the determination of CBD in lipolysis fractions, CM emulsions, rat plasma, and tissue homogenates. Very simple and time-efficient extraction steps were used. These extraction steps are highly cost-efficient compared to the use of solid-phase extraction method reported by other groups [220-222]. Run times are equal to or less than 20 min, which permit high-throughput sample analysis. All the developed methods were validated according to internationally acceptable guidelines [185]. The methods are selective to CBD, no matrix related peaks elute at the same elution times of CBD (**Figure 3.1, 3.2, 3.3, 3.4, 3.5, 3.7, 3.8,** and **3.9**). RSD and RE values are within the acceptable limits for all QC samples (**Table 3.1, 3.2, 3.3,** and **3.6**) indicating that methods are precise and accurate for the determination of CBD.

To the best of our knowledge there are no reported methods for the determination of CBD in lipolysis fractions, CM emulsion, or rat tissue homogenates using HPLC-UV. Compared to previously developed and validated assays in rat plasma, the LLOQ of CBD obtained in our study is similar to the LLOQ (10 ng/mL) reported by Deiana *et al* [209] in a study for the determination of CBD in rat plasma using LC–MS/MS. Therefore, the method reported here for the determination of CBD in rat plasma provides a technique with a similar sensitivity to reported LC-MS/MS methods, but in a more cost-efficient and simple way. The above mentioned results confirm that the developed methods are suitable for routine analysis.

To our knowledge, this study reports for the first time detailed stability data for CBD in rat plasma. The stability of CBD was previously evaluated in human plasma [223] and the results were consistent with those obtained in our study for rat plasma. In addition, we demonstrated that the developed method for the determination of CBD in rat plasma is suitable for pharmacokinetic

studies. Few pharmacokinetic studies have been reported for CBD in rats. Different bioanalytical methods were used in these previous studies, including unspecific radioactivity assays in early reports [38, 42]. Therefore, the variability of pharmacokinetic parameters obtained in previous works is very high. Further studies, however, will be required to accurately assess the pharmacokinetic parameters for CBD after intravenous and oral administrations.

The assay of CBD in rat plasma was published in the Journal of Pharmaceutical and Biomedical Analysis [224]. It is worth noting that this assay has attracted considerable interest. We have been contacted by academic and industrial research groups to help establish their in-house assays.

3.5. Conclusions

Simple, sensitive, and cost-efficient HPLC-UV methods were developed and validated for the determination of CBD in different biological matrices. The stability of CBD in rat plasma was investigated for the first time, and was found to be satisfactory under all tested conditions. In addition, the method for the determination of CBD in rat plasma was applied to a pharmacokinetic study after IV administration of CBD to rats. The bioanalytical methods described in this study were successfully used in this project and can also be used to support preclinical studies in other laboratories where sophisticated instrumentation such as LC-MS/MS is not available.

4. INTRALUMINAL PROCESSING AND INTESTINAL LYMPHATIC TRANSPORT POTENTIAL OF ORALLY ADMINISTERED CANNABIDIOL (CBD)

4.1. Introduction

Orally administered drugs are commonly classified, based on their rate of dissolution and permeability, to four main classes according to the Biopharmaceutics Classification System (BCS) [225]. Cannabidiol (CBD) has poor water solubility and high intestinal permeability (predicted by ACD/I-Lab software, online interface, http://ilab.cds.rsc.org/), which fulfil the criteria of BCS II drugs [225]. For BCS II drugs, intestinal solubilisation is the rate limiting step for absorption following oral administration [226]. Different approaches have been applied to enhance intestinal solubilisation and therefore the absorption of BCD II drugs [227]. Of these approaches, lipid-based formulation is common [156, 228]. Lipid content of the lipid-based formulations, similar to dietary lipids in food, are digested in the small intestine to form mixed micelles, which can solubilise lipophilic drugs of BCS class II and thereby greatly enhance their diffusion toward the absorptive membrane of enterocytes (**Figure 4.1**) [129, 156, 229]. Another advantage of lipid-based formulations is the prolongation of gastric emptying time. This can increase the residence time of lipophilic drugs in the small intestine, which permits more time for solubilisation and absorption [230]. In addition, oral administration of long-chain triglycerides (LCT) or long-chain fatty acids (but not shorter lipids) leads to the assembly of triglyceride-rich lipoproteins, particularly chylomicrons (CM), in the enterocytes

[162, 163]. CM are then secreted by exocytosis through the basolateral membrane of enterocytes. Being large particles, CM cannot pass the walls of vascular capillaries, but are absorbed to the lymph lacteals instead (**Figure 4.1**) [130-133]. Some lipophilic drugs can associate with CM in the enterocyte and be transported to the intestinal lymphatic system [132]. Indeed, high intestinal lymphatic transport was reported as the main absorption pathway for highly lipophilic drugs that have high association values with CM, when orally co-administered with LCT to rats [165, 166]. Therefore, oral administration of lipophilic drugs of BCS class II in LCT-based formulation can augment intestinal solubilisation and potentially promote intestinal lymphatic transport [231].

In recent years, there has been an escalating interest for the assessment of intestinal processing of lipid-based formulations using experimental models. *In vitro* lipolysis model is one of the most popular techniques used to simulate physiological lipid digestion processes in the small intestine, and is commonly applied in the design and development of oral lipid-based drug delivery systems [188, 189, 232-235]. *In vitro* lipolysis is conducted by the dispersion of the lipid-based formulation in a temperature and pH controlled biorelevant medium, simulating the content of the upper part of the small intestine. Triglyceride components of lipid-based formulations are digested to fatty acids by the addition of lipase enzyme. The released fatty acids are titrated with sodium hydroxide to maintain the pH of the medium at controlled band [188, 189, 232-237]. Many experimental parameters are therefore involved in the optimisation of the model, which could significantly affect the outcome of lipolysis. These parameters include buffer capacity, the activity of lipase enzyme, pH, and the concentration of bile salts and phospholipids in the digestion medium [226, 237]. Recently, these parameters were optimised and validated by our research group for the lipolysis of LCT-based formulations (**Table 2.2**) [189]. The

validated parameters were therefore applied in the current study to assess the solubilised fraction of CBD that would be available for absorption following oral administration in a LCT-based formulation.

As mentioned above, following absorption, lipophilic drugs might associate with CM in the enterocytes and gain access to the intestinal lymphatic system. The precise mechanism governing the association of lipophilic drugs with CM is far from clear and might happen at any stage of CM assembly [158, 164, 166]. Nevertheless, the degree of association of a lipophilic drug with CM can serve as a predictive measure for the intestinal lymphatic transport potential [166]. In this regard, a number of studies have focused on developing *in silico* models for the prediction of intestinal lymphatic transport [190, 238]. Based on molecular structure, Holm and Hoest developed a computational model to predict the lymphatic absorption of drugs when co-administered with LCT [238]. The predictive level of this model was higher than previously described log *P* - and triglyceride solubility-dependent models [238]. However, this model was described by authors as an initial non-validated approach, and to the best of our knowledge the subsequent practical use of this model was not reported [239]. A more accurate multi-parameter *in silico* model was later developed by Gershkovich *et al* [190]. This model could reasonably predict the association of a drug with CM in enterocytes, and hence the fraction of absorbed drug to be delivered to intestinal lymphatics rather than systemic circulation. Moreover, a linear correlation between the *ex vivo* uptake of some lipophilic compounds by plasma-derived CM and the intestinal lymphatic bioavailability of these compounds was established by Gershkovich and Hoffman [166]. Predicted values by this correlation represent the lymphatic bioavailability of the tested lipophilic compound when co-administered with LCT in an *in vivo* rat model [166].

Taken together the above mentioned approaches, this study has two main aims. Firstly, the assessment of intestinal solubilisation of CBD following oral administration in LCT-based formulation using *in vitro* lipolysis model. Secondly, it aims to assess the potential of intestinal lymphatic transport of CBD when orally co-administered with LCT by assessing the uptake of CBD by CM.

.

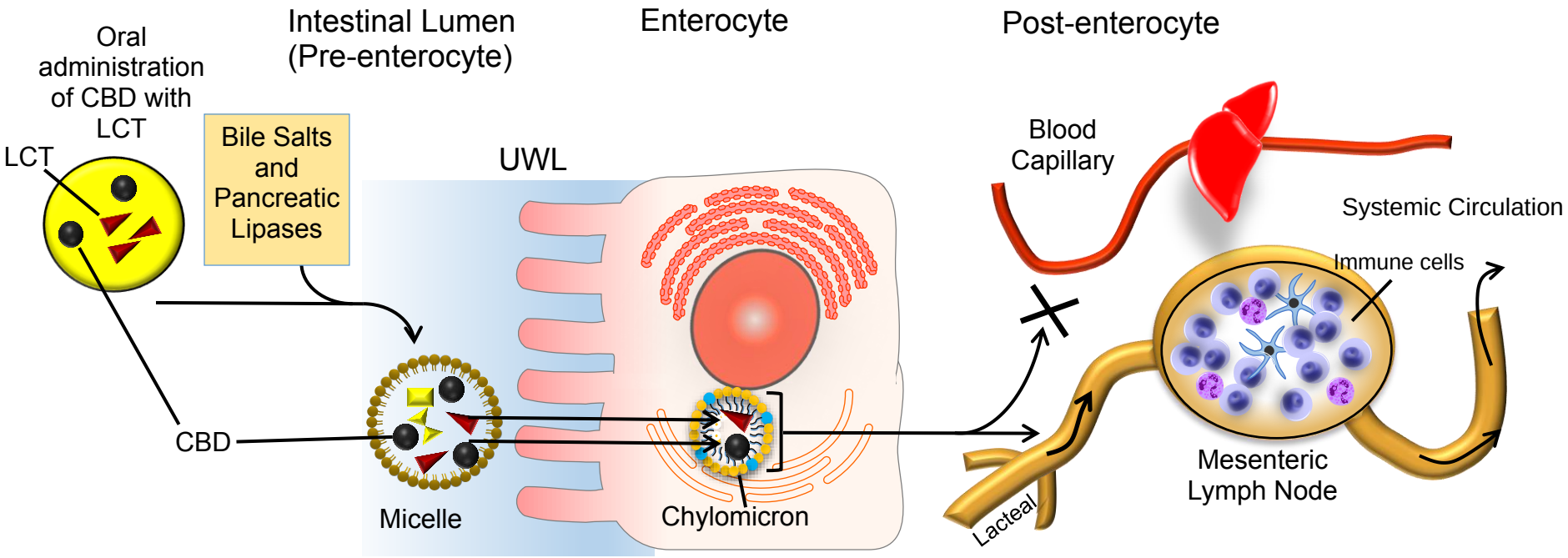

Figure 4.1. Schematic representation for the oral administration of cannabidiol (CBD) in a long-chain triglycerides (LCT)-based formulation showing intestinal solubilisation and the potential of intestinal lymphatic transport. UWL, unstirred water layer.

4.2. Experimental design

Lipid-based formulations can be further classified, according to the added excipients, to four main classes [240]. Type I is the simplest and it is a solution of the drug in triglycerides [228, 240, 241]. In this study, CBD was formulated as a solution of LCT (Type I lipid-based formulation). The effect of LCT on intestinal processing of CBD was assessed using an *in vitro* lipolysis model as described in chapter 2, section 2.7.1. The rationale of selecting 160 µL as the volume of LCT-based formulations of CBD in the lipolysis experiments is based on the assumption that CBD could be administered to humans in one-mL capsule with a glass of water (~ 250 mL). Considering the final volume of the simulated digestion medium in the reaction vessel (~ 40 mL), one-mL was scaled down to 160 µL to simulate oral administration of capsules to human.

The intestinal lymphatic transport potential of orally administered CBD was assessed by evaluating the uptake of CBD by CM as described in chapter 2, section 2.7.2.

4.2.1. Statistical analysis

Results are expressed as mean ± standard error of the mean (SEM). Statistical differences between data sets were assessed using one-way analysis of variance (ANOVA) followed by the Tukey's correction for multiple comparisons. $p < 0.05$ was considered to represent a significant difference.

4.3. Results

4.3.1. Intraluminal processing of CBD co-administered with LCT

The distribution of CBD in the lipid, micellar, and sediment fractions following the lipolysis of 160 µL of sesame oil containing 2.5, 5, 10, 20, 40, 80,

and 160 mg/mL of CBD is shown in **Figure 4.2**. Upon lipolysis of sesame oil, around one-third of CBD dose was solubilised in the micellar fraction when the concentration of CBD in the formulation is in the range of 2.5-40 mg/mL (**Figure 4.2 A, B, C, D** and **E**; **Figure 4.3**). However, increasing the concentration of CBD in the formulation to 80 and 160 mg/mL significantly decreased the distribution of CBD to the micellar fraction (**Figure 4.3**). The solubilised amount of CBD in the micellar fractions corresponds to the fraction readily available for absorption. The remaining amount of CBD was distributed between the undigested lipid fraction (50-80%) and the sediment layer (6-12%). This amount corresponds the proportion of the drug that is not readily available for absorption following oral administration with lipids [226, 242].

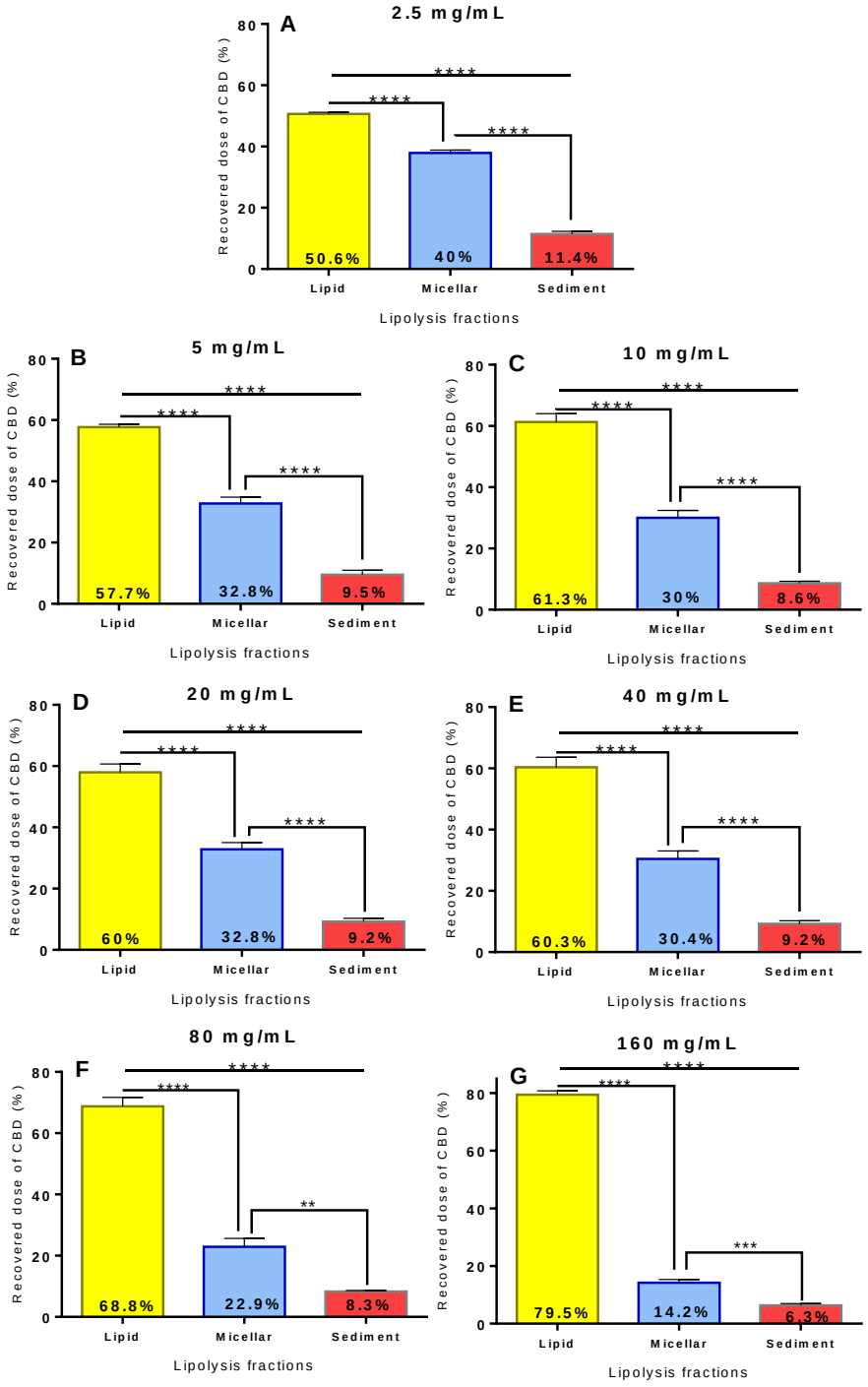

Figure 4.2. Distribution of cannabidiol (CBD) in the lipid, micellar and sediment layers after lipolysis of 160 µl of the LCT sesame oil containing 2.5, 5, 10, 20, 40, 80, and 160 mg of CBD (n = 6). The data are shown as mean ± SEM. One-

way ANOVA with Tukey's post-hoc test was used for statistical analysis. ** p < 0.01; *** p < 0.001; **** p < 0.0001.

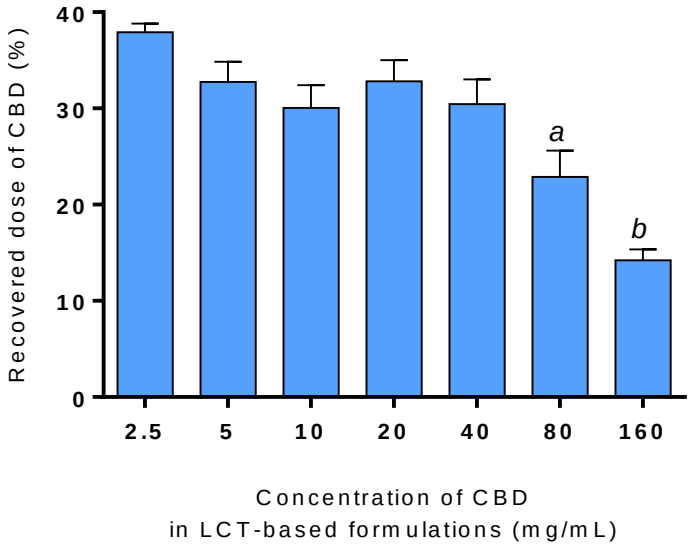

Figure 4.3. The distribution of cannabidiol (CBD) (mean ± SEM, n = 6) in the micellar fractions following the lipolysis of 160 µl of sesame oil containing 2.5, 5, 10, 20, 40, 80, and 160 (mg/mL) of CBD. One-way ANOVA with Tukey's post-hoc test was used for statistical analysis. *a*, significant statistical differences from 2.5, 5, and 20 mg/mL experimental sets (p < 0.05); *b*, significant statistical differences from 2.5, 5, 10, 20, and 40 mg/mL experimental sets (p < 0.05).

4.3.1. Intestinal lymphatic transport potential of cannabinoids

4.3.1.1. *In silico* prediction of CBD association with CM

The physicochemical properties of CBD used in the *in silico* model are summarised in **Table 4.1** along with their LOGIT values (the result of adjusting CBD's physicochemical properties with their relevant unscaled regression coefficients). This model predicted the association of CBD with CM to be 39.4%. Applying this value in the linear correlation described between CM association and intestinal lymphatic bioavailability [190], it can be calculated that 11.5% of CBD dose is expected to be delivered to the intestinal lymphatic system following oral co-administration with LCT in rats (red lines, **Figure 4.4**).

Table 4.1. *In silico* calculation for the association of cannabidiol (CBD) with chylomicrons (CM) based on physicochemical properties. The unscaled regression coefficients were developed by Gershkovich *et al* [190].

Physicochemical Property		Unscaled regression coefficients	LOGIT values
Log D 7.4	6.53	0.299879	1.9582
Log *P* - Log D	0	-0.238127	0
PSA (Å^2)	40.46	-0.00855215	-0.3460
HBA	2	-0.184359	-0.3687
FRB	6	0.0805226	0.4831
Density (g/cm^3)	1.025	1.45337	1.4897
Molar Volume (cm^3)	306.644	0.00545912	1.6740
HBD	2	0.0823094	0.1646
Total LOGIT Values			5.0549
Constant			-5.2414
Degree of Association (X)			-0.1865
% Association with CM			**39.4%**

PSA, polar surface area; HBA, number of hydrogen bond acceptors; FRB, freely rotatable bonds; HBD, number of hydrogen bond donors; CM, chylomicrons.

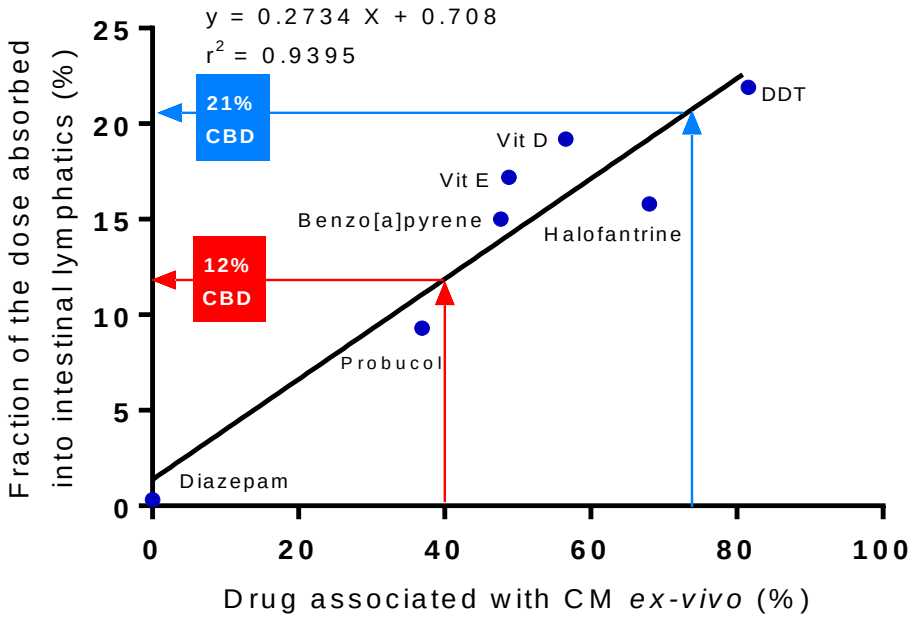

Figure 4.4. The intestinal lymphatic bioavailability (% of dose) vs. the *ex vivo* uptake (% association) by rat plasma-derived chylomicrons (CM) for some lipophilic compounds (modified from Gershkovich and Hoffman [166]). Arrows describe the application of the *in silico*-calculated (39%, red lines) and *ex vivo*-assessed (74%, blue lines) uptake values of CBD by CM to this correlation to predict intestinal lymphatic bioavailability.

4.3.1.2. The uptake of CBD by artificial chylomicron-like lipid particles and natural rat and human CM

The results of the uptake are shown in **Figure 4.5**. The association values of CBD with artificial lipid particles and natural CM were in the range of 70-80%. No significant differences were seen between the uptake of CBD by artificial lipid particles, rat CM, or human CM (**Figure 4.5**). Applying the association value of CBD with rat plasma-derived CM to the linear equation described in **Figure 4.4** predicts an intestinal lymphatic bioavailability of 20.9% (blue lines, **Figure 4.4**)

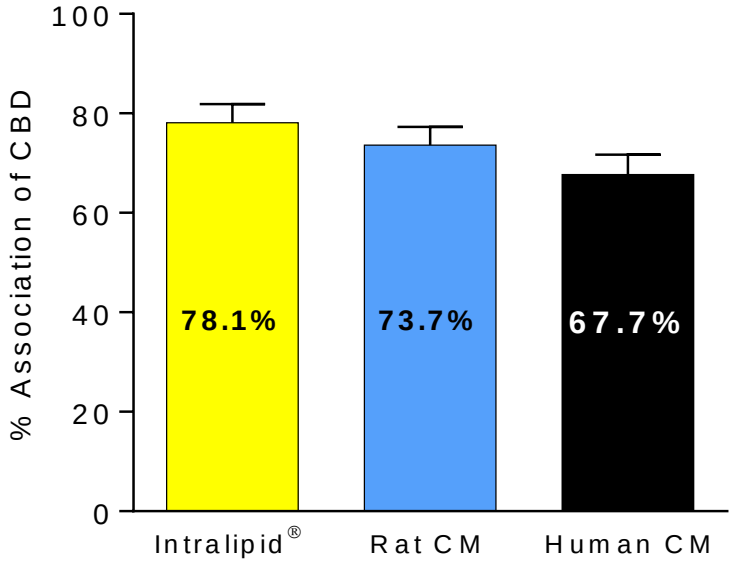

Figure 4.5. The uptake of cannabidiol (CBD) by lipid particles (from Intralipid®, n = 9) and plasma-derived chylomicrons (CM) isolated from rats (n = 7) or humans (n = 5). The data are shown as mean ± SEM of % association. One-way ANOVA with Tukey's post-hoc test was used for statistical analysis. Differences between data sets were statistically non-significant.

4.4. Discussion

It is generally accepted that intraluminal (intestinal) solubilisation is the main obstacle that hinders the absorption of lipophilic drugs of BCS II, such as CBD [226]. One of the most commonly used approaches to overcome this obstacle is lipid-based formulations [160]. The digestion of formulation-derived lipids, or dietary lipids in food, results in the formation of micellar structures [156]. These are spherical structures of hydrophobic core and hydrophilic surface, which are mainly composed of bile salts, cholesterol, monoglycerides, fatty acids, phospholipids, and some other components of lipid digestion products [226, 229]. The distribution of lipophilic drugs into the micellar structures facilitates the diffusion of drugs across the unstirred water layer and thereby enhances their absorption [242]. In addition, oral administration of LCT promotes the formation of CM which can act as a carriers for the drug from the enterocytes to the intestinal lymphatic system [164]. In this study, we aimed to assess the effect of lipids on the intraluminal solubilisation and to evaluate the intestinal lymphatic transport of CBD following oral administration in LCT-based formulation.

Our results showed that following the lipolysis of LCT-based formulations containing CBD in the range of 2.5-40 mg/mL, around 30-40% of CBD was recovered in the micellar fraction (**Figure 4.2**). This corresponds to the fraction readily available for absorption. However, at higher concentrations (80 and 160 mg/mL), the solubilised fraction has significantly decreased (**Figure 4.2 F** and **G**; **Figure 4.3**). This in turn means that the ability of mixed micelles to solubilise CBD started to reach saturation. Similar trends were also observed in our laboratory for Δ^9-tetrahydrocannabinol (THC) [194]. In addition, significantly higher amounts of CBD were retained in the undigested lipid fractions compared

to the micellar fractions (**Figure 4.2**). The distribution of CBD in the lipid fractions seems to be increased as the concentration of CBD in the formulation increases (50% at 2.5 mg/mL increased to 80% at 160 mg/mL formulations). Similar pattern of preferential partitioning toward the undigested LCT was also reported for other highly lipophilic compounds, such as halofantrine, probucol, and phytosterols (log *P* 7.27 – 10.72) [243-245]. In contrast, less lipophilic drugs, such as dexamethasone, diazepam, and griseofulvin (log *P* 1.87 – 3.35), were primarily found in the micellar fractions [231, 243]. It has been suggested that following lipolysis, high lipophilicity drives the drug to the undigested lipids rather than being partitioned to the micellar fractions [226, 246]. This proposition has been challenged by the solubilisation behaviour demonstrated for vitamin D_3 and cholesterol (highly lipophilic compounds), which were mostly recovered in the micellar fractions [235, 244]. Nevertheless, incomplete lipid digestion is one of the major drawbacks of *in vitro* lipolysis model that is not expected *in vivo* [226]. In fact, in humans, under normal physiological conditions, all ingested triglycerides are efficiently digested and absorbed [247]. Therefore, it is possible that more CBD could be solubilised in the micellar fraction *in vivo*. In addition, in this study, significantly less CBD was precipitated in the sediment fractions compared with micellar and lipid fractions (**Figure 4.2**). This demonstrates the efficiency of LCT-based formulation to prevent CBD precipitation. Similar effect was also reported for all the lipophilic drugs mentioned above [231, 235, 243-245]. Overall, it can be suggested that following oral administration of LCT-based formulation containing CBD at concentrations equal to or less than 40 mg/mL, at least one-third of the administered dose will be readily available for absorption.

Following absorption to the enterocytes, the potential of intestinal lymphatic transport is primarily dependent on the ability of lipophilic drugs to

associate with CM (**Figure 4.1**). The *in silico* model applied in this study predicted that CBD would have 39% association with CM (**Table 4.1**). Based on this value, the potential of intestinal lymphatic bioavailability of CBD in rats following oral administration in LCT-based formulation would be in the range of 12% (calculated by incorporating the *in silico* results in the linear correlation described by Gershkovich and Hoffman [166]) (red lines, **Figure 4.4**). The extent of intestinal lymphatic transport predicted by the *in silico* model has therefore supported that CBD is a promising candidate for further investigations. It can be proposed that CBD, based on physicochemical properties, might have intrinsic ability to associate with CM. In addition, the lymphatic transport potential was investigated by assessing the uptake of CBD by artificial CM-like lipid particles. These particles have previously been shown to provide a reasonably close estimate for the degree of association with CM before proceeding with experiments that require materials from animals or humans [190, 191]. In this study, CBD showed remarkable association with lipid particles (~ 78%, **Figure 4.5**). Yet, lipid particles lack the surface apoproteins found in natural CM which might affect the process of association [190]. Therefore, association experiments were also performed with natural CM isolated from rats and showed association values of 73.7 ± 3.6% (**Figure 4.5**). This has further confirmed the high association ability of CBD with CM. The *ex vivo* uptake of CBD by CM isolated from rat plasma was also applied in the linear correlation shown above in **Figure 4.4** (the blue lines). The intestinal lymphatic bioavailability revealed by the linear equation was ~ 21%. This is almost double the lymphatic bioavailability calculated using values predicted by the *in silico* model, which apparently underestimated the uptake of CBD by CM. Noteworthy, the *ex vivo* uptake of CBD by rat CM was performed the same way as the compounds used to build the linear correlation described above (**Figure 4.4**).

Therefore, it can be suggested, based on the uptake by rat CM, that CBD has high potential of intestinal lymphatic transport following oral administration with LCT to rats. The impact of CM association on the intestinal lymphatic transport was previously demonstrated for the synthetic lipophilic cannabinoids PRS-211,220 and dexanabinol [165]. The authors showed that the *ex vivo* uptake values of PRS-211,220 and dexanabinol by rat CM were 66 and 32%, respectively, and the intestinal lymphatic bioavailability of PRS-211,220 was 6-fold higher than that of dexanabinol [165].

In order to assess if intestinal lymphatic transport of CBD could happen in humans, the uptake of CBD by CM isolated from human volunteers was also assessed in our study. Association values observed in this experiment were similar to the uptake profile seen in rat CM (**Figure 4.5**). Therefore, it is reasonable to assume that similar effects of enhanced intestinal lymphatic bioavailability to orally administered CBD when co-administered with LCT would occur in humans. To the best of our knowledge, this study has described for the first time the *ex vivo* uptake of a drug by isolated human CM and demonstrated no significant difference between the uptake of CBD by human and rat CM. Apparently, both human and rat CM can interchangeably be used to assess CBD's, and perhaps other drugs', uptake. To note, simultaneous with CBD experiments, THC was also shown in our laboratory to have comparable association values with CM isolated from rats and humans [194].

4.5. Conclusions

This study demonstrated that at least one-third of CBD dose would be solubilised and readily available for absorption when orally administered in LCT-formulation at a concentration ≤ 40 mg/mL. Above that concentration, however, the solubilised fraction is inversely proportional to the concentration

of CBD in the formulation. Therefore, *in vitro* lipolysis was successfully applied to determine the optimum concentration of CBD in LCT-based formulation to be used for subsequent *in vivo* experiments. In addition, oral administration of LCT can promote the formation of CM, which can deliver significant fraction of the absorbed CBD to the intestinal lymphatic system. The high potential of intestinal lymphatic transport demonstrated for CBD following oral co-administration of LCT in rats, is likely to occur in humans as well.

5. EFFECT OF LONG-CHAIN TRIGLYCERIDES (LCT) ON PLASMA PHARMACOKINETICS AND BIODISTRIBUTION OF ORALLY ADMINISTERED CANNABIDIOL (CBD) AND Δ^9-TETRAHYDROCANNABINOL (THC)

5.1. Introduction

Cannabis is typically consumed by either smoking or oral ingestion. For many people, smoking is the preferred way of consuming medical cannabis as it allows tailoring of the dose to achieve rapid therapeutic effects [3]. However, this method of delivery is not appropriate in considerable number of patients due to the irritant effects of some components in the smoke, the difficulty of consuming cannabis in smoke-free places, and other potential risks and difficulties associated with the smoking process [248]. Oral ingestion of cannabis or cannabis-based medicines is therefore the preferred route of administration in many cases. When patients self-medicate with cannabis, it is frequently added to cookies or cakes. The vast majority of cannabis-cooking recipes involve the use of dietary lipids (whole milk, butter, or vegetable oil) for the preparation of these cannabis-containing foods. This was attributed to the fact that therapeutically-active cannabinoids are lipid-soluble and therefore easily extracted from cannabis upon preparation with dietary fats [249]. It has also been proposed that the longer the fatty-acid chains in the lipids, the more potent cannabis-effect is expected following oral administration [249, 250]. Cannabidiol (CBD) and Δ^9-tetrahydrocannabinol (THC) are currently available as pharmaceutical formulations. The oral formulations of CBD and THC

(Epidiolex® and Marinol®, respectively) contain sesame oil, which is mostly composed of long-chain triglycerides (LCT). It has been stated that the rationale for adding sesame oil to the formulations is to dissolve the lipid-soluble cannabinoids, CBD and THC [3, 251]. Moreover, many clinical trials have also reported the use of vegetable oils as vehicles to prepare capsules containing cannabis extracts [252-255].

Thus, the available evidence suggests that the use of dietary fats and pharmaceutical lipid-based excipients is common practice in the preparation of cannabis-containing foods and cannabis-based medicinal formulations. However, despite the widespread use of lipids in cannabis formulations, to our knowledge the effect of lipid excipients on the exposure of patients to orally administered cannabis or cannabinoids has not been investigated. Therefore, the aim of this study is to elucidate the effect of oral co-administration of lipids on the exposure to the main cannabinoids, and hence on the therapeutic effect or potential toxicity of cannabis-based treatments.

5.2. Experimental design

5.2.1. Plasma pharmacokinetics experiments

For the determination of plasma pharmacokinetics of cannabinoids following IV and oral administrations to rats, animals were divided into the following 5 treatment groups: IV bolus of CBD at a dose of 4 mg/kg (8 mg/mL solution in propylene glycol–ethanol–sterile water (80:10:10, v/v/v)), oral gavage of CBD or THC at a dose of 12 mg/kg in lipid-free formulation (12 mg/mL solution in propylene glycol–ethanol–sterile water (80:10:10, v/v/v)), and oral gavage of CBD or THC in lipid (LCT)-based formulation at a dose of 12 mg/kg (12 mg/mL solution in sesame oil).

Blood samples were withdrawn and processed for the determination of CBD and THC concentrations as described in chapter 2, sections 2.4 and 2.8.

In addition, THC was administered by IV bolus administration (4 mg/kg, similar to the formulation described above for CBD) to 5 male SD rats. This experiment was performed together with my colleague Jonathan Wong [194]. The plasma concentration-time data of IV THC was used in the current study for the purpose of calulating the absolute bioavailability of THC following oral administration in lipid-free and lipid-based formulations.

5.2.2. Biodistribution experiments

The biodistribution of CBD and THC to MLN was assessed following oral administration in lipid-free and LCT-based formulations (similar to the formulations used in plasma pharmacokinetic studies) to rats. Animals were euthanized at the pre-determined times of maximum plasma concentrations (t_{max}) and one-hour before t_{max} (t_{max} – 1h). These points were obtained from the plasma pharmacokinetic studies. The selection of these points was based on the rational assumption that the transport of a drug to the systemic circulation via the intestinal lymphatic system increases the time-course of drug appearance in plasma. Therefore, at these points, achieving peak levels in the intestinal lymphatic system is likely. Full experimental details are described in chapter 2, sections 2.8.4.1, 2.5, and 2.6. In addition, the biodistribution of cannabinoids to intestinal lymph, spleen, and brain was assessed two hours following oral administration (t_{max} – 1h) to rats as descried in chapter 2, sections 2.8.4.3, 2.4, 2.5, and 2.6.

5.2.3. The dose of lipid

The dose of LCT administered to rats for the plasma pharmacokinetics and biodistribution experiments was 1 mL/kg. This lipid dose was selected as it

allows experimentally feasible measurement and administration of accurate doses of cannabinoids to rats. However, it was demonstrated that lower lipid dose, approximately 0.15 mL/kg, was enough to enhance the intestinal lymphatic transport in rats [134].

5.2.4. Statistical analysis

Results are expressed as mean ± standard error of the mean (SEM). Statistical differences between data sets were assessed using either one-way analysis of variance (ANOVA) with Fisher's LSD test or unpaired two-tailed Student's *t*-test, as appropriate. A p value < 0.05 was considered to represent a significant difference.

5.3. Results

5.3.1. Effect of lipids on plasma pharmacokinetics of orally administered cannabinoids

The plasma concentration-time profiles of CBD following IV bolus administration and oral administrations in lipid-free vehicle and lipid-based formulation are presented in **Figure 5.1**. Plasma concentrations of CBD have markedly increased following the administration of LCT-based formulation compared to the lipid-free formulation. In addition, the co-administration of LCT seems to delay the appearance of quantifiable concentrations of CBD in plasma, implying delayed absorption. Plasma concentration-time profiles following the oral administration of THC in lipid-free vehicle and lipid-based formulation are shown in **Figure 5.2**. Similar to CBD, higher concentrations of THC were recovered in the plasma following oral administration of LCT-based formulation compared to lipid-free formulation. The administration of LCT-based formulation also showed delayed absorption as manifested by the low plasma concentrations

of THC after the co-administration LCT compared to lipid-free formulation at the first assessed time point (30 min). Interestingly, the elimination phase after oral administration of both formulations (LCT-based and lipid-free) was comparable for both cannabinoids.

5.3.1.1. Pharmacokinetic analysis

5.3.1.1.1.Non-compartmental approach

The pharmacokinetic parameters derived from plasma concentration-time profiles of CBD are summarised in **Table 5.1**. The absolute bioavailability of CBD was increased by almost 3-fold following oral administration in lipid-based formulation compared to lipid-free vehicle. For THC, the pharmacokinetic parameters are summarised in **Table 5.2**. The absolute bioavailability of THC was also increased following oral administration in LCT-based formulation by more than 2.5-fold.

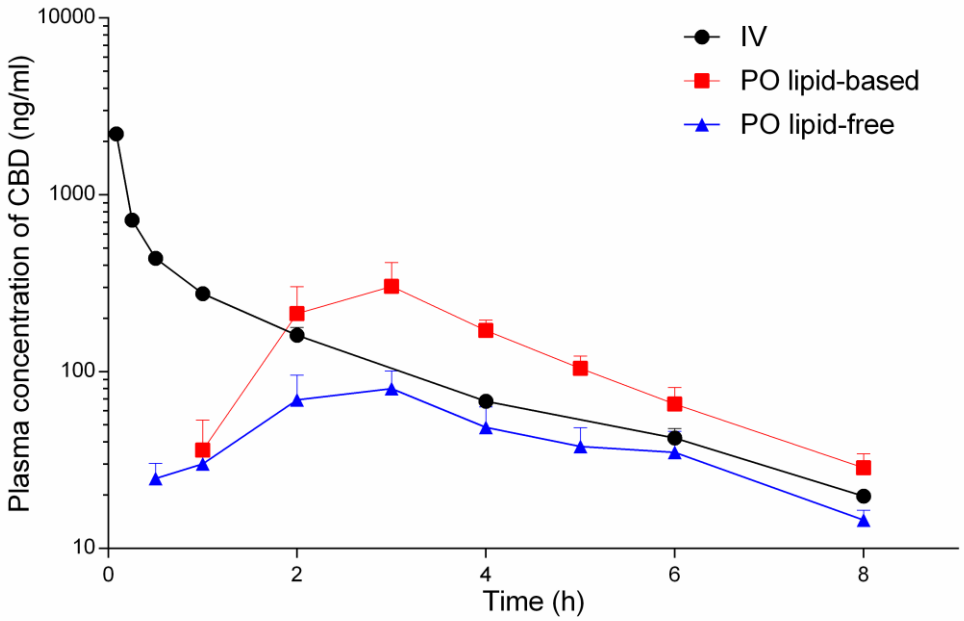

Figure 5.1. Plasma concentration-time profiles of cannabidiol (CBD) following IV bolus (4 mg/kg, n = 4), oral lipid-free formulation (12 mg/kg, n = 4), and long-chain triglyceride (LCT)-based formulation (12 mg/kg, n = 4) to rats. The data are shown as mean ± SEM. Plasma concentrations of CBD assessed at 30 min following the oral administration in LCT-based formulation and 12 h after IV and oral administrations (LCT-based and lipid-free) were below the lower

limit of quantification (LLOQ, 10 ng/mL). Therefore, these concentrations were not reported.

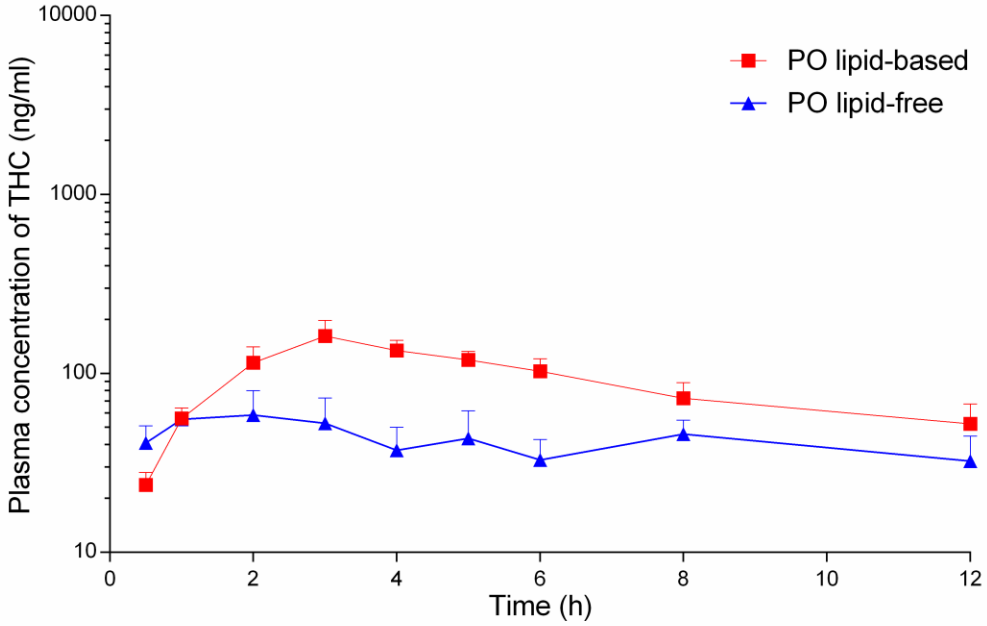

Figure 5.2. Plasma concentration-time profiles of Δ^9-tetrahydrocannabinol (THC) following oral administration of lipid-free formulation (12 mg/kg, n = 6) and long-chain triglyceride (LCT)-based formulation (12 mg/kg, n = 5) to rats. The data are shown as mean ± SEM.

Table 5.1. Pharmacokinetic parameters (mean ± SEM) derived from plasma concentration-time profiles following the administration of IV bolus (4 mg/kg), oral lipid-free formulation (12 mg/kg), and oral long-chain triglyceride (LCT)-based formulation (12 mg/kg) of cannabidiol (CBD) to rats using non-compartmental analysis.

Administration/ formulation	$AUC_{0-\infty}$ (h.ng/mL)	AUC_{0-t} (h.ng/mL)	$V_{d\ ss}$ (mL/kg)	CL (mL/h/kg)	$t_{1/2}$ (h)	C_{max} (ng/mL)	t_{max} (h)	F (%)	n
IV bolus	1436 ± 50	1380 ± 43	5220 ± 145	2794 ± 85	2.0 ± 0.1	-	-	-	4
Oral lipid-free	379 ± 85	327 ± 91	-	-	2.5 ± 0.4	87 ± 25	3	7.9 ± 2.2	4
Oral LCT-based	999 ± 185*	932 ± 188*	-	-	1.6 ± 0.1	308 ± 109	3	22.3 ± 4.6*	4

$AUC_{0-\infty}$, the area under the plasma concentration-time curve from 0 to infinite time; AUC_{0-t}, AUC from 0 to time of last measurable concentration; $V_{d\ ss}$, apparent volume of distribution at steady state; CL, clearance; C_{max}, maximum concentration in plasma; and t_{max}, time to maximum concentration in plasma.
Unpaired *t*-test was used for statistical analysis. * Statistically different from oral lipid-free formulation ($p < 0.05$).

Table 5.2. Pharmacokinetic parameters (mean ± SEM) derived from plasma concentration-time profiles following the administration of IV bolus (4 mg/kg), oral lipid-free formulation (12 mg/kg), and oral long-chain triglyceride (LCT)-based formulation (12 mg/kg) of Δ^9-tetrahydrocannabinol (THC) to rats using non-compartmental analysis.

Administration/ formulation	$AUC_{0-\infty}$ (h.ng/mL)	AUC_{0-t} (h.ng/mL)	$V_{d\ ss}$ (mL/kg)	CL (mL/h/kg)	$t_{1/2}$ (h)	C_{max} (ng/mL)	t_{max} (h)	F (%)	n
IV bolus	1972 ± 438#	1624 ± 334#	9267 ± 2682#	2671 ± 680#	4.6 ± 2.0#	-	-	-	5
Oral lipid-free	790 ± 293	414 ± 130	-	-	6.9 ± 2.0	65 ± 17	2	8.5 ± 2.6	6
Oral LCT-based	1826 ± 615*	1050 ± 169*	-	-	7.4 ± 2.6	172 ± 34	3	21.5 ± 3.5*	5

$AUC_{0-\infty}$, the area under the plasma concentration-time curve from 0 to infinite time; AUC_{0-t}, AUC from 0 to time of last measurable concentration; $V_{d\ ss}$, apparent volume of distribution at steady state; CL, clearance; C_{max}, maximum concentration in plasma; and t_{max}, time to maximum concentration in plasma.
Unpaired *t*-test was used for statistical analysis. * Statistically different from oral lipid-free formulation ($p < 0.05$).
values calculated from the plasma concentration-time profiles of THC following IV bolus administration obtained from [194].

5.3.1.1.2.Compartmental approach

5.3.1.1.2.1. Compartmental analysis of intravenous and oral CBD data

The compartmental analysis of IV data of CBD executed plasma concentration-time profile as one- and two-compartmental models. Three weighing factors were applied for each model: uniform (W_1), $W_{1/C}$ (gives more value to low concentration points), and W_{1/C^2} (gives more value to high concentration points). **Table 5.3** shows the values of Akaike Information Criterion (AIC) and Bayesian information criterion (BIC) for the compartmental analysis of the IV data of CBD. Plots of observed mean plasma concentration-time profile of IV CBD and the predicted values by the compartmental analysis are shown in **Figure 5.3**. Based on AIC and BIC values, and plots of observed and predicted plasma concentrations, two-compartment model calculated by applying a weighing factor of W_{1/C^2} was the best fit for the IV data of CBD (**Table 5.3**, **Figure 5.3 F**). The pharmacokinetic parameters derived from the mean plasma concentration-time profile of IV CBD calculated by two-compartmental analysis are described in **Table 5.4**.

Table 5.3. Akaike Information Criterion (AIC) and Bayesian information criterion (BIC) values calculated by compartmental analysis of mean plasma concentration-time profile of cannabidiol (CBD) following IV bolus administration to rats (4 mg/kg, n = 4).

	One-compartment model			Two-compartment model		
	Weighing factor			Weighing factor		
	W_1	$W_{1/C}$	W_{1/C^2}	W_1	$W_{1/C}$	W_{1/C^2}
AIC	100.7	90.3	66.3	69.4	65.2	52.2
BIC	100.8	90.5	66.5	70	65.5	52.5

Table 5.4. The pharmacokinetic parameters derived from compartmental analysis of mean plasma concentration-time profile of cannabidiol (CBD) following the administration of IV bolus (4 mg/kg, n = 4), oral long-chain triglycerides (LCT)-based formulation (12 mg/kg, n = 4), and oral lipid-free formulation (12 mg/kg, n = 4) to rats.

Variable	IV bolus	Oral LCT-based	Oral lipid-free
$AUC_{0-\infty}$ (h.ng/mL)	1396.3	971.3	347
$V_{d\ ss}$ (mL/kg)	5464.4	-	-
CL (mL/h/kg	2864.6	-	-
C_{max} (ng/mL)	NA	243.9	58.3
t_{max} (h)	NA	3	3
$t_{1/2\alpha}$ (h)	0.1	NA	NA
$t_{1/2\beta}$ (h)	1.9	NA	NA
α (1/h)	8	NA	NA
β (1/h)	0.4	NA	NA
A (ng/mL)	3410.5	NA	NA
B (ng/mL)	359.9	NA	NA
K01 (1/h)	NA	0.97	0.46
K10 (1/h)	2.7	0.5	0.5
K12 (1/h)	4.6	NA	NA
K21 (1/h)	1.1	NA	NA
T lag (h)	NA	0.9	0.2

For the oral data of CBD, only two compartmental models could be fitted. These are one-compartment and one-compartment with lag time for absorption. Three weighing factors were also applied for oral data. The values of AIC and BIC for the compartmental analysis of mean plasma concentration-time profiles following oral administration of CBD in LCT-based and lipid-free formulations are presented in **Table 5.5**. Plots of observed mean plasma concentration-time profiles of oral CBD and the predicted values by the compartmental analysis are shown in **Figure 5.4** and **Figure 5.5** for LCT-based and lipid-free formulations, respectively. Based on lowest AIC and BIC values, and plots of observed and predicted plasma concentrations, oral data of CBD (both from lipid-based and

lipid-free oral administrations) fit one-compartment with lag time for absorption model applying a weighing factor of W_{1/C^2} (**Table 5.5**, **Figure 5.4 F** and **Figure 5.5 F**). The pharmacokinetic parameters derived from mean plasma concentration-time profile of oral CBD calculated by two-compartmental analysis are described in **Table 5.4**.

Table 5.5. Akaike Information Criterion (AIC) and Bayesian information criterion (BIC) values calculated by compartmental analysis of mean plasma concentration-time profiles following oral administration of cannabidiol (CBD) in long-chain triglycerides (LCT)-based and lipid-free formulations.

		One-compartment no lag time for absorption			One-compartment with lag time for absorption		
		Weighing factor			Weighing factor		
		W_1	$W_{1/C}$	W_{1/C^2}	W_1	$W_{1/C}$	W_{1/C^2}
LCT-based formulation	AIC	78.4	75	65.6	68	58.7	46.1
	BIC	78.3	74.9	65.5	67.9	58.5	45.9
lipid-free formulation	AIC	60.4	57	51.3	57.9	54.9	49.8
	BIC	60.7	57.3	51.5	58.2	55.3	50

5.3.1.1.2.2. Compartmental analysis of oral THC data

The values of AIC and BIC for the compartmental analysis of mean plasma concentration-time profiles following oral administration of THC in LCT-based and lipid-free formulations are presented in **Table 5.6**. Plots of observed mean plasma concentration-time profiles of oral THC and the predicted values by the compartmental analysis are shown in **Figure 5.6** and **Figure 5.7** for LCT-based and lipid-free formulations, respectively. Based on lowest AIC and BIC values, and the plots of observed and predicted plasma concentrations, oral data of THC following the administration of LCT-based formulation fit one-compartment with lag time for absorption model applying a weighing factor of W_{1/C^2} (**Table 5.6**, **Figure 5.6 F**). Whereas, oral data of THC following the administration of lipid-

free formulation fit one-compartment model (without lag time for absorption) applying a weighing factor of W_1 (**Table 5.6**, **Figure 5.7 A**). The pharmacokinetic parameters derived from mean plasma concentration-time profiles of oral THC calculated by compartmental analysis are described in **Table 5.7**.

Table 5.6. Akaike Information Criterion (AIC) and Bayesian information criterion (BIC) values calculated by compartmental analysis of mean plasma concentration-time profiles following oral administration of Δ^9-tetrahydrocannabinol (THC) in long-chain triglycerides (LCT)-based and lipid-free formulations.

		One-compartment no lag time for absorption			One-compartment with lag time for absorption		
		Weighing factor			Weighing factor		
		W_1	$W_{1/C}$	$W_{1/C}^2$	W_1	$W_{1/C}$	$W_{1/C}^2$
LCT-based formulation	AIC	75.2	73.8	68.7	70.8	67.5	60.5
	BIC	75.8	74.4	69.3	71.6	68.3	61.3
lipid-free formulation	AIC	57.9	58.3	58.2	74	74.3	74.2
	BIC	58.5	58.9	58.8	74.8	75	75

Table 5.7. The pharmacokinetic parameters derived from mean plasma concentration-time profiles following oral administration of Δ^9-tetrahydrocannabinol (THC) in long-chain triglycerides (LCT)-based formulation (12 mg/kg, n = 5) and lipid-free formulation (12 mg/kg, n = 6)

Variable	Oral LCT-based	Oral lipid-free
$AUC_{0-\infty}$ (h.ng/mL)	1364.5	1022
C_{max} (ng/mL)	127	58.3
t_{max} (h)	3	2
K01 (1/h)	0.6	2.8
K10 (1/h)	0.2	0.06
T lag (h)	0.3	NA

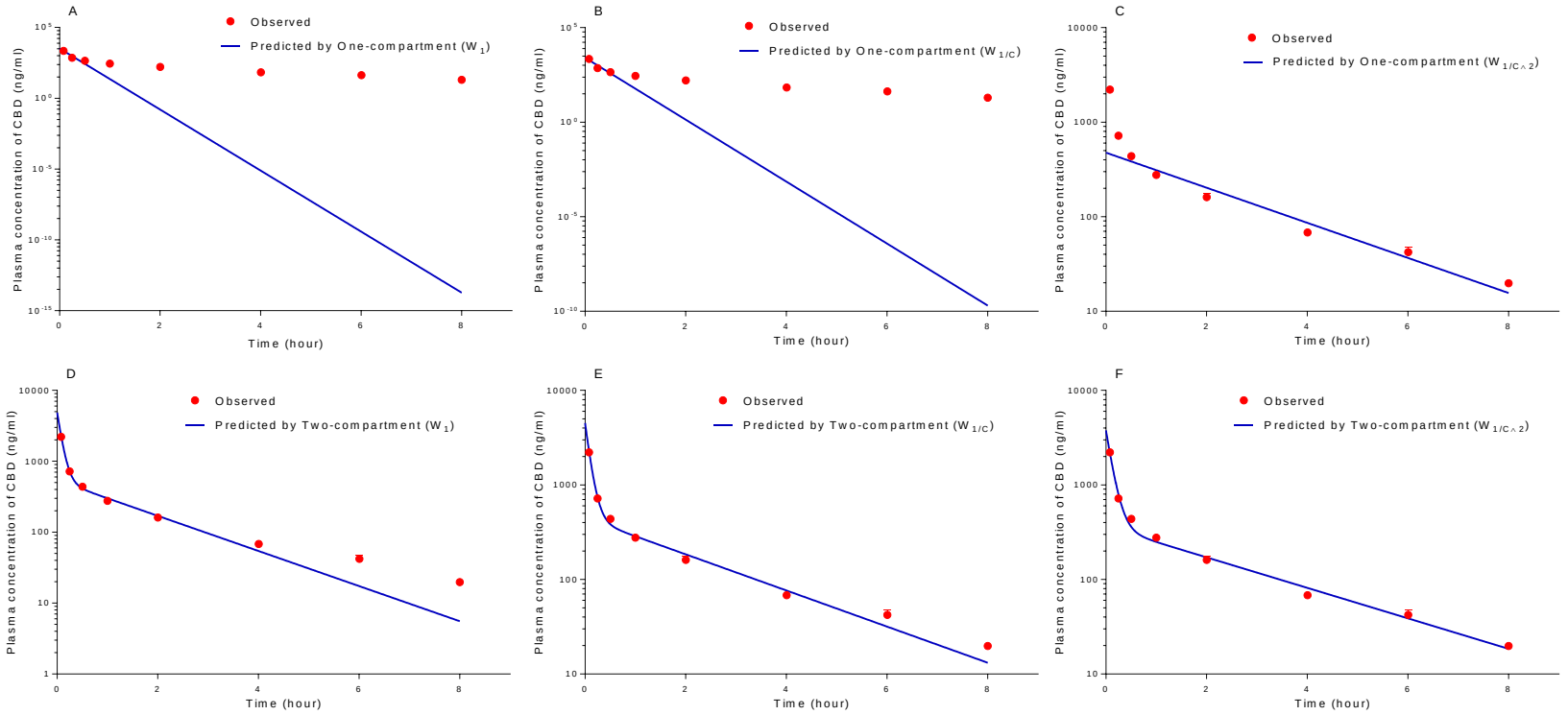

Figure 5.3. Plots of observed mean plasma concentration-time profile of IV bolus administration of cannabidiol (CBD) to 4 SD rats and the predicted values by compartmental analysis. **Panel A**: one-compartment model applying uniform (W_1) weighing factor. **Panel B**: one-compartment model applying weighing factor of $W_{1/C}$. **Panel C**: one-compartment model applying weighing

factor of $W_{1/C}^2$. **Panel D**: two-compartment model applying uniform (W_1) weighing factor. **Panel E**: two-compartment model applying weighing factor of $W_{1/C}$. **Panel F**: two-compartment model applying weighing factor of $W_{1/C}^2$.

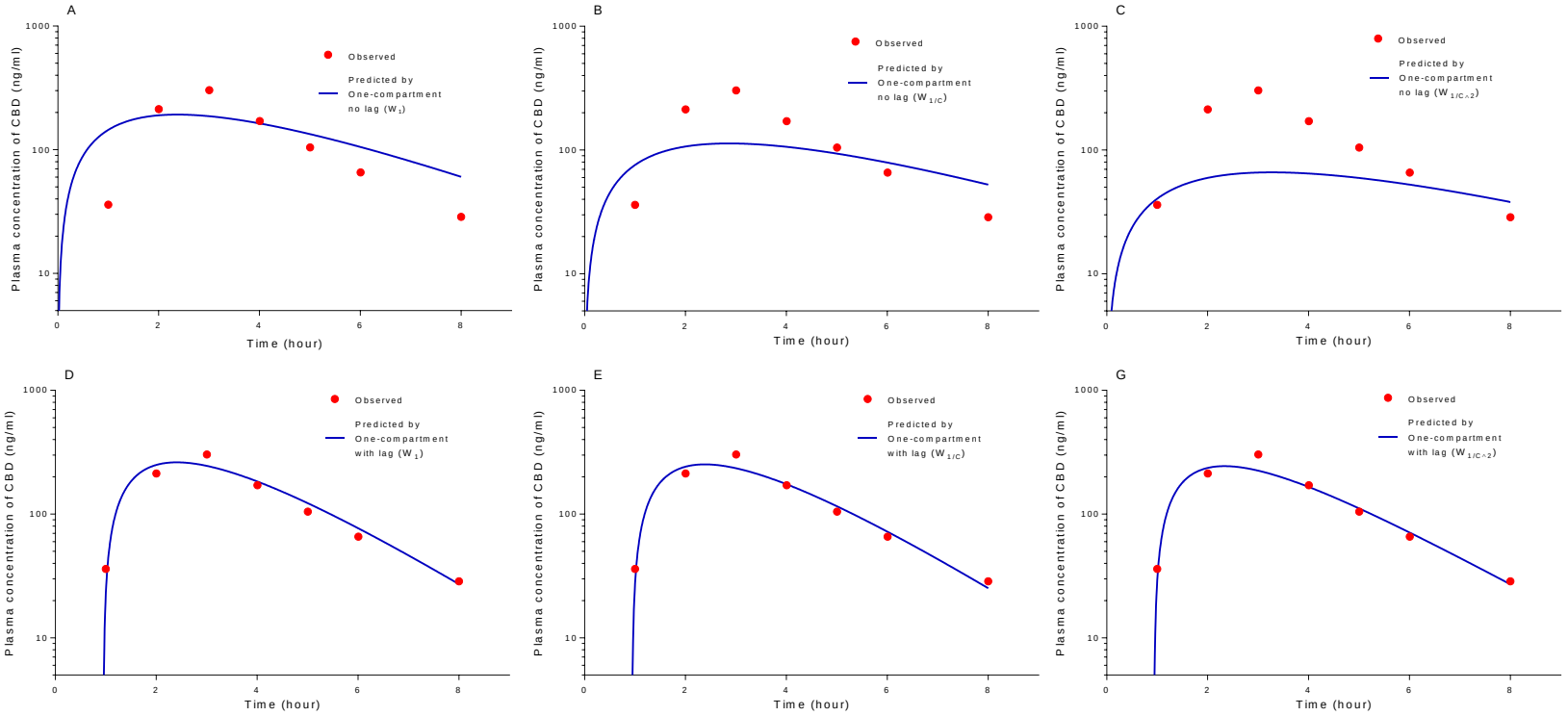

Figure 5.4. Plots of observed mean plasma concentration-time profile following oral administration of cannabidiol (CBD, 12 mg/kg) in long-chain triglycerides (LCT)-based formulation to 4 SD rats and the predicted values by compartmental analysis. **Panel A**: one-compartment without lag time for absorption model applying uniform (W_1) weighing factor. **Panel B**: one-compartment without lag time for absorption model applying weighing factor of $W_{1/C}$. **Panel C**: one-compartment without lag time for absorption model applying weighing factor of $W_{1/C}^2$. **Panel D**: one-compartment with lag time for absorption model

applying uniform (W_1) weighing factor. **Panel E**: one-compartment with lag time for absorption model applying weighing factor of $W_{1/C}$. **Panel F**: one-compartment with lag time for absorption model applying weighing factor of $W_{1/C}^2$.

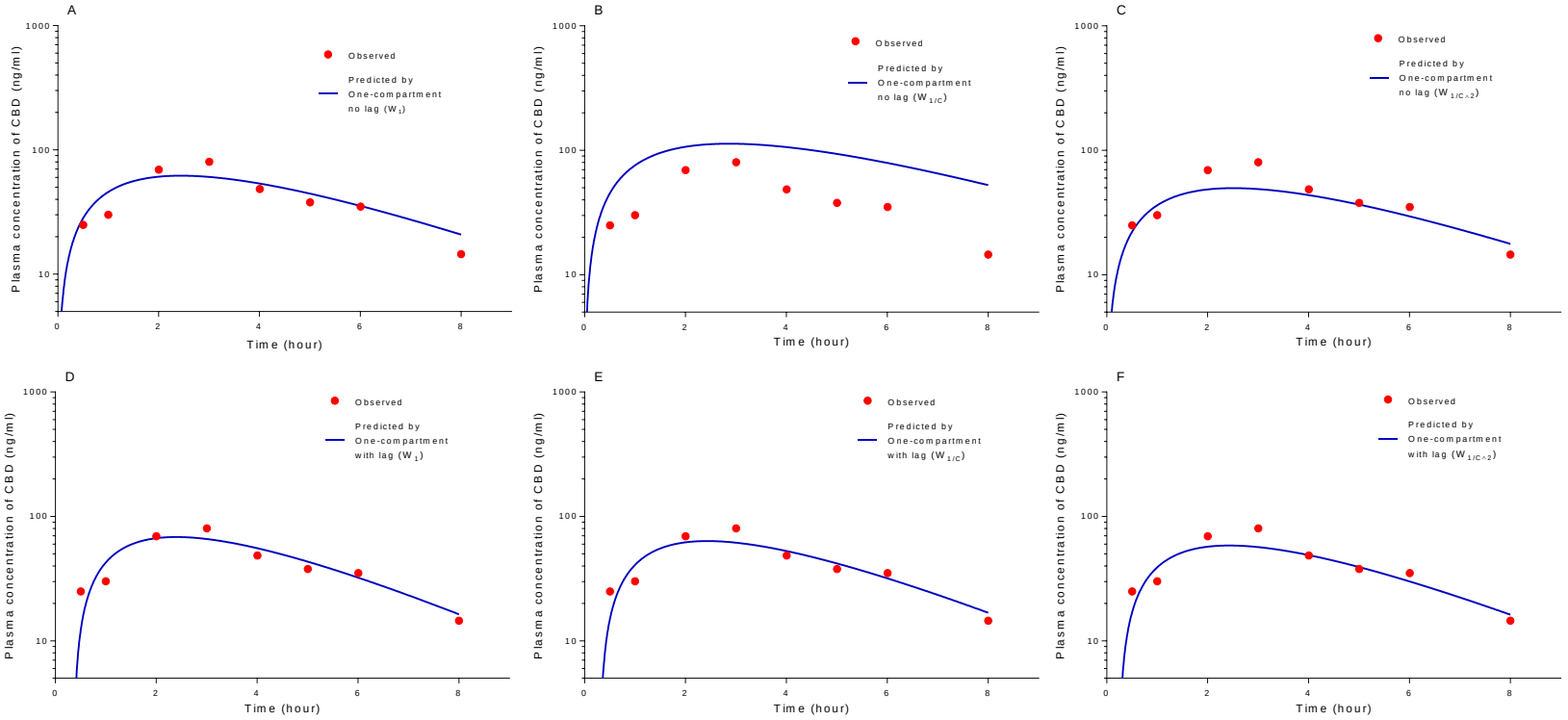

Figure 5.5. Plots of observed mean plasma concentration-time profile following oral administration of cannabidiol (CBD, 12 mg/kg) in lipid-free formulation to 4 SD rats and the predicted values by compartmental analysis. **Panel A**: one-compartment without lag time for absorption model applying uniform (W_1) weighing factor. **Panel B**: one-compartment without lag time for absorption model applying weighing factor of $W_{1/C}$. **Panel C**: one-compartment without lag time for absorption model applying weighing factor of $W_{1/C}^2$. **Panel D**: one-compartment with lag time for absorption model applying uniform (W_1) weighing factor.

Panel E: one-compartment with lag time for absorption model applying weighing factor of $W_{1/C}$. **Panel F**: one-compartment with lag time for absorption model applying weighing factor of $W_{1/C}^2$.

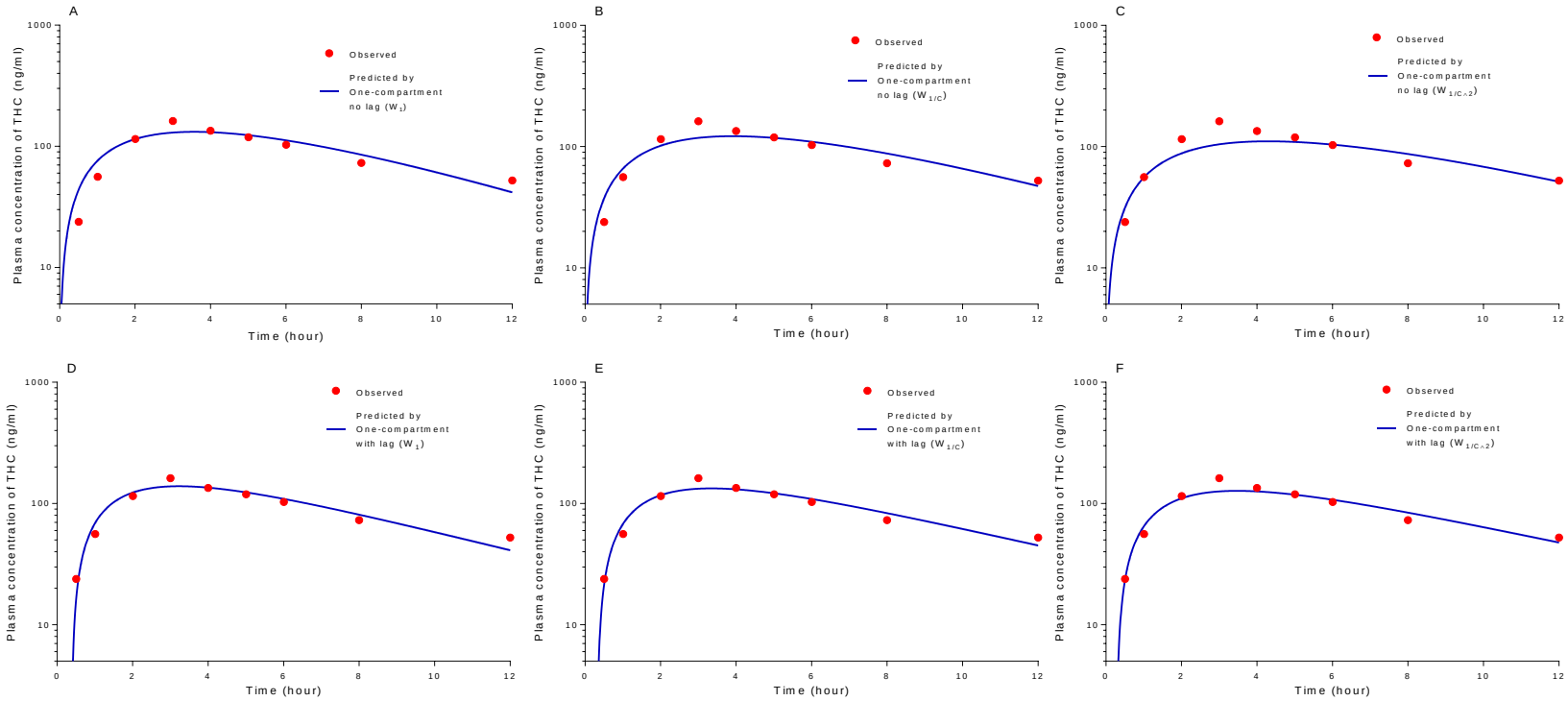

Figure 5.6. Plots of observed mean plasma concentration-time profile following oral administration of Δ^9-tetrahydrocannabinol (THC, 12 mg/kg) in long-chain triglycerides (LCT)-based formulation to 5 SD rats and the predicted values by compartmental analysis. **Panel A**: one-compartment without lag time for absorption model applying uniform (W_1) weighing factor. **Panel B**: one-compartment without lag time for absorption model applying weighing factor of $W_{1/C}$. **Panel C**: one-compartment without lag time for absorption model applying weighing factor of $W_{1/C}^2$. **Panel D**: one-compartment with lag time for absorption model

applying uniform (W_1) weighing factor. **Panel E**: one-compartment with lag time for absorption model applying weighing factor of $W_{1/C}$. **Panel F**: one-compartment with lag time for absorption model applying weighing factor of $W_{1/C}^2$.

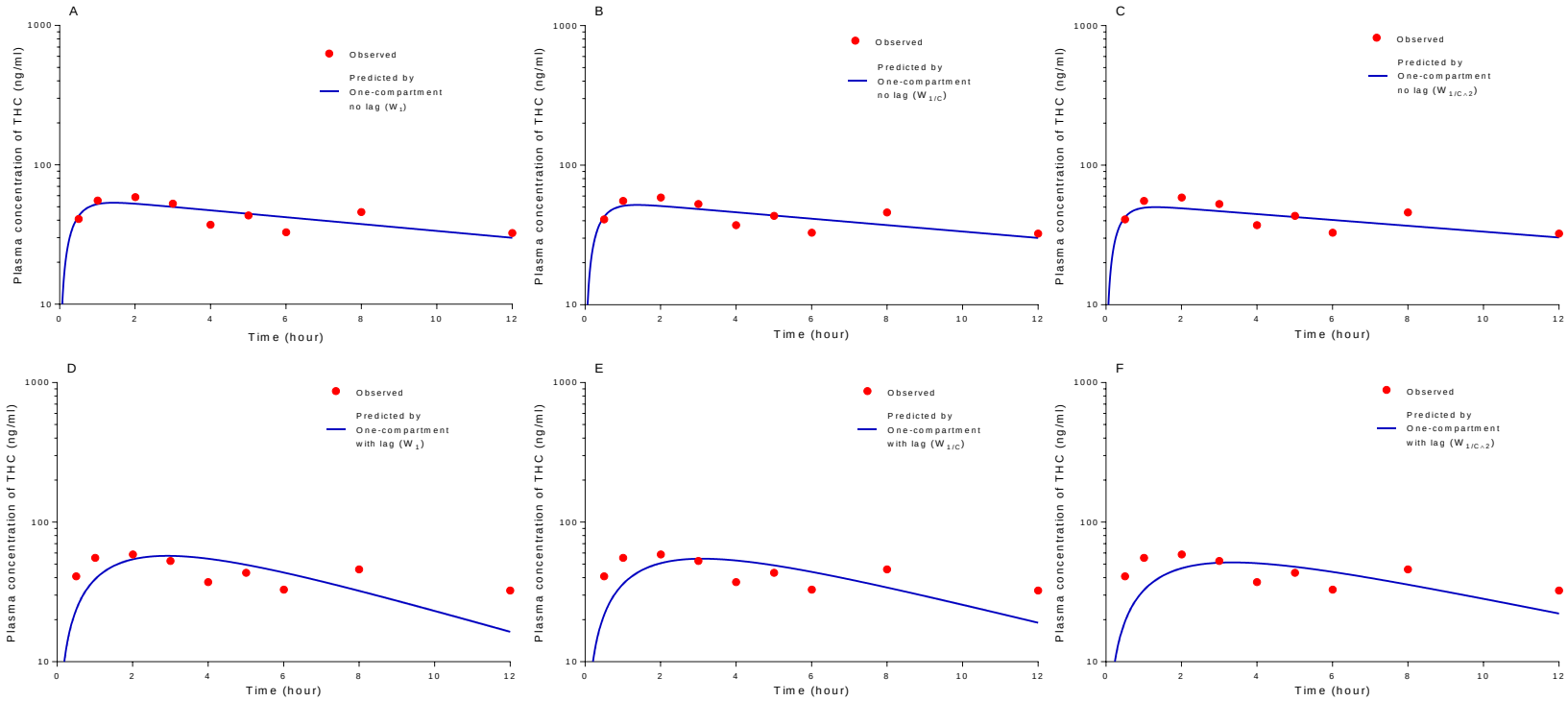

Figure 5.7. Plots of observed mean plasma concentration-time profile following oral administration of Δ^9-tetrahydrocannabinol (THC, 12 mg/kg) in lipid-free formulation to 6 SD rats and the predicted values by compartmental analysis. **Panel A**: one-compartment without lag time for absorption model applying uniform (W_1) weighing factor. **Panel B**: one-compartment without lag time for absorption model applying weighing factor of $W_{1/C}$. **Panel C**: one-compartment without lag time for absorption model applying weighing factor of $W_{1/C}^2$. **Panel D**: one-compartment with lag time for absorption model applying uniform (W_1) weighing

factor. **Panel E**: one-compartment with lag time for absorption model applying weighing factor of $W_{1/C}$. **Panel F**: one-compartment with lag time for absorption model applying weighing factor of $W_{1/C}^2$.

5.3.2. Effect of lipids on the biodistribution of orally administered cannabinoids

5.3.2.1. Biodistribution of cannabinoids to the mesenteric lymph nodes (MLN) of rats

The concentrations of CBD and THC found in MLN following oral administration with LCT were profoundly higher than those observed after administration in lipid-free formulations to rats at t_{max} and one-hour prior to t_{max} (**Figure 5.8 A** and **B**).

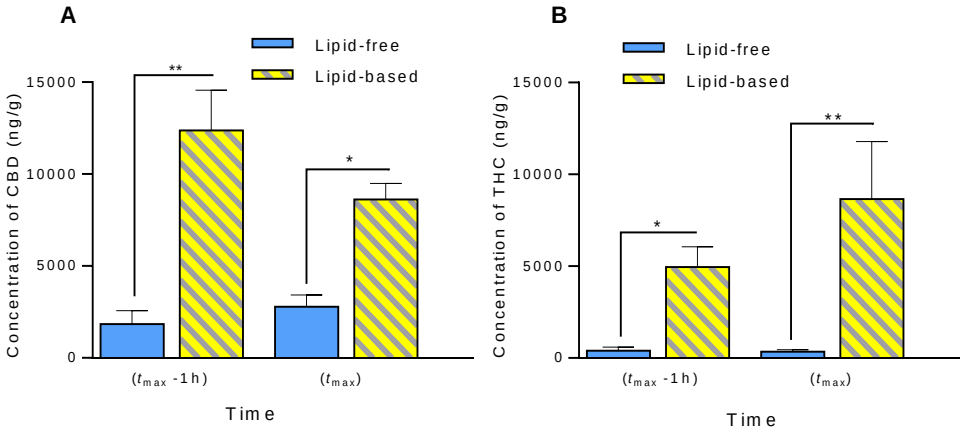

Figure 5.8. Distribution of cannabinoids to mesenteric lymph nodes (MLN) following oral administration of lipid-free and lipid-based formulations (solution of cannabinoids in sesame oil) to rats. **Panel A**: concentration of cannabidiol (CBD) found in MLN at time of maximum concentration in plasma (t_{max}) and one-hour prior to t_{max} (t_{max} – 1 h) following oral administration of lipid-free formulation (12 mg/kg, n = 3 at t_{max}, n = 3 at t_{max} – 1h), and long-chain triglycerides (LCT)-based formulation (12 mg/kg, n = 3 at t_{max}, n = 3 at t_{max} – 1h) to rats. **Panel B**: concentration of Δ^9-tetrahydrocannabinol (THC) found in MLN at t_{max} and t_{max} – 1h following oral administration of lipid-free formulation (12 mg/kg, n = 5 at t_{max}, n = 4 at t_{max} – 1h), and LCT-based formulation (12 mg/kg, n = 3 at t_{max}, n = 4 at t_{max} – 1h) to rats. Values are expressed as mean ± SEM. Statistical analysis was performed using unpaired two-tailed Student's *t*-test. * $p < 0.05$; ** $p < 0.01$. The concentrations of THC found in MLN at t_{max}

were obtained together with my colleague Jonathan Wong [194] and are used here for the purpose of comparison.

5.3.2.2. Biodistribution of cannabinoids to plasma, intestinal lymph fluid, spleen, and brain of rats.

Figure 5.9 shows the concentrations of CBD and THC in lymph fluid, plasma, spleen, and brain one-hour prior to t_{max} following oral administration of CBD and THC in LCT-based formulations. Profoundly higher concentrations of cannabinoids were observed in lymph fluid compared with plasma, spleen, and brain. CBD concentration in intestinal lymph fluid was as much as 250-, 500-, and 360-fold higher than the concentration in plasma, spleen, and brain, respectively (**Figure 5.9 A**). The concentration of THC was 100-, 270-, and 600-fold higher in lymph than in plasma, spleen, and brain, respectively (**Figure 5.9 B**). No significant differences were observed in the distribution of CBD and THC between plasma, spleen, and brain (**Figure 5.9**).

To assess the effect of LCT co-administration on the biodistribution of CBD and THC to lymphoid tissues in the intestinal lymphatic system (MLN) and the distribution to the largest lymphatic tissue in the central compartment (the spleen), the concentrations of cannabinoids in MLN were compared with those found in spleen (**Figure 5.10**). **Figure 5.10** shows that significantly higher levels of cannabinoids were found in MLN compared to spleen. The concentrations in MLN were more than 50-fold and 20-fold higher than in spleen for CBD and THC, respectively (**Figure 5.10**).

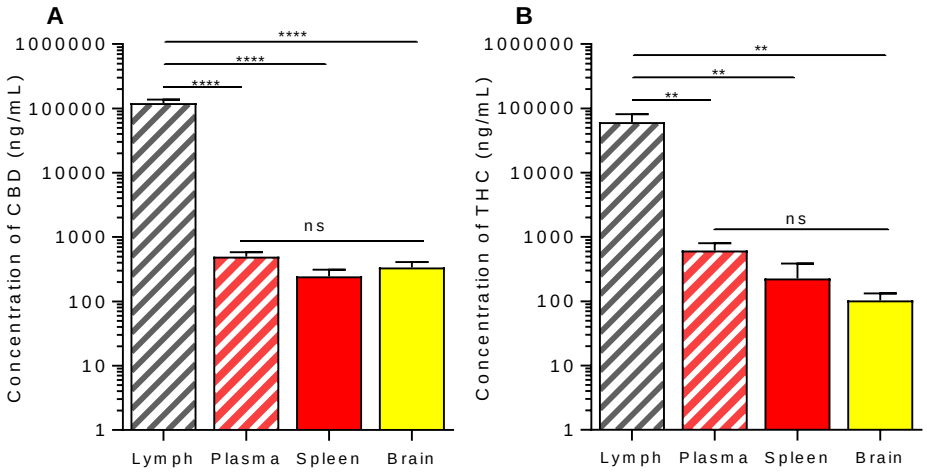

Figure 5.9. Concentration of cannabinoids recovered in intestinal lymph fluid, plasma, spleen, and brain following oral administration of lipid-based formulations (solution of cannabinoids in sesame oil) to rats. **Panel A:** concentration of cannabidiol (CBD) in lymph fluid (n = 3), plasma (n = 3), spleen (n = 6), and brain (n = 7) two hours (one-hour prior to t_{max}) following oral administration of long-chain triglyceride (LCT)-based formulation (12 mg/kg) to rats. **Panel B:** concentration of Δ^9-tetrahydrocannabinol (THC) in lymph fluid (n = 4), plasma (n = 4), spleen (n = 3), and brain (n = 3) two hours (one-hour prior to t_{max}) following oral administration of LCT-based formulation (12 mg/kg) to rats. Values are expressed as mean ± SEM. Statistical analysis

was performed using one-way ANOVA with Fisher's LSD test. ** $p < 0.01$; **** $p < 0.0001$.

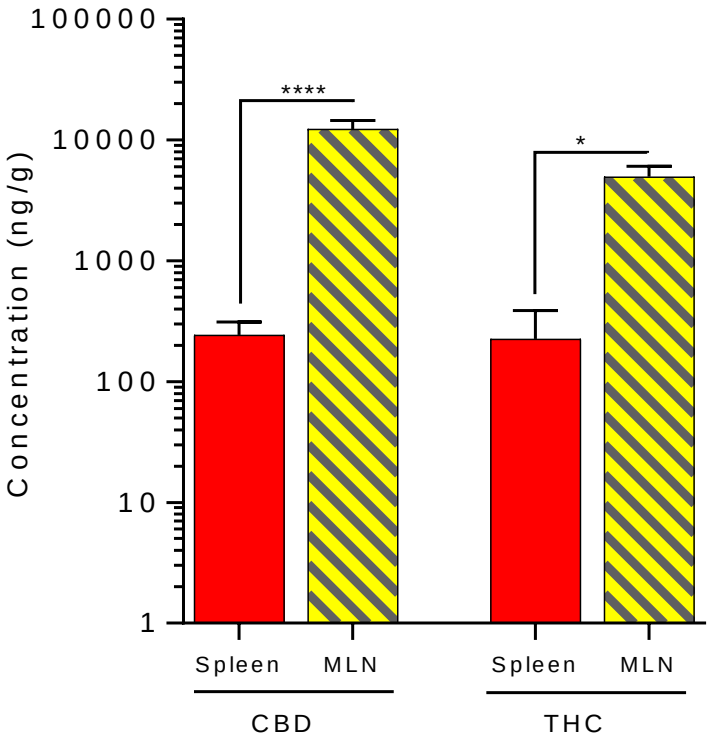

Figure 5.10. Concentration of cannabidiol (CBD) and Δ^9-tetrahydrocannabinol (THC) recovered in spleen (n = 6 and 3, respectively) and mesenteric lymph nodes (MLN, n = 3 and 4, respectively) two hours (one-hour prior to t_{max}) following oral administration of long-chain triglycerides (LCT)-based formulations to rats. Values are expressed as mean ± SEM. Statistical analysis was performed using unpaired two-tailed Student's *t*-test. * $p < 0.05$; **** $p < 0.0001$.

5.4. Discussion

Over the last few years, the medicinal use of cannabis has gained growing interest after a long period of marginalization [256]. The legalisation of medical cannabis programs has noticeably increased the access of patients to cannabis and cannabis-based medicines in many countries [11]. For many patients, orally administered cannabis and cannabis-based medicines are preferred over other

routes of administration [3, 26]. Orally administered cannabis is often consumed with dietary fat-containing food (such as cookies). Lipids are also commonly used in pharmaceutical formulations of cannabis or cannabinoids. The rationale for the use of dietary fats and lipids is to enhance the extraction of the lipid-soluble active constituents [3, 249, 250]. However, the impact of dietary fats or pharmaceutical lipid excipients on the systemic exposure of patients to the cannabinoids has not previously been explored. This could be of particular importance when it comes to therapeutic efficacy or potential toxicity. We have demonstrated in the previous chapter the effect of lipids, particularly LCT, on the intestinal solubilisation of orally administered CBD (comparable results were also demonstrated for THC [194]). In this study we aimed to assess the effect of lipids on the systemic exposure to CBD and THC following oral consumption with dietary fats or oral administration of cannabis-based medicines.

5.4.1. Effect of lipids on the systemic bioavailability of orally administered cannabinoids

Based on the non-compartmental analysis of the plasma concentration-time profiles, the co-administration of cannabinoids with lipids enhances the bioavailability of CBD in rats by almost 3-fold (**Figure 5.1** and **Table 5.1**) and of THC by more than 2.5-fold (**Figure 5.2** and **Table 5.2**). Such a profound increase in systemic exposure can significantly affect the therapeutic effects or toxicity of these cannabinoids. To the best of our knowledge there are no previously reported studies of absolute oral bioavailability of these cannabinoids in rats. In humans, the reported bioavailabilities of CBD and THC, based on a very limited available number of studies, were less than 10% [24, 28, 29]. In our study, oral administration of THC and CBD in lipid-free formulations to rats

showed similar range of bioavailability to that reported in humans (**Table 5.1** and **Table 5.2**). The low oral bioavailability of CBD and THC following oral administration of lipid-free formulations is consistent with the fact that CBD and THC exhibit substantial first-pass metabolism [37, 38]. Indeed, higher bioavailabilites were reported after administration by routes that avoid hepatic first-pass metabolism such as inhalation of CBD [24] and THC [29, 257], or rectal administration of THC [37]. The absorption of dietary lipids from the LCT-based formulations involves the formation of chylomicrons (CM) in enterocytes [162, 163]. These CM could therefore act as carriers to transfer CBD and THC to the systemic circulation via the intestinal lymphatic system (high association values were demonstrated for CBD (chapter 4, section 4.3.1.2) and THC [194] with rat and human CM). Drugs that are transported via the intestinal lymphatic system avoid hepatic first-pass metabolism and therefore achieve significantly higher bioavailability than after administration in lipid-free formulation [165]. Therefore, it is prudent to propose that the primary mechanism underlying the enhanced exposure to CBD and THC when co-administered with LCT in rats is intestinal lymphatic transport. Similar observations were previously reported for the synthetic lipophilic cannabinoid PRS-211,220, which had association values with rat CM comparable to CBD and THC, and showed 3-fold increase in oral bioavailability following oral administration with LCT compared to lipid-free formulation to rats [165]. As mentioned earlier, the association values of CBD and THC with CM isolated from human volunteers were similar to the uptake profile seen in rat CM. Therefore, it is reasonable to assume that similar effects of increased systemic exposure to orally administered cannabinoids when co-administered with lipids would occur in humans.

It remains unclear if there is a minimal amount of lipids that is required to activate intestinal lymphatic transport mechanism. Some studies show that

as little as 1 g of lipid emulsion was sufficient to activate intestinal lymphatic transport of a highly lipophilic compound in dogs [258]. In contrast, it has been demonstrated that the administration of a low dose of lipids to rats (equivalent to 1 g in humans) was not sufficient to enhance intestinal lymph flow. However, a higher lipid dose (equivalent to 10 g in humans) significantly increased lymph flow [134]. These amounts of lipids can easily be obtained from the average meal in Western diet [259]. It currently remains unclear if the administration of a small-volume capsule with lipid-based formulation of cannabinoids (such as Marinol®; contains synthetic THC) in fasting conditions would activate lymphatic transport and increase significantly the bioavailability of cannabinoids. Indeed, low bioavailability of cannabinoids were reported in humans after oral administration in low volumes of lipid-based formulations (0.25 – 0.5 mL capsules containing the drug dissolved in sesame oil) under fasting conditions [23, 28]. However, our results suggest that the same lipid-based formulation-containing capsule administered with a meal, or lipid-rich cannabis-containing cookies, may result in a profound increase in systemic exposure, similar to what has been observed in this study in a rat model.

In addition to the non-compartmental analysis described above, plasma concentration-time profiles were also assessed by compartmental approach. The disposition (distribution and elimination) of IV CBD showed the characteristic biexponential curve of two-compartment model (**Figure 5.1**). AIC and BIC values (**Table 5.3**), and plots of observed vs predicted concentrations (**Figure 5.3 F**) also confirmed that the two-compartment model is the best fit for IV CBD data. The rapid distribution phase observed for CBD is consistent with its high lipophilic nature (log *P* 6.53), which suggests rapid penetration and distribution to highly blood-perfused tissues as well as high metabolism in the liver. For oral CBD, plasma profiles following the administration of LCT-based

and lipid-free formulations were fitted to one-compartment with lag time for absorption model, guided by AIC and BIC values and visual inspection of observed vs predicted concentrations plots (**Table 5.5**, **Figure 5.4 F**, and **Figure 5.5 F**). The mono-exponential elimination phase of the semi-log plasma concentration-time profiles of oral data confirms further the one-compartment kinetic model (**Figure 5.1**). A comparison of the lag times for absorption of LCT-based and lipid-free formulations (0.9 and 0.2 h, respectively (**Table 5.4**)), reveals possible effect of formulation on gastric emptying time and/or the rate of drug dissolution. In fact, it was previously demonstrated that oral administration of LCT can increase gastric emptying time [230]. In addition, intestinal lymphatic transport could be another reason for the increase in time-course appearance of CBD in plasma following administration in LCT-formulation compared to lipid-free formulation.

In regards to oral THC, plasma profile following the administration of LCT-based formulation was best fitted to one-compartment with lag time for absorption model whereas lipid-free formulation fitted to one-compartment model without lag time (**Table 5.6** and **Table 5.7**). Similar to CBD, the LCT-based formulation of THC showed delayed absorption compared with lipid-free formulation, which could also imply the involvement of gastric emptying time and intestinal lymphatic transport.

It should be noted that the compartmental approach is based on the theoretical assumption that the body is composed of one or more compartment that might not have direct physiological meaning [260]. Therefore, the kinetic parameters from compartmental analysis should be integrated with caution and only be used as a guide for further investigations.

5.4.2. Effect of lipids on the biodistribution of orally administered cannabinoids

As mentioned above, the systemic bioavailability of CBD and THC was significantly enhanced when administered orally in conditions facilitating intestinal lymphatic transport, specifically co-administration with LCT. The results of biodistribution experiments indicate that the intestinal lymphatic transport of CBD and THC was, indeed, enhanced following oral co-administration of lipids as denoted by the dramatic increase in the concentrations recovered in MLN (**Figure 5.8 A** and **B**). It is important to note the extremely high concentrations of cannabinoids recovered in intestinal lymph fluid compared with plasma, spleen, and brain (**Figure 5.9**). The concentrations of CBD and THC in intestinal lymph fluid were in the range of 120 and 60 µg/mL compared to 0.5 and 0.6 µg/mL in plasma, respectively. Similar trends were previously reported for other lipophilic compounds, dexanabinol and PRS-211,220, when orally administered with LCT to rats [165]. To note, the concentrations of CBD and THC in the intestinal lymph fluid were 10 and 12-fold, respectively, higher than in MLN (**Figure 5.9** and **5.10**). This is related to the fact that cannabinoids are delivered to the MLN via the intestinal lymph fluid, which flows through the sinuses compartment of MLN (**Figure 1.5**). Other lymph-free compartments of MLN architecture, particularly the lobules and capsule [261], as well as the surrounding connective tissue act as dilution to the lymph fluid contained in MLN when MLN are homogenised for the determination of cannabinoids. In addition, CBD and THC showed comparable distribution to plasma, spleen, and brain (**Figure 5.9**). These results are in line with the results reported by Deiana *et al* [209] who demonstrated comparable concentrations of CBD in plasma and brain two hours following oral

administration to rats. Alozie *et al* [42], however, reported higher concentrations of THC in plasma compared to brain following IV bolus administration. The discrepancy between our results and those reported by Alozie *et al* [42] could be related to the fact that radioactivity-based assay was used for the determination of THC in that study, which is often non-specific in terms of differentiating THC from its metabolites. Moreover, our study has demonstrated, for the first time, that the biodistribution of CBD and THC to lymphoid tissues in the intestinal lymphatic system (MLN) was substantially higher than the distribution to the largest lymphatic tissue in the central compartment, the spleen (**Figure 5.10**). Therefore, given our findings, we suggest that oral administration with dietary lipids represents a valid targeting approach of CBD and THC to lymphoid tissues in the intestinal lymphatic system.

It is well recognised that the intestinal lymphatic system is the major host of immune cells [127, 133, 134], the main pathway of intestinal tumour metastases [157, 158], and the place where some viruses like human immunodeficiency virus spread and develop [159]. Thus, the approach described in this study could be of high therapeutic value for targeting pharmacological agents such as immunomodulators, some chemotherapeutic agents, and anti-infective agents to the intestinal lymphatic system.

5.5. Conclusions

In conclusion, co-administration of dietary lipids or pharmaceutical lipid excipients can substantially increase the systemic exposure to orally administered cannabis or cannabis-based medicines. Our data indicate that the primary mechanism of the increased absorption of cannabinoids in the presence of lipids is intestinal lymphatic transport. The amount of lipids present in

cannabis-containing foods, or following a high-fat meal, is sufficient to activate intestinal lymphatic transport and lead to increased systemic exposure to cannabinoids. The increase in systemic exposure to cannabinoids in humans is of potentially high clinical importance as it could turn a barely effective dose of orally administered cannabis into highly effective one, or indeed a therapeutic dose into a toxic one. Therefore, it is important for cannabis-prescribing clinicians and those who self-medicate with cannabis to carefully consider the effect of the co-administration of lipids on the therapeutic outcomes of orally administered cannabis or cannabis-based medicines. Even of a higher importance is the fact that the co-administration of cannabis or cannabis-based medicines with lipids results in extremely high levels of lipophilic cannabinoids in the intestinal lymphatic system. At these high local concentrations, cannabinoids could produce pharmacological effects on immune cells within the intestinal lymphatic system.

6. IMMUNOMODULATORY EFFECTS OF CANNABIDIOL (CBD) AND Δ^9-TETRAHYDROCANNABINOL (THC)

6.1. Introduction

The therapeutic immunomodulatory effects of cannabidiol (CBD) and Δ^9-tetrahydrocannabinol (THC) have recently been receiving considerable attention [57, 184]. CBD has been shown to be effective following oral administration in lipid-based formulations or parenteral injections in animal models of a number of debilitating diseases caused by over-reactive immune responses (autoimmune and inflammatory diseases) including multiple sclerosis (MS) [116], rheumatoid arthritis [262], diabetes mellitus [263], allergic asthma [264], autoimmune hepatitis [265] and colitis [266]. Similarly, THC has been shown to be beneficial following oral administration in lipid-based formulations or parenteral injections in MS [267], diabetes mellitus [268], and allergic asthma [264] animal models. The proposed mechanisms governing these effects involve the ability of CBD and THC at relatively high concentrations to suppress lymphocyte proliferation and inflammatory cytokine production [116, 262-266, 269]. This is supported by immunosuppressive effects that have been detected in *in vitro* studies [61, 62]. Nevertheless, only a few human studies have been conducted to assess the immunomodulatory effects of cannabinoids in patients suffering from autoimmune diseases, particularly MS. These studies showed no clear evidence for the immunosuppressive effects following oral administration of low-amount lipid-containing formulations of cannabinoids [270, 271]. In fact, Killestein *et al* [270] suggested a moderate pro-

inflammatory potential in MS patients treated with orally administered cannabis extract. Katona *et al* [271] showed that the discrepancy between animal and human studies could be, in part, due to the high oral doses of cannabinoids used in animals (8-40 mg/kg) compared to around 0.25 mg/kg in human trials, which results in plasma levels in human in the range of 5 ng/mL. These low levels of cannabinoids detected in human plasma are consistent with the extensive first-pass metabolism reported for CBD and THC after oral administration [37, 38].

We have demonstrated in chapter 5 that oral co-administration of CBD and THC with sufficient amount of long-chain triglycerides (LCT), equivalent to moderate- to high-fat meals in humans, can enhance systemic bioavailability in rats (**Figure 5.1** and **Figure 5.2**). Even more important, extremely high concentrations of cannabinoids were recovered in the intestinal lymphatic system but not in plasma (**Figure 5.9**). Noteworthy, the intestinal lymphatic system is an essential contributor to the immune functions of the body [272]. It is the largest lymphatic organ and contains more than half of the body's lymphocytes [152, 153]. Therefore, the primary aim of our work was to assess whether the concentrations of CBD and THC found in the intestinal lymphatic system following oral co-administration with lipids could produce immunomodulatory effects. An additional aim was to assess if such effects are of potential therapeutic value to improve the treatment outcomes of autoimmune diseases such as MS, or can lead to potential safety considerations in immunocompromised patients such as those under chemotherapy regimens.

6.2. Experimental design

In this study, we evaluated whether the concentrations of cannabinoids achieved in the intestinal lymphatic system had immunomodulatory effects on

immune cells isolated from MLN and the spleen of rats. In addition, the immunomodulatory effects of CBD and THC were assessed on peripheral blood mononuclear cells (PBMC) isolated from human participants. Human samples were obtained from healthy volunteers, autoimmune disease patients (MS patients; **Table 2.4**), and cancer patients on chemotherapy (non-seminomatous germ cell tumour (NSGCT) patients; **Table 2.5**). These cases correspond to different status of the immune function. Proliferation assays and flow cytometry analysis of the pro-inflammatory cytokines were used to evaluate the immunomodulatory effects of cannabinoids as described in chapter 2, sections 2.9.3, 2.9.4, 2.9.5, 2.9.6, and 2.9.7.

6.2.1. Statistical analysis

Results are expressed as mean ± standard error of the mean (SEM). Statistical differences between data sets were assessed using one-way analysis of variance (ANOVA) with Fisher's LSD test. A p value < 0.05 was considered to represent a significant difference.

6.3. Results

6.3.1. Effect of CBD and THC on the proliferation of immune cells isolated from MLN and spleen of rats

Proliferation assays are commonly used to assess lymphocyte responses to a variety of stimuli [273]. We evaluated whether the concentrations of cannabinoids achieved in the intestinal lymphatic system had immunomodulatory effects on immune cells isolated from MLN and the spleen of rats. CBD significantly suppressed mitogen-stimulated proliferation of immune cells from both MLN and spleen at concentrations equal to and above 2.5 µg/mL (**Figure 6.1 A** and **B**). Slightly higher concentrations of THC were

required to inhibit the proliferation of immune cells isolated from MLN and spleen, at and above 7.5 and 5 µg/mL, respectively (**Figure 6.1 C** and **D**).

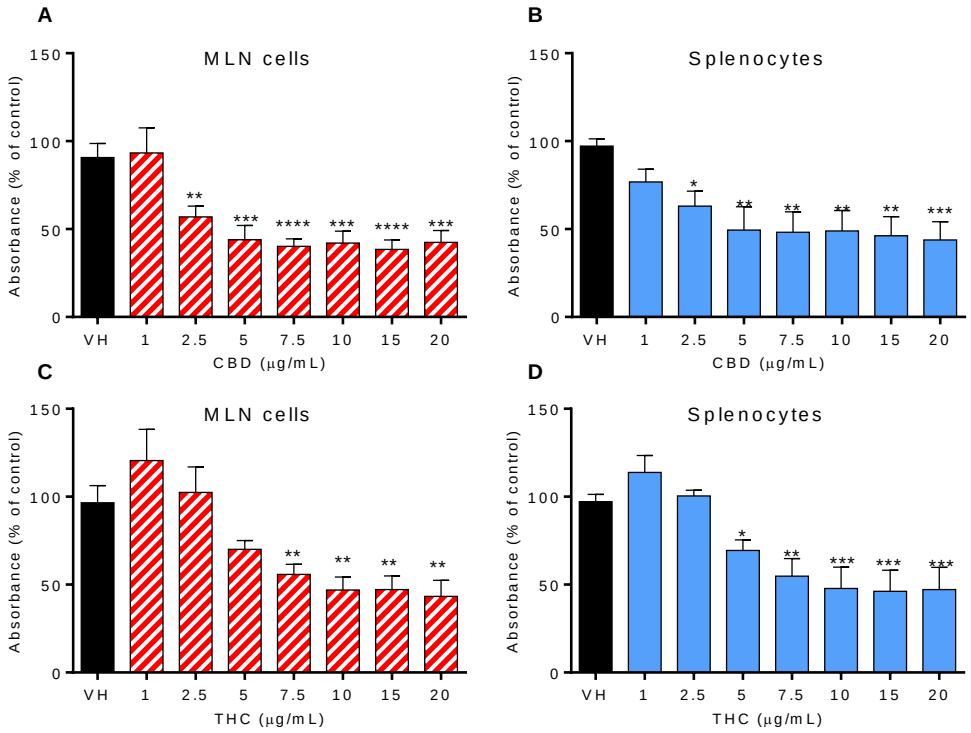

Figure 6.1. Proliferation of immune cells isolated from mesenteric lymph nodes (MLN) and spleen of rats (n = 5). Cells were stimulated by phytohaemagglutinin (PHA, 10 µg/mL) after incubation with cannabidiol (CBD) or Δ^9-tetrahydrocannabinol (THC) at concentrations of 1 – 20 µg/mL. **Panel A:** effect of CBD on the proliferation of immune cells isolated from MLN, **Panel B:** effect of CBD on the proliferation of immune cells isolated from spleen, **Panel C:** effect of THC on the proliferation of immune cells isolated from MLN, and **Panel D:** effect of THC on the proliferation of immune cells isolated from spleen. Values are expressed as mean ± SEM. Samples run in triplicates. Statistical analysis was performed using one-way ANOVA with Fisher's LSD test. Statistical differences compared to the vehicle (DMSO)-treated cells (VH); * $p < 0.05$; ** $p < 0.01$; *** $p < 0.001$; **** $p < 0.0001$.

6.3.2. CBD and THC attenuate the intracellular expression of pro-inflammatory cytokines, TNF-α and IFN-γ, in $CD3^+$ T cells isolated from rats

In addition to lymphocyte proliferation, the immunomodulatory effects of CBD and THC were assessed by measuring the intracellular expression of TNF-α and IFN-γ in $CD3^+$ T cells isolated from MLN and spleen of rats. As shown in **Figure 6.2 A** and **B**, CBD significantly decreased TNF-α expressing T cells from both MLN and spleen only at relatively high concentrations (20 µg/mL). However, a more potent effect was observed for CBD on IFN-γ. Similar to CBD, THC also significantly reduced TNF-α expressing T cells from MLN and spleen at the highest tested concentration of 20 µg/mL. However, lower concentrations were required to significantly reduce IFN-γ expressing T cells from MLN and spleen, 5 and 1 µg/mL, respectively (**Figure 6.2 C** and **D**).

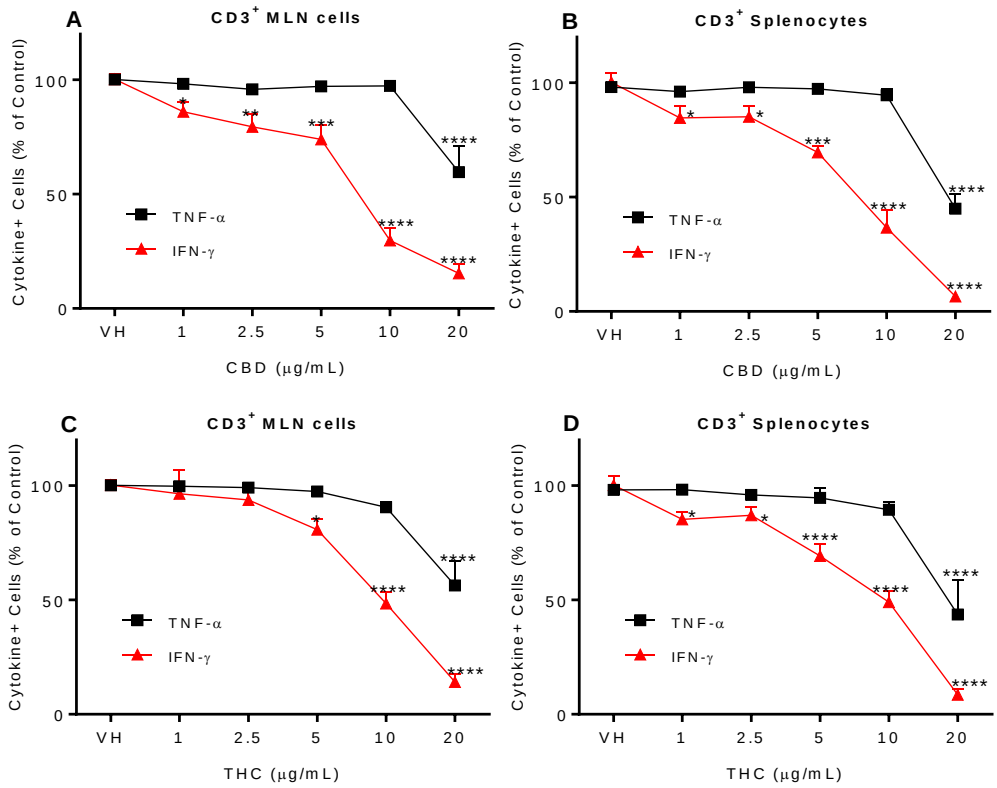

Figure 6.2. Percentage (% of control, mean ± SEM) of TNF-α and IFN-γ expressing $CD3^+$ immune cells isolated from mesenteric lymph nodes (MLN) and spleen of rats. Cells were stimulated by phorbol myristate acetate and ionomycin (PMA & I) in the presence of brefeldin A after incubation with cannabidiol (CBD) or Δ^9-tetrahydrocannabinol (THC) at concentrations of 1 – 20 μg/mL. **Panel A:** effect of CBD on the cytokine profile of immune cells isolated from MLN (n = 7), **Panel B:** effect of CBD on the cytokine profile of immune cells isolated from spleen (n = 5), **Panel C:** effect of THC on the cytokine profile of immune cells isolated from MLN (n = 7), and **Panel D:** effect of THC on the cytokine profile of immune cells isolated from spleen (n = 5). Statistical analysis was performed using one-way ANOVA with Fisher's LSD test. Statistical differences compared to the vehicle (DMSO)-treated cells (VH); * $p < 0.05$; ** $p < 0.01$; *** $p < 0.001$; **** $p < 0.0001$.

6.3.3. Effect of CBD and THC on the proliferation of PBMC isolated from human blood

The immunomodulatory effects of CBD and THC were assessed on PBMC isolated from human blood. Proliferation results showed that solubilised CBD and THC can significantly inhibit the proliferation of PBMC isolated from healthy volunteers at concentrations equal to or above 5 and 10 µg/mL, respectively (**Figure 6.3 A** and **B**).

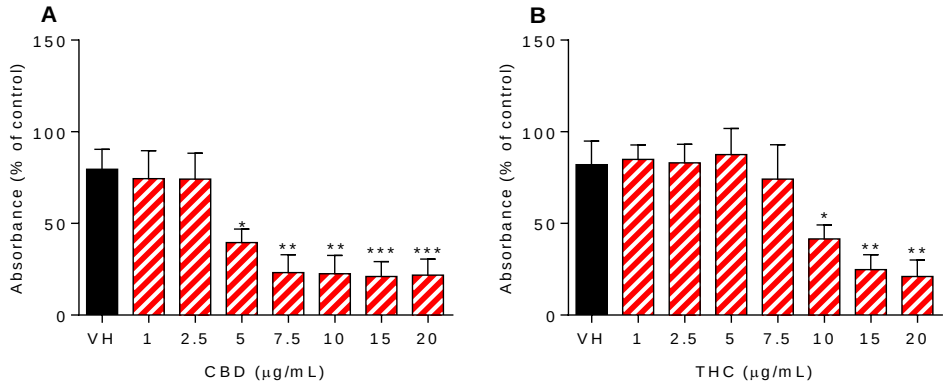

Figure 6.3. Proliferation of peripheral blood mononuclear cells (PBMC) isolated from healthy human volunteers. Cells were stimulated by phytohaemagglutinin (PHA, 10 µg/mL) after incubation with DMSO-dissolved cannabidiol (CBD, **Panel A**) or Δ^9-tetrahydrocannabinol (THC, **Panel B**) at concentrations of 1 – 20 µg/mL. Values are expressed as mean ± SEM (n = 4). Samples run in triplicates. Statistical analysis was performed using one-way ANOVA with Fisher's LSD test. Statistical differences compared to the vehicle-treated cells (VH); * $p < 0.05$; ** $p < 0.01$; *** $p < 0.001$; **** $p < 0.0001$.

Orally administered cannabinoids are delivered to the intestinal lymphatic system in chylomicrons (CM)-associated form following oral administration with lipids. Therefore, in this study, CM-associated CBD was incubated with PBMC isolated from healthy volunteers. At these conditions, CM-associated CBD has suppressed the proliferation of PBMC at concentrations similar to what have

been observed for CBD solution (**Figure 6.4**). In regards to CM-associated THC, it was demonstrated in our lab that it suppresses the proliferation of PBMC at concentrations equivalent to those produced by THC solution [194].

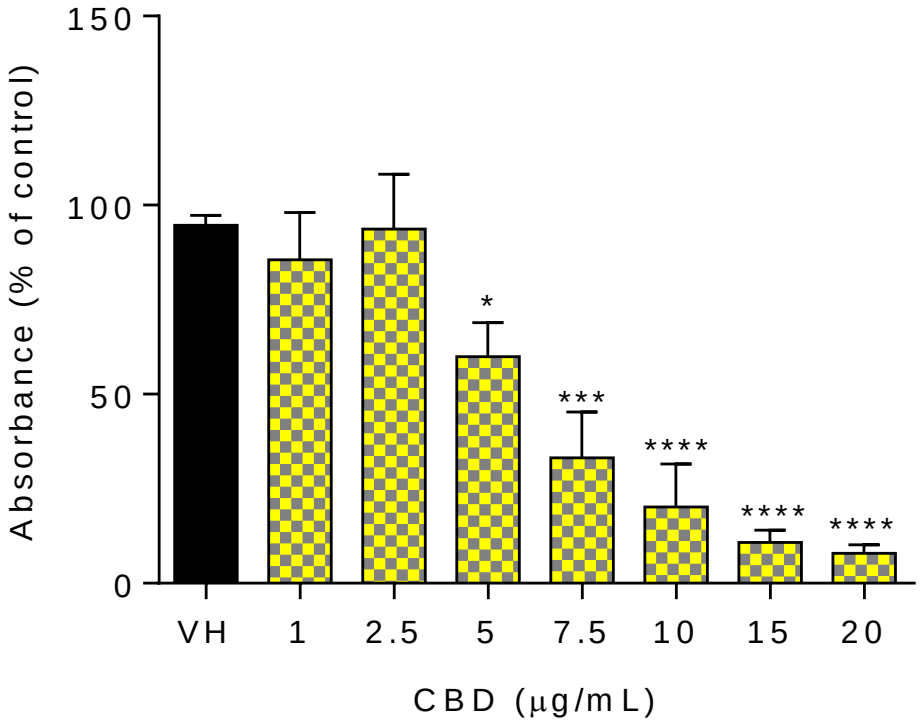

Figure 6.4. Proliferation of peripheral blood mononuclear cells (PBMC) isolated from healthy human volunteers. Cells were stimulated by phytohaemagglutinin (PHA, 10 μg/mL) after incubation with chylomicrons (CM)-associated cannabidiol (CBD) at concentrations of 1 – 20 μg/mL. Values are expressed as mean ± SEM (n = 3). Samples run in triplicates. Statistical analysis was performed using one-way ANOVA with Fisher's LSD test. Statistical differences compared to CM emulsion-treated cells (VH); * $p < 0.05$; *** $p < 0.001$; **** $p < 0.0001$.

To assess the potential therapeutic value of targeting lipophilic cannabinoids to the intestinal lymphatic system, the immunosuppressive effects of cannabinoids on PBMC isolated from patients suffering from autoimmune

disease, particularly MS patients, (**Table 2.4**) were evaluated. In this patient group, CBD markedly suppressed the proliferation of PBMC at half of the concentrations observed for healthy volunteers PBMC (**Figure 6.5 A**). Similar results were also found for THC (**Figure 6.5 B**).

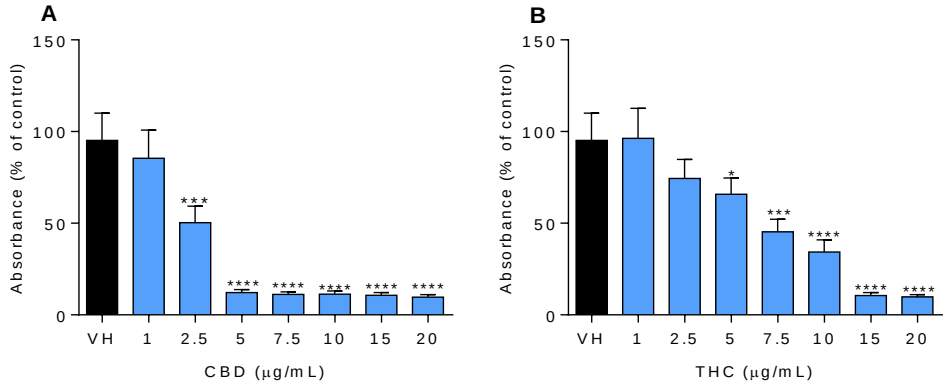

Figure 6.5. Proliferation of peripheral blood mononuclear cells (PBMC) isolated from multiple sclerosis (MS) patients. Cells were stimulated by phytohaemagglutinin (PHA, 10 µg/mL) after incubation with DMSO-dissolved cannabidiol (CBD, **Panel A**) or Δ^9-tetrahydrocannabinol (THC, **Panel B**) at concentrations of 1 – 20 µg/mL. Values are expressed as mean ± SEM (n = 7). Samples run in triplicates. Statistical analysis was performed using one-way ANOVA with Fisher's LSD test. Statistical differences compared to the vehicle-treated cells (VH); * $p < 0.05$; ** $p < 0.01$; *** $p < 0.001$; **** $p < 0.0001$.

Furthermore, proliferation experiments were also conducted on PBMC isolated from patients on chemotherapy regimens for the treatment of non-seminomatous germ cell tumours (NSGCT, **Table 2.5**). In this set, CBD showed anti-proliferative effects on PBMC from NSGCT patients which were comparable to healthy volunteers, i.e. immunosuppressive effects at concentrations equal to and above 5 µg/mL (**Figure 6.6**). THC also suppressed the proliferation of cancer patients PBMC at concentrations equal to and above 10 µg/mL, which are similar to the concentrations observed for healthy volunteers PBMC [194].

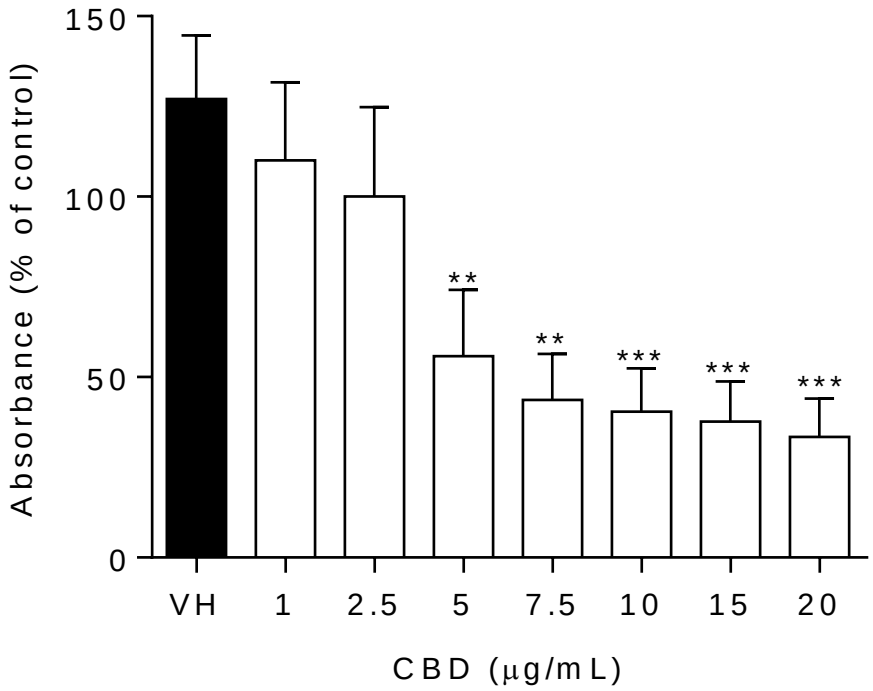

Figure 6.6. Proliferation of peripheral blood mononuclear cells (PBMC) isolated from patients on chemotherapy regimens for the treatment of non-seminomatous germ cell tumours (NSGCT). Cells were stimulated by phytohaemagglutinin (PHA, 10 µg/mL) after incubation with DMSO-dissolved cannabidiol (CBD) at concentrations of 1 – 20 µg/mL. Values are expressed as mean ± SEM (n = 7). Samples run in triplicates. Statistical analysis was performed using one-way ANOVA with Fisher's LSD test. Statistical differences compared to the vehicle-treated cells (VH); ** $p < 0.01$; *** $p < 0.001$.

6.3.4. Effects of CBD and THC on cytokine profiles of human lymphocytes

Following *in vitro* activation of PBMC, the intracellular expression of TNF-α, IFN-γ, IL-2, IL-17A, and granulocyte-macrophage colony-stimulating factor (GM-CSF) was assessed by means of flow cytometry. Similar to the proliferation assay, PBMC were isolated from healthy volunteers, MS patients, and NSGCT

patients. In PBMC isolated from healthy volunteers, CBD significantly decreased TNF-α, IFN-γ, and IL-17A expressing T cells when incubated with cells at the highest tested concentration (20 µg/mL). IL-2 and GM-CSF expressing T cells, however, were suppressed at CBD concentrations at and above 5 µg/mL (**Figure 6.7 A**). In regards to THC, no appreciable effect was observed on TNF-α, IFN-γ, and IL-17A expressing T cells compared to the vehicle-treated cells. However, IL-2 and GM-CSF expressing T cells were inhibited at concentrations equal to and above 5 µg/mL (**Figure 6.7 D**). For PBMC isolated from MS patients, the immunosuppressive effects of CBD and THC on the expression of the tested cytokines were significantly higher compared to the effects on cells isolated from healthy volunteers (**Figure 6.7 B** and **E**). Moreover, the effects of CBD and THC on the expression of the assessed cytokines from NSGCT patient T cells were comparable to healthy volunteer cells with some exceptions (**Figure 6.7**). These exceptions include more prominent immunosuppressive effects of CBD on TNF-α and IFN-γ expressing T cells as well as the effects of THC on TNF-α and IL-2 expressing T cells from NSGCT patients (**Figure 6.7 C** and **G**). Representative flow cytometry histograms are shown in **Figure 6.8**.

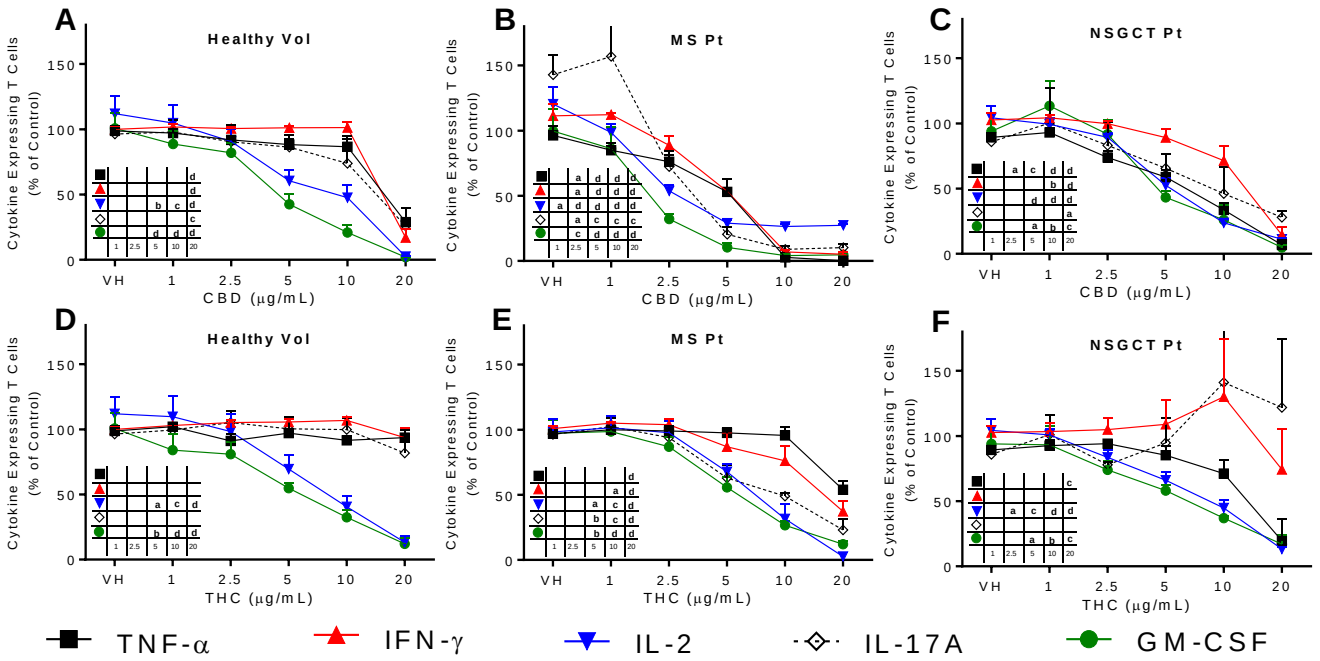

Figure 6.7. Percentage (% of control, mean ± SEM) of TNF-α, IFN-γ, IL-2, IL-17A, and GM-CSF expressing $CD3^+$ T cells isolated from human participants. Cells were stimulated by phorbol myristate acetate and ionomycin (PMA & I) in the presence of brefeldin A after incubation with cannabidiol (CBD) or Δ^9-tetrahydrocannabinol (THC) at concentrations of 1 – 20 µg/mL. **Panel A:** effect of CBD on PBMC from healthy volunteers (n = 5), **Panel B:** effect of CBD on PBMC from multiple sclerosis (MS) patients (n = 4), **Panel C:** effect of CBD on PBMC from patients on chemotherapy to treat non-seminomatous germ cell tumours (NSGCT) (n = 3), **Panel D:** effect of THC on PBMC from healthy volunteers (n = 5), **Panel E:** effect of THC on PBMC from MS patients (n = 3), **Panel F:** effect of THC on PBMC from patients on chemotherapy to treat NSGCT (n = 3). Statistical analysis was performed using

one-way ANOVA with Fisher's LSD test. The inset table in the lower left corner of each panel refers to the statistical differences compared to the vehicle (DMSO)-treated cells (VH); a $p < 0.05$; b $p < 0.01$; c $p < 0.001$; d $p < 0.0001$.

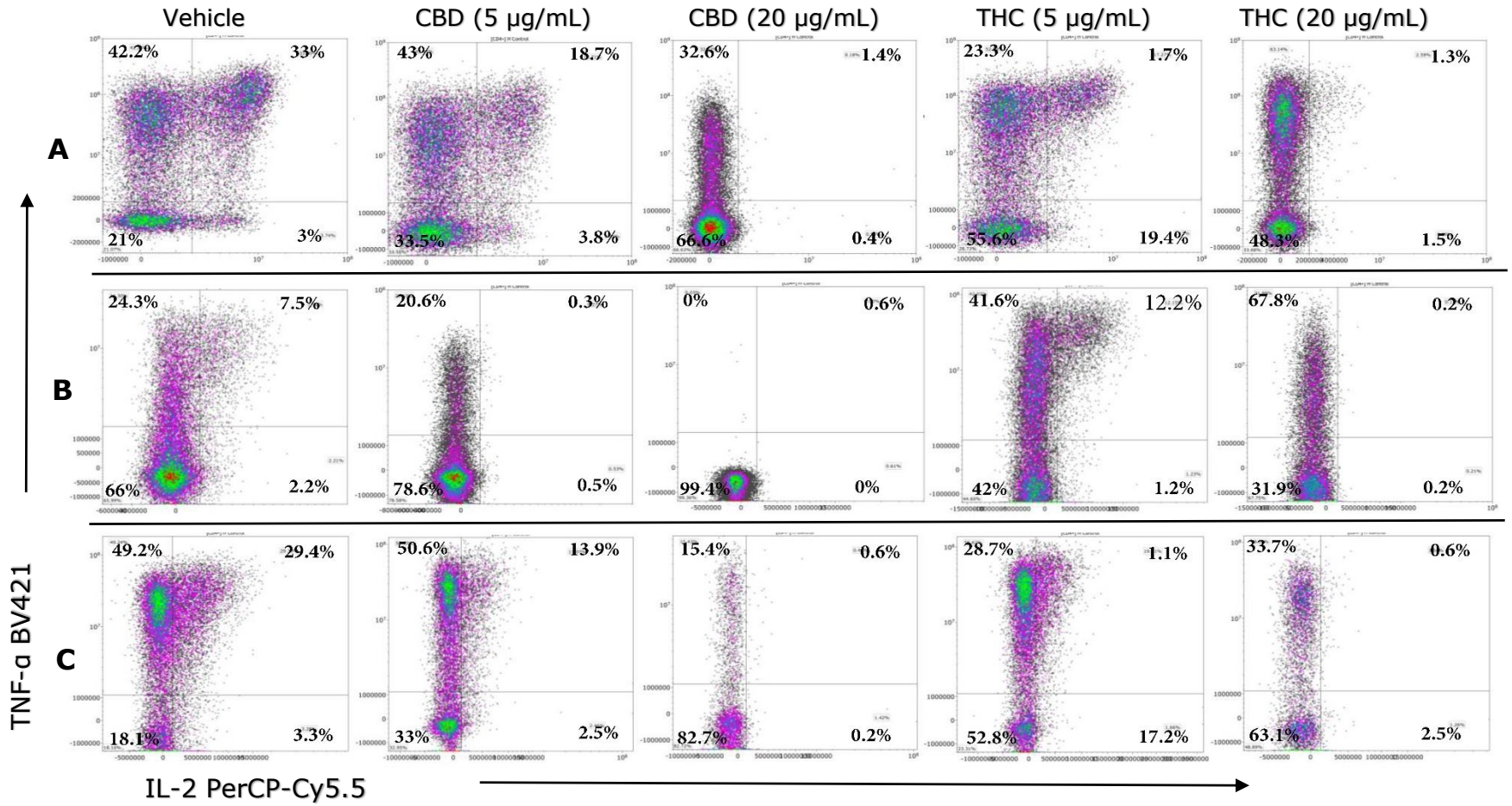

Figure 6.8. Representative flow cytometry histograms showing the effect of cannabidiol (CBD) and Δ^9-tetrahydrocannabinol (THC) at concentrations of 5 and 20 µg/mL on TNF-α and IL-2 expressing $CD3^+$ T cells isolated from human participants. Cells were stimulated by phorbol myristate acetate and ionomycin (PMA & I) in the presence of brefeldin A. **Panel A:** effect of CBD

and THC on PBMC from a healthy volunteer, **Panel B:** effect of CBD and THC on PBMC from a multiple sclerosis (MS) patient, **Panel C:** effect of CBD and THC on PBMC from a patient on chemotherapy to treat non-seminomatous germ cell tumours (NSGCT).

6.1. Discussion

The intestinal lymphatic system is the major host of immune cells. It has been proposed that the lymphatic system is an attractive target for immunomodulators, because drugs can achieve high local concentrations and avoid systemic dilution [274, 275]. This concept is supported by the fact that immune cells within the lymphatic system move slower and experience lower shear stress relative to those within the systemic circulation [123]. In this study, the effect of CBD and THC on the proliferation of lymphocytes isolated from lymphoid tissues in the intestinal lymphatic system and spleen of rats was assessed. Both cannabinoids significantly inhibited the proliferation of mitogen-stimulated lymphocytes from MLN and spleen at concentrations that are highly unlikely to be achieved in rat plasma, but can be easily obtained in the intestinal lymphatic system after co-administration with lipids (**Figure 6.1**). In addition, the results suggest that CBD has more potent anti-proliferative effect than THC (**Figure 6.1**). Moreover, in this study, CBD and THC attenuated the expression of TNF-α and IFN-γ, key pro-inflammatory cytokines in the pathogenesis of autoimmune diseases [276], by T cells isolated from MLN and spleen (**Figure 6.2**). In line with the anti-proliferative effect, cannabinoids also suppressed the expression of inflammatory cytokines at micromolar range concentrations, which are achievable in the intestinal lymphatic system, but not in general circulation. The immunosuppressive effects of CBD and THC on murine immune cells in the same concentration range were also reported elsewhere [62, 63]. It is conceivable that intestinal lymphatic transport is a potential underlying mechanism of previously reported therapeutic effects of CBD and THC in murine models of autoimmune diseases in which cannabinoids were administered orally with large amounts of lipids [116, 268].

To assess the immunomodulatory effect of cannabinoids on human cells, proliferation assays were performed on PBMC isolated from venous blood of human volunteers. Our results demonstrate that CBD and THC, at relatively high concentrations, inhibits the proliferation of mitogen-stimulated PBMC isolated from healthy volunteers (**Figure 6.3**). These results are consistent with previous reports [61]. Importantly, these concentrations would not be achievable in systemic blood circulation even when high oral doses of cannabinoids are consumed. Consroe *et al* [28] reported that the maximum plasma concentration recovered following repeated oral administration of 10 mg/kg/day CBD (in a small-volume lipid-based formulation) in humans was 25 ng/mL. This is profoundly lower than the 5 µg/mL concentration required to significantly inhibit PBMC proliferation in this study (**Figure 6.3 A**). In contrast, high doses of THC are limited by the psychotropic side effects reported for this drug [277]. Nevertheless, given the results obtained in rats (chapter 5), it is likely that oral administration of CBD and THC in humans in conditions facilitating intestinal lymphatic transport (with lipid dose in the range of 10 g [134]) can result in very high concentrations in the intestinal lymphatic system. It should be noted, however, that CM association in the enterocytes is a prerequisite for the intestinal lymphatic delivery of lipophilic compounds when orally administered with lipids [165, 166, 278, 279]. Importantly, in the current study, CM-associated CBD was still able to inhibit the proliferation of PBMC isolated from healthy volunteers, showing similar effects to CBD in solution (**Figure 6.3 A** and **Figure 6.4**). Similarly, CM-associated THC showed similar antiproliferative effects as THC in solution [194]. Therefore, these results suggest that the fact that cannabinoids are delivered to the intestinal lymphatic system in a CM-associated form would not reduce the immunomodulatory effects. A possible explanation for this maintained effect in CM-associated form

is that lymphocytes possess lipoprotein lipase enzyme activity, which enables them to utilise fatty acids and triglycerides from CM [280] and therefore be exposed to cannabinoids.

In addition, our results indicate that PBMC isolated from MS patients are more sensitive to the immunomodulatory effects of cannabinoids compared to PBMC isolated from healthy volunteers (**Figure 6.5**). This could be related to the up-regulation of cannabinoid CB_2 receptors on the immune cells of MS patients [281]. These receptors are thought to be involved in the immunosuppressive effect of cannabinoids [63, 282]. Interestingly, some other reports suggested that cannabinoids exert their immunosuppressive effect by CB_2-independent mechanisms as well [283]. Another aspect addressed in this study is the anti-proliferative effects of CBD on PMBC isolated from cancer patients under chemotherapy regimens. In this case, CBD showed anti-proliferative effects comparable to those showed on PBMC isolated from healthy volunteers (**Figure 6.6**). Similar effects were also demonstrated for THC in our laboratory [194]. However, cancer patients on chemotherapy usually have low or low-borderline blood lymphocyte counts [284], which was also the case in this study (**Table 2.5**). Hence, there is potential risk of further immunosuppression when cannabinoids are administered in conditions that facilitate intestinal lymphatic transport, raising concerns regarding adverse effects in cancer patients who self-medicate with cannabinoids or are prescribed cannabinoids as part of their supportive medication.

It is generally been accepted that TNF-α, IFN-γ, and IL-2 produced by T_H1 cells are actively involved in the pathogenesis of many autoimmune diseases [285]. Recently, T_H17 cells (which produce IL-17A) have emerged as a major factor in the pathogenesis of autoimmune diseases as well as the contribution of GM-CSF to drive the inflammatory effects of T_H17 [97] and T_H1 [286, 287]

cells. These cells are of particular importance in the initiation and propagation of MS [288]. In this study, CBD and THC induced a profound decrease in IL-2 and GM-CSF expressing T cells separated from healthy volunteers. This is consistent with the demonstration of a link between IL-2 production and GM-CSF induction [289]. CBD showed higher immunosuppressive effect than THC as manifested by the effect on TNF-α, IFN-γ, and IL-17A (**Figure 6.7 A** and **D**). For PBMC isolated from MS patients, similar to the anti-proliferative effect, cannabinoids displayed more potent suppression of cytokine expression compared to cells from healthy volunteers (**Figure 6.7 B** and **E**). Yet, these effects were only observed at micromolar concentrations, which are consistent with previous reports [61, 290]. Collectively, the effects of cannabinoids on lymphocyte proliferation and cytokine profile explored in the current study suggest that targeting lipophilic cannabinoids to the intestinal lymphatic system for enhanced immunomodulatory effects in the treatment of autoimmune diseases could be a promising therapeutic approach. This approach could extend the therapeutic value of cannabinoids currently being used for symptomatic relief in MS patients [39] to a disease-modifying treatment, which could delay the progression of MS. In fact, the immunomodulatory effects of cannabinoids described in this study are consistent with the proposed mechanisms of action of disease-modifying therapies currently used in the treatment of MS (**Table 1.5**) [291]. Moreover, the results suggest that CBD has higher therapeutic effectiveness in autoimmune diseases compared with THC as it has more pronounced immunomodulatory effects, is devoid of psychotropic side effects, and is well tolerated in humans following acute and chronic intake of relatively high doses [292].

On the other hand, adequate levels of the above mentioned cytokines are important to maintain adaptive immune reposes to fight infections [293, 294].

In this study, a substantial decrease in cytokines produced by T cells has been demonstrated with cannabinoids in PBMC isolated from cancer patients under chemotherapy regimen (**Figure 6.7 C** and **F**). This can potentially further deteriorate chemotherapy-induced immunosuppression in these patients. It is well recognised that some cancer patients self-medicate and consume cannabis or cannabis-based medicinal formulations orally to alleviate nausea and vomiting associated with chemotherapy [295]. Given the results of this study, in this patients group, oral administration of immunosuppressive drugs such as cannabinoids in conditions facilitating intestinal lymphatic transport requires caution and should possibly be avoided.

6.2. Conclusions

It has been demonstrated in this work that cannabinoids produce prominent immunomodulatory effects on murine and human lymphocytes with CBD being more immunosuppressive than THC. In addition, lymphocytes from MS patients were more susceptible to the immunosuppressive effects of cannabinoids than those from healthy volunteers or cancer patients. Yet, these effects are only feasible at high cannabinoid levels which are highly unlikely to be achieved in plasma but can be found in the intestinal lymphatic system after oral co-administration with lipids. Thus, administering cannabinoids, in particular CBD, with a high-fat meal, as cannabis-containing food, or in lipid-based formulations could represent a valid therapeutic approach to improve the treatment of MS, or indeed other autoimmune disorders. However, in immunocompromised patients, administration of cannabinoids in this way may deepen the immunosuppressive effects.

7. IMPLICATIONS AND FUTURE PROSPECTS

7.1. Key findings and implications

This study demonstrated conclusively that oral administration of cannabinoids in a simple lipid-based formulation (solution of cannabinoids in long-chain triglycerides (LCT)) results in extremely high levels in the intestinal lymphatic system and prominent immunomodulatory effects.

The concentrations of cannabidiol (CBD) and Δ^9-tetrahydrocannabinol (THC) found in the intestinal lymphatic system were more than hundred-fold higher than plasma concentrations. Importantly, at concentrations achieved in the intestinal lymphatic system but not in plasma, both cannabinoids can produce substantial immunomodulatory effects. These effects include the ability to suppress lymphocyte proliferation and the production of pro-inflammatory cytokines from murine and human lymphocytes. In addition, cannabinoids showed more immunosuppressive effects on immune cells from multiple sclerosis (MS) patients than those from healthy volunteers. It is important to stress here that suppressing lymphocyte proliferation and inhibiting the release of inflammatory cytokines are key therapeutic mechanisms for the treatment of autoimmune diseases such as MS [291, 296]. Therefore, oral administration of cannabinoids with LCT represents a targeting approach to the intestinal lymphatic system, a major host of immune cells, for enhanced immunomodulatory effects in the treatment of autoimmune diseases. Moreover, CBD showed more pronounced immunomodulatory effects than THC. Combining this observation with the fact that CBD is devoid of psychotropic side effects and well tolerated in humans following the intake of high doses [292], it can be

suggested that CBD has higher therapeutic effectiveness in autoimmune diseases than THC.

It was also demonstrated in this study that cannabinoids have immunosuppressive effects on immune cells isolated from cancer patients on chemotherapy. This can weaken adaptive immune reposes to fight infections and potentially further deteriorate chemotherapy-induced immunosuppression in these patients. Therefore, oral administration of immunosuppressive drugs such as cannabinoids in conditions facilitating intestinal lymphatic transport requires caution and should possibly be avoided in cancer patients on chemotherapy.

Another important finding demonstrated in this work is that oral co-administration with lipids of the two main active cannabinoids, CBD and THC, substantially enhances the systemic exposure to these cannabinoids in a rat model. Our data demonstrate that the primary mechanism of the increased absorption of cannabinoids in the presence of lipids is intestinal lymphatic transport. The amount of lipids present in cannabis-containing foods, or following a high-fat meal, is sufficient to activate intestinal lymphatic transport and lead to increased systemic exposure to cannabinoids in humans, similar to what has been observed in this study in a rat model.

The mechanisms underlying enhanced intestinal lymphatic transport and systemic exposure to CBD and THC following oral co-administration with LCT were explored in this study. We have demonstrated that oral administration of cannabinoids in LCT-based formulation results in efficient intestinal solubilisation. At least one-third of CBD dose would be solubilised and readily available for absorption when administered in fasted conditions. For optimum solubilisation, the concentration of CBD in LCT-based formulation should apparently be limited to 40 mg/mL. Above that concentration, the solubilised

fraction is inversely proportional to the concentration of CBD in the formulation. It should not be ignored, however, that most *in vitro* lipolysis models, including the one used in this study, reflect intestinal lipid digestion but not gastric contribution [236]. Lipid digestion by gastric lipases could further enhance, at least partially, the solubilisation of lipophilic drugs in the intestinal milieu [156]. In addition, long intestinal transit times and the ability of human pancreas to produce larger quantities of lipase than needed permit almost complete lipid lipolysis *in vivo* [226]. Thus, the solubilised fraction of CBD demonstrated in our study represents the minimum expected range and it is likely that more CBD could be solubilised *in vivo* following oral administration with LCT.

The digestion of LCT from a lipid-based formulation, or from a high-fat meal, does not only enhance the intestinal solubilisation of cannabinoids (pre-enterocyte events) but can also augment the synthesis and trafficking of chylomicrons (CM) inside the enterocytes [162, 163]. CBD and THC showed high association values with CM, which can therefore divert the absorption pathway of cannabinoids toward the intestinal lymphatic system instead of the portal circulation (**Figure 4.1**). This pathway avoids first-pass metabolism in the liver, which is thought to be the main cause of low oral bioavailability of cannabinoids [37, 38]. Hence, the results of CM-association suggest that there is a high potential of intestinal lymphatic transport and enhanced exposure following oral administration with LCT to rats as well as humans.

7.1.1. Translational aspect

Given the high local levels of cannabinoids recovered in the intestinal lymphatic system, oral administration of cannabinoids with lipids could represent a valid therapeutic approach to improve the treatment of MS, or perhaps other autoimmune disorders. This approach could extend the

therapeutic value of cannabinoids currently being used for symptomatic relief in MS patients [39] to a disease-modifying treatment, which could delay the progression of MS. On the contrary, oral administration of cannabinoids with dietary lipids might further deepen the immunosuppressive state of cancer patients on chemotherapy. Therefore, the practice of administering oral cannabinoids to alleviate nausea and vomiting associated with chemotherapy requires caution and should possibly be avoided in conditions facilitating intestinal lymphatic transport.

In addition, the increase in systemic exposure to cannabinoids in humans is of potentially high clinical importance as it could turn a barely effective dose of orally administered cannabis into highly effective one, or indeed a therapeutic dose into a toxic one. Therefore, it is important for cannabis-prescribing clinicians and those who self-medicate with cannabis to carefully consider the effect of the co-administration of lipids on the therapeutic outcomes of orally administered cannabis or cannabis-based medicines.

7.2. Future prospects

While the results of the current study provide a novel insight into the impact of intestinal lymphatic transport on the immunomodulatory effects of orally administered cannabinoids, further research should be undertaken to investigate these effects *in vivo*. Animal models of autoimmune diseases have advanced better understanding of disease pathogenesis and the development of efficient therapeutic approaches. These models can, therefore, be used to assess the therapeutic potential of targeting lipophilic cannabinoids to the intestinal lymphatic system. Considering the remarkable immunomodulatory effects of cannabinoids demonstrated in this study on immune cells from MS patients, an animal model of MS is of particular interest for further research.

Over the last century, experimental autoimmune encephalomyelitis (EAE) has established and evolved as a reasonably valid preclinical model for MS [297, 298]. In fact, EAE has been successfully used for the development of immunotherapies, which are currently among the first line therapies for the treatment of MS. These therapies include glatiramer acetate, mitoxantrone, fingolimod, and natalizumab [111]. Successful demonstration of the therapeutic efficacy of cannabinoids in EAE can support the conduction of a small randomized controlled clinical trial in MS patients.

The potential detrimental consequences of enhancing the intestinal lymphatic transport of orally administered cannabinoids to immunocompromised patients can also be explored using animal models. Experimental chemotherapy-induced leukopenia (low white blood cell count) model was previously described in mice, rats, and hamsters [299-301]. This model could be a useful tool to assess the impact of intestinal lymphatic transport of cannabinoids on the physiological functions of already challenged immune system.

7.2.1. Assessing the therapeutic effects of orally administered cannabinoids

7.2.1.1. Experimental autoimmune encephalomyelitis (EAE)

MS is a unique and complex human disease that can't be represented by a single animal model. However, animal models of MS have significantly improved our overall knowledge of MS pathogenesis and supported the development of novel therapeutics. Currently, three animal models of MS are commonly used in research. These are EAE, virally-induced demyelinating model, and toxin-induced demyelinating model [112]. EAE is by far the model of choice to simulate the inflammatory nature of MS. It has been established in

rabbits as early as 1920s and developed later to include rodents, which are currently the most commonly used species [113].

As described earlier in the introduction of this thesis, the relapsing-remitting course of MS (RRMS) represents the active inflammatory phase of the disease and it is the most prevalent form of MS (corresponds to around 85% of the cases) [88, 113]. At this stage of the disease, patients might benefit from the disease-modifying effects (immunomodulatory effects) of cannabinoids following oral administration with LCT. The therapeutic effects of cannabinoids on the clinical symptoms of MS will be assessed using both rat and mouse models of EAE. In rats, EAE can be induced by subcutaneous injection of the myelin-derived antigen myelin basic protein (MBP) emulsified in complete Freund's adjuvant (CFA) to Lewis rats as described by Bruin *et al* [302]. This induction protocol results in monophasic EAE characterised by acute onset of the disease followed by spontaneous recovery. These features resemble the clinical sign of relapse in MS [303]. Therefore, the rat model of MS can be used to assess the therapeutic potentials of orally administered cannabinoids on the acute episodes of T cell-mediated neuroinflammations. The steady neurological signs of MS in this model can permit reliable follow up for cannabinoids-induced changes in the clinical symptoms. Yet, this model can't be described as a complete model of RRMS as it lacks an important hallmark of the disease, the remission phase. Thus, the ability of cannabinoids to prevent relapses after the quiescent remission periods can't be explored using this model. A relapsing-remitting pattern of MS can be induced in SJL/J mice by subcutaneous injection of the myelin-derived antigen proteolipid protein (PLP) emulsified in CFA [304]. This model can, therefore, provide valued information about the potential therapeutic effects of cannabinoids to prevent relapses and/or the development of new neurological lesions.

The change in clinical symptoms can be assessed using a ten-point scoring scale as previously described [305, 306]. In addition, the immunomodulatory effects of cannabinoids can be assessed using lymphocyte proliferation assay and flow cytometry analysis as described in chapter 2, sections 2.9.6 and 2.9.7, respectively.

7.2.1.2. The effect of oral cannabinoids on disease progression and symptoms of MS in RRMS patients

The novel findings of this research provided invaluable insights toward the therapeutic applications of targeting the intestinal lymphatic system in the treatment of MS. This view highlights the need for a clinical research to assess the use of oral cannabinoids as disease-modifying drugs in the treatment of MS. In fact, CBD and THC are currently used to relieve spasticity due to MS [39]. In addition, both cannabinoids are available as oral formulations. These facts might aid the approval of a small randomized controlled clinical trial in which already available formulations of cannabinoids are administered to RRMS patients in conditions facilitating the intestinal lymphatic transport. The clinical symptoms can be evaluated by using Kurtzke Expanded Disability Status Score (EDSS). In addition, the immunomodulatory effects of cannabinoids can be evaluated in peripheral blood mononuclear cells (PBMC) isolated from the patients using the techniques described in chapter 2, sections 2.9.6 and 2.9.7.

It is worth mentioning that the results of the current study have provided a very promising direction for the potential therapeutic application of targeting cannabinoids to the intestinal lymphatic system in the treatment of MS. Yet, this approach is not limited to MS and can possibly be used as a treatment strategy in other autoimmune diseases like rheumatoid arthritis, diabetes mellitus, autoimmune hepatitis, colitis, systemic lupus erythematosus (SLE), and psoriasis.

7.2.2. Assessing the potential detrimental effects of orally administered cannabinoids

In addition to the therapeutic effects of enhancing the intestinal lymphatic transport of orally administered cannabinoids, the results of our study suggest potential detrimental immunosuppressive effects in immunocompromised individuals, such as cancer patients on chemotherapy. It is well recognised that cancer patients on chemotherapy are highly predisposed to secondary infections [307]. Leukopenia was described as a common cause for these infections [308]. To address this issue, an animal model of chemotherapy-induced immunocompromised state will be used. In a study by Campos *et al* [300], leukopenia was induced in Wistar rats by two intraperitoneal injections of the chemotherapeutic agent 5-fluorouracil (5-FU). In addition, oral mucositis (a common secondary infection in cancer patients on chemotherapy [309]) can be induced by superficial scratch on the check pouch mucosa as previously described [310]. Cannabinoids can then be administered orally to these rats in lipid-free and lipid-based formulations. The effect of cannabinoids on the progression of oral mucositis can be assessed by macroscopic and microscopic test as described by Medeiros *et al* [311]. The systemic immunomodulatory effects of cannabinoids can be evaluated using leukocyte differential count, lymphocyte proliferation assay, and the expression of inflammatory cytokines as well as assessing the development of bacteremia in the blood of rats.

8. REFERENCES

1. Abel EL. Marihuana: The First Twelve Thousand Years: Springer US; 1980.

2. Zuardi AW. History of cannabis as a medicine: a review. Revista Brasileira de Psiquiatría. 2006;28(2):153-7.

3. Iversen LL. The Science of Marijuana: Oxford University Press; 2007.

4. Kalant H. Medicinal use of cannabis: history and current status. Pain Research and Management. 2001;6(2):80-94.

5. Mikuriya TH. Marijuana in medicine: past, present and future. Calif Med. 1969;110(1):34.

6. Zuardi AW. History of cannabis as a medicine: a review. Rev Bras Psiquiatr. 2006;28(2):153-7.

7. Robson P. Therapeutic aspects of cannabis and cannabinoids. Br J Psychiatry. 2001;178:107-15. Epub 2001/02/07.

8. Rasmusson X. History and Policy of Clinical Cannabis versus Medical Marijuana: US History and Policy. Journal of Social Science for Policy Implications. 2014;2(1):15-30.

9. Armentano P. Emerging Clinical Applications For Cannabis and Cannabinoids: A Review of the Recent Scientific Literature. Washington, DC: The National Organization for the Reform of Marijuana Laws; 2014 [cited 2015]; 6th:[Available from: http://norml.org/library/recent-research-on-medical-marijuana.

10. Robson P. Human studies of cannabinoids and medicinal cannabis. Cannabinoids: Springer; 2005. p. 719-56.

11. Sznitman SR, Zolotov Y. Cannabis for therapeutic purposes and public health and safety: a systematic and critical review. Int J Drug Policy. 2015;26(1):20-9. Epub 2014/10/12.

12. Pertwee RG. Cannabinoid pharmacology: the first 66 years. Br J Pharmacol. 2006;147:S163-S71.

13. ElSohly M, Gul W. Constituents of cannabis sativa. Handbook of Cannabis. 2014;3:1093.

14. Brenneisen R. Chemistry and analysis of phytocannabinoids and other Cannabis constituents. Marijuana and the Cannabinoids: Springer; 2007. p. 17-49.

15. Pertwee RG. Pharmacological actions of cannabinoids. Cannabinoids: Springer; 2005. p. 1-51.

16. Koppel BS, Brust JC, Fife T, Bronstein J, Youssof S, Gronseth G, et al. Systematic review: efficacy and safety of medical marijuana in selected neurologic disorders: report of the Guideline Development Subcommittee of the American Academy of Neurology. Neurology. 2014;82(17):1556-63. Epub 2014/04/30.

17. Mackie K. Cannabinoid receptors: Where they are and what they do. J Neuroendocrinol. 2008;20:10-4.

18. Seely KA, Prather PL, James LP, Moran JH. Marijuana-based Drugs: Innovative Therapeutics or Designer Drugs of Abuse? Mol Interv. 2011;11(1):36-51.

19. Raymon LP, Walls HC. Pharmacology of cannabinoids. Marijuana and the Cannabinoids: Springer; 2007. p. 97-123.

20. Pertwee RG. Handbook of cannabis: Oxford University Press, USA; 2014.

21. Mechoulam R, Peters M, Murillo-Rodriguez E, Hanus LO. Cannabidiol--recent advances. Chemistry & biodiversity. 2007;4(8):1678-92. Epub 2007/08/23.

22. Hazekamp A, Pappas G. Self-medication with cannabis. Handbook of Cannabis. 2014:319.

23. Grotenhermen F. Pharmacokinetics and pharmacodynamics of cannabinoids. Clin Pharmacokinet. 2003;42(4):327-60. Epub 2003/03/22.

24. Ohlsson A, Lindgren JE, Andersson S, Agurell S, Gillespie H, Hollister LE. Single-dose kinetics of deuterium-labelled cannabidiol in man after smoking and intravenous administration. Biomed Environ Mass Spectrom. 1986;13(2):77-83. Epub 1986/02/01.

25. Lindgren J-E, Ohlsson A, Agurell S, Hollister L, Gillespie H. Clinical effects and plasma levels of Δ 9-tetrahydrocannabinol (Δ 9-THC) in heavy and light users of cannabis. Psychopharmacology (Berl). 1981;74(3):208-12.

26. Wang T, Collet JP, Shapiro S, Ware MA. Adverse effects of medical cannabinoids: a systematic review. CMAJ. 2008;178(13):1669-78. Epub 2008/06/19.

27. Nadulski T, Pragst F, Weinberg G, Roser P, Schnelle M, Fronk E-M, et al. Randomized, double-blind, placebo-controlled study about the effects of cannabidiol (CBD) on the pharmacokinetics of Δ9-tetrahydrocannabinol (THC) after oral application of THC verses standardized cannabis extract. Ther Drug Monit. 2005;27(6):799-810.

28. Consroe P, Kennedy K, Schram K. Assay of plasma cannabidiol by capillary gas chromatography/ion trap mass spectroscopy following high-dose repeated daily oral administration in humans. Pharmacol Biochem Behav. 1991;40(3):517-22. Epub 1991/11/01.

29. Ohlsson A, Lindgren JE, Wahlen A, Agurell S, Hollister LE, Gillespie HK. Plasma delta-9 tetrahydrocannabinol concentrations and clinical effects after oral and intravenous administration and smoking. Clin Pharmacol Ther. 1980;28(3):409-16. Epub 1980/09/01.

30. Collins TR. Special Report: What Neurologists Are Doing About Medical Marijuana. Neurology Today. 2014;14(8):1-28.

31. Fasinu PS, Phillips S, ElSohly MA, Walker LA. Current status and prospects for cannabidiol preparations as new therapeutic agents. Pharmacotherapy: The Journal of Human Pharmacology and Drug Therapy. 2016;36(7):781-96.

32. Geffrey AL, Pollack SF, Bruno PL, Thiele EA. Drug–drug interaction between clobazam and cannabidiol in children with refractory epilepsy. Epilepsia. 2015;56(8):1246-51.

33. Wempe MF, Oldland A, Stolpman N, Kiser TH. Stability of dronabinol capsules when stored frozen, refrigerated, or at room temperature. Am J Health Syst Pharm. 2016;73(14).

34. Sporkert F PF, Ploner CJ, Tschirch A, Stadelmann AM. Pharmacokinetic investigations and delta-9-tetrahydrocannabinol and its metabolites after single administration of 10 mg Marinol in attendance of a psychiatric study. The Annual Meeting of The International Association of Forensic Toxicologists; 2001 Aug 26-30; Prague, Czech Republic2001.

35. Huestis MA. Human cannabinoid pharmacokinetics. Chemistry & biodiversity. 2007;4(8):1770-804. Epub 2007/08/23.

36. Klumpers LE, Beumer TL, van Hasselt JG, Lipplaa A, Karger LB, Kleinloog HD, et al. Novel Δ9-tetrahydrocannabinol formulation Namisol® has beneficial pharmacokinetics and promising pharmacodynamic effects. Br J Clin Pharmacol. 2012;74(1):42-53.

37. Mattes RD, Shaw LM, Edling-Owens J, Engelman K, Elsohly MA. Bypassing the first-pass effect for the therapeutic use of cannabinoids. Pharmacol Biochem Behav. 1993;44(3):745-7. Epub 1993/03/01.

38. Siemens AJ, Walczak D, Buckley FE. Characterization of blood disappearance and tissue distribution of [3H]cannabidiol. Biochemical pharmacology. 1980;29(3):462-4. Epub 1980/02/01.

39. Wright S, Guy G. Licensed Cannabis-Based Medicines: Benefits and Risks. Handbook of Cannabis. 2014:373.

40. Karschner EL, Darwin WD, Goodwin RS, Wright S, Huestis MA. Plasma cannabinoid pharmacokinetics following controlled oral delta9-tetrahydrocannabinol and oromucosal cannabis extract administration. Clin Chem. 2011;57(1):66-75. Epub 2010/11/17.

41. Huestis M. Pharmacokinetics and metabolism of the plant cannabinoids, Δ 9-tetrahydrocannibinol, cannabidiol and cannabinol. Cannabinoids: Springer; 2005. p. 657-90.

42. Alozie SO, Martin BR, Harris LS, Dewey WL. 3H-delta 9-Tetrahydrocannabinol, 3H-cannabinol and 3H-cannabidiol: penetration and regional distribution in rat brain. Pharmacol Biochem Behav. 1980;12(2):217-21. Epub 1980/02/01.

43. Pop E. Pharmacology and Medicinal Chemistry of THC. Cannabinoids. 2004:8.

44. Jiang R, Yamaori S, Takeda S, Yamamoto I, Watanabe K. Identification of cytochrome P450 enzymes responsible for metabolism of cannabidiol by human liver microsomes. Life Sci. 2011;89(5-6):165-70. Epub 2011/06/28.

45. Ujváry I, Hanuš L. Human metabolites of cannabidiol: a review on their formation, biological activity, and relevance in therapy. Cannabis and Cannabinoid Research. 2016;1(1):90-101.

46. Huestis MA, Smith ML. Cannabinoid pharmacokinetics and disposition in alternative matrices. Handbook of Cannabis, Oxford University Press, Oxford. 2014:296-319.

47. Zhornitsky S, Potvin S. Cannabidiol in humans—the quest for therapeutic targets. Pharmaceuticals. 2012;5(5):529-52.

48. Benowitz NL, Nguyen TL, Jones RT, Herning RI, Bachman J. Metabolic and psychophysiologic studies of cannabidiol-hexobarbital interaction. Clin Pharmacol Ther. 1980;28(1):115-20.

49. Pertwee RG. Endocannabinoids and their pharmacological actions. Endocannabinoids: Springer; 2015. p. 1-37.

50. McPartland J, Glass M, Pertwee R. Meta-analysis of cannabinoid ligand binding affinity and receptor distribution: interspecies differences. Br J Pharmacol. 2007;152(5):583-93.

51. Pertwee RG, Ross RA, Craib SJ, Thomas A. (−)-Cannabidiol antagonizes cannabinoid receptor agonists and noradrenaline in the mouse vas deferens. Eur J Pharmacol. 2002;456(1):99-106.

52. Thomas A, Baillie G, Phillips A, Razdan R, Ross R, Pertwee R. Cannabidiol displays unexpectedly high potency as an antagonist of CB1 and CB2 receptor agonists in vitro. Br J Pharmacol. 2007;150(5):613-23.

53. Laprairie R, Bagher A, Kelly M, Denovan-Wright E. Cannabidiol is a negative allosteric modulator of the cannabinoid CB1 receptor. Br J Pharmacol. 2015;172(20):4790-805.

54. Morales P, Hurst DP, Reggio PH. Molecular Targets of the Phytocannabinoids: A Complex Picture. Phytocannabinoids: Springer; 2017. p. 103-31.

55. Turner SE, Williams CM, Iversen L, Whalley BJ. Molecular Pharmacology of Phytocannabinoids. Phytocannabinoids: Springer; 2017. p. 61-101.

56. Pertwee R. Tolerance to and dependence on psychotropic cannabinoids. The Biological Bases of Drug Tolerance and Dependence. 1991:231-63.

57. Pertwee RG. Pharmacological and therapeutic targets for Δ9 tetrahydrocannabinol and cannabidiol. Euphytica. 2004;140(1-2):73-82.

58. Booz GW. Cannabidiol as an emergent therapeutic strategy for lessening the impact of inflammation on oxidative stress. Free Radical Biology and Medicine. 2011;51(5):1054-61.

59. Tanasescu R, Constantinescu CS. Cannabinoids and the immune system: an overview. Immunobiology. 2010;215(8):588-97.

60. Luo Y, Patel M, Wiederhold M, Ou D. Effects of cannabinoids and cocaine on the mitogen-induced transformations of lymphocytes of human and mouse origins. Int J Immunopharmacol. 1992;14(1):49-56.

61. Jenny M, Santer E, Pirich E, Schennach H, Fuchs D. Delta9-tetrahydrocannabinol and cannabidiol modulate mitogen-induced tryptophan degradation and neopterin formation in peripheral blood mononuclear cells in vitro. J Neuroimmunol. 2009;207(1-2):75-82. Epub 2009/01/27.

62. Kaplan BL, Springs AE, Kaminski NE. The profile of immune modulation by cannabidiol (CBD) involves deregulation of nuclear factor of activated T cells (NFAT). Biochem Pharmacol. 2008;76(6):726-37. Epub 2008/07/29.

63. Robinson RH, Meissler JJ, Breslow-Deckman JM, Gaughan J, Adler MW, Eisenstein TK. Cannabinoids inhibit T-cells via cannabinoid receptor 2 in an in vitro assay for graft rejection, the mixed lymphocyte reaction. Journal of neuroimmune pharmacology : the official journal of the Society on NeuroImmune Pharmacology. 2013;8(5):1239-50. Epub 2013/07/05.

64. Ribeiro A, Ferraz-de-Paula V, Pinheiro ML, Vitoretti LB, Mariano-Souza DP, Quinteiro-Filho WM, et al. Cannabidiol, a non-psychotropic plant-derived cannabinoid, decreases inflammation in a murine model of acute lung injury: Role for the adenosine A 2A receptor. Eur J Pharmacol. 2012;678(1):78-85.

65. Liou GI, Auchampach JA, Hillard CJ, Zhu G, Yousufzai B, Mian S, et al. Mediation of cannabidiol anti-inflammation in the retina by equilibrative nucleoside transporter and A2A adenosine receptor. Invest Ophthalmol Vis Sci. 2008;49(12):5526-31.

66. Novotna A, Mares J, Ratcliffe S, Novakova I, Vachova M, Zapletalova O, et al. A randomized, double-blind, placebo-controlled, parallel-group, enriched-design study of nabiximols*(Sativex®), as add-on therapy, in subjects with refractory spasticity caused by multiple sclerosis. Eur J Neurol. 2011;18(9):1122-31.

67. Phillips TJ, Cherry CL, Cox S, Marshall SJ, Rice AS. Pharmacological treatment of painful HIV-associated sensory neuropathy: a systematic review

and meta-analysis of randomised controlled trials. PLoS One. 2010;5(12):e14433.

68. Borgelt LM, Franson KL, Nussbaum AM, Wang GS. The pharmacologic and clinical effects of medical cannabis. Pharmacotherapy: The Journal of Human Pharmacology and Drug Therapy. 2013;33(2):195-209.

69. Xiong W, Cui T, Cheng K, Yang F, Chen S-R, Willenbring D, et al. Cannabinoids suppress inflammatory and neuropathic pain by targeting α3 glycine receptors. J Exp Med. 2012:jem. 20120242.

70. Martin WJ, Coffin PO, Attias E, Balinsky M, Tsou K, Walker JM. Anatomical basis for cannabinoid-induced antinociception as revealed by intracerebral microinjections. Brain Res. 1999;822(1):237-42.

71. Rock E, Bolognini D, Limebeer C, Cascio M, Anavi-Goffer S, Fletcher P, et al. Cannabidiol, a non-psychotropic component of cannabis, attenuates vomiting and nausea-like behaviour via indirect agonism of 5-HT1A somatodendritic autoreceptors in the dorsal raphe nucleus. Br J Pharmacol. 2012;165(8):2620-34.

72. Rock EM, Sticht MA, Parker LA. Effect of phytocannabinoids on nausea and vomiting. Handbook of Cannabis Oxford Scholarship, Oxford. 2014:435-54.

73. Pryce G, Riddall DR, Selwood DL, Giovannoni G, Baker D. Neuroprotection in experimental autoimmune encephalomyelitis and progressive multiple sclerosis by cannabis-based cannabinoids. Journal of neuroimmune pharmacology. 2015;10(2):281-92.

74. Croxford JL, Pryce G, Jackson SJ, Ledent C, Giovannoni G, Pertwee RG, et al. Cannabinoid-mediated neuroprotection, not immunosuppression, may be more relevant to multiple sclerosis. J Neuroimmunol. 2008;193(1):120-9.

75. Pryce G, Ahmed Z, Hankey DJ, Jackson SJ, Croxford JL, Pocock JM, et al. Cannabinoids inhibit neurodegeneration in models of multiple sclerosis. Brain. 2003;126(10):2191-202.

76. Hampson A, Grimaldi M, Axelrod J, Wink D. Cannabidiol and (−) Δ9-tetrahydrocannabinol are neuroprotective antioxidants. Proceedings of the National Academy of Sciences. 1998;95(14):8268-73.

77. Russo EB. Cannabis and cannabinoids: pharmacology, toxicology, and therapeutic potential: Routledge; 2013.

78. Ablin J, Ste-Marie P, Schäfer M, Häuser PDW, Fitzcharles M-A. Medical use of cannabis products. Der Schmerz. 2016;30(1):3-13.

79. Bolognini D, Ross R. Medical cannabis vs. synthetic cannabinoids: what does the future hold? Clin Pharmacol Ther. 2015;97(6):568-70.

80. Whiting PF, Wolff RF, Deshpande S, Di Nisio M, Duffy S, Hernandez AV, et al. Cannabinoids for medical use: a systematic review and meta-analysis. JAMA. 2015;313(24):2456-73.

81. Lucas P, Walsh Z. Medical cannabis access, use, and substitution for prescription opioids and other substances: A survey of authorized medical cannabis patients. International Journal of Drug Policy. 2017;42:30-5.

82. Abbas AK, Lichtman AH, Pillai S. Basic immunology: functions and disorders of the immune system: Elsevier Health Sciences; 2014.

83. Zabriskie JB. Essential Clinical Immunology: Cambridge University Press; 2009.

84. Chapel H, Haeney M, Misbah S, Snowden N. Essentials of clinical immunology: John Wiley & Sons; 2013.

85. Burmester GR, Pezzutto A. Color Atlas of Immunology: Georg Thieme Verlag; 2003.

86. Kasper DL, Fauci AS, Hauser S, Longo D, Jameson JL, Loscalzo J. Harrison's Principles of Internal Medicine 19/E (Vol.1 & Vol.2): McGraw-Hill Education; 2015.

87. Hemmer B, Kerschensteiner M, Korn T. Role of the innate and adaptive immune responses in the course of multiple sclerosis. The Lancet Neurology. 2015;14(4):406-19.

88. Fauci AS. Harrison's principles of internal medicine / editors, Anthony S. Fauci ... [et al.]. 17th ed. New York: McGraw-Hill Medical; 2008. v. <1-2 > p.

89. Ramagopalan SV, Sadovnick AD. Epidemiology of multiple sclerosis. Neurol Clin. 2011;29(2):207-17.

90. Leray E, Moreau T, Fromont A, Edan G. Epidemiology of multiple sclerosis. Rev Neurol (Paris). 2016;172(1):3-13.

91. Gold R, Wolinsky J. Pathophysiology of multiple sclerosis and the place of teriflunomide. Acta Neurol Scand. 2011;124(2):75-84.

92. Gold R, Wolinsky JS. Pathophysiology of multiple sclerosis and the place of teriflunomide. Acta Neurol Scand. 2011;124(2):75-84. Epub 2010/10/01.

93. Werring DJ, Brassat D, Droogan AG, Clark CA, Symms MR, Barker GJ, et al. The pathogenesis of lesions and normal-appearing white matter changes in multiple sclerosis: a serial diffusion MRI study. Brain. 2000;123 (Pt 8):1667-76. Epub 2000/07/25.

94. Smith KJ, McDonald WI. The pathophysiology of multiple sclerosis: the mechanisms underlying the production of symptoms and the natural history of the disease. Philos T Roy Soc B. 1999;354(1390):1649-73.

95. Lubetzki C, Stankoff B. Demyelination in multiple sclerosis. Handb Clin Neurol. 2014;122:89-99. Epub 2014/02/11.

96. Wingerchuk DM, Lucchinetti CF, Noseworthy JH. Multiple sclerosis: current pathophysiological concepts. Lab Invest. 2001;81(3):263-81.

97. McGeachy MJ. GM-CSF: the secret weapon in the TH17 arsenal. Nature immunology. 2011;12(6):521-2.

98. Dutta R, Trapp BD. Mechanisms of neuronal dysfunction and degeneration in multiple sclerosis. Prog Neurobiol. 2011;93(1):1-12. Epub 2010/10/16.

99. Gonsette RE. Neurodegeneration in multiple sclerosis: The role of oxidative stress and excitotoxicity. Journal of the Neurological Sciences. 2008;274(1–2):48-53.

100. Damal K, Stoker E, Foley JF. Optimizing therapeutics in the management of patients with multiple sclerosis: a review of drug efficacy, dosing, and mechanisms of action. Biologics. 2013;7:247-58.

101. Dolati S, Babaloo Z, Jadidi-Niaragh F, Ayromlou H, Sadreddini S, Yousefi M. Multiple sclerosis: Therapeutic applications of advancing drug delivery systems. Biomed Pharmacother. 2017;86:343-53.

102. Du Pasquier RA, Pinschewer DD, Merkler D. Immunological mechanism of action and clinical profile of disease-modifying treatments in multiple sclerosis. CNS Drugs. 2014;28(6):535-58.

103. Bigi S, Yeh EA. Symptomatic treatment in multiple sclerosis. US Neurol. 2013;9:35-40.

104. Toosy A, Ciccarelli O, Thompson A. Symptomatic treatment and management of multiple sclerosis. Handb Clin Neurol. 2014;122:513-62.

105. Zajicek J, Sanders H, Wright D, Vickery P, Ingram W, Reilly S, et al. Cannabinoids in multiple sclerosis (CAMS) study: safety and efficacy data for 12 months follow up. J Neurol Neurosurg Psychiatry. 2005;76(12):1664-9.

106. Zajicek JP, Hobart JC, Slade A, Barnes D, Mattison PG, Group MR. Multiple sclerosis and extract of cannabis: results of the MUSEC trial. J Neurol Neurosurg Psychiatry. 2012;83(11):1125-32.

107. Svendsen KB, Jensen TS, Bach FW. Does the cannabinoid dronabinol reduce central pain in multiple sclerosis? Randomised double blind placebo controlled crossover trial. BMJ. 2004;329(7460):253.

108. Rog DJ, Nurmikko TJ, Friede T, Young CA. Randomized, controlled trial of cannabis-based medicine in central pain in multiple sclerosis. Neurology. 2005;65(6):812-9.

109. Iskedjian M, Bereza B, Gordon A, Piwko C, Einarson TR. Meta-analysis of cannabis based treatments for neuropathic and multiple sclerosis-related pain. Curr Med Res Opin. 2007;23(1):17-24.

110. Freeman R, Adekanmi O, Waterfield M, Waterfield A, Wright D, Zajicek J. The effect of cannabis on urge incontinence in patients with multiple sclerosis: a multicentre, randomised placebo-controlled trial (CAMS-LUTS). International Urogynecology Journal. 2006;17(6):636-41.

111. t Hart BA, Gran B, Weissert R. EAE: imperfect but useful models of multiple sclerosis. Trends in molecular medicine. 2011;17(3):119-25. Epub 2011/01/22.

112. Denic A, Johnson AJ, Bieber AJ, Warrington AE, Rodriguez M, Pirko I. The relevance of animal models in multiple sclerosis research. Pathophysiology : the official journal of the International Society for Pathophysiology. 2011;18(1):21-9. Epub 2010/06/12.

113. Robinson AP, Harp CT, Noronha A, Miller SD. The experimental autoimmune encephalomyelitis (EAE) model of MS: utility for understanding disease pathophysiology and treatment. Handb Clin Neurol. 2014;122:173-89. Epub 2014/02/11.

114. Kipp M, van der Star B, Vogel DY, Puentes F, van der Valk P, Baker D, et al. Experimental in vivo and in vitro models of multiple sclerosis: EAE and beyond. Multiple Sclerosis and Related Disorders. 2012;1(1):15-28.

115. Kipp M, Nyamoya S, Hochstrasser T, Amor S. Multiple sclerosis animal models: a clinical and histopathological perspective. Brain Pathol. 2017.

116. Kozela E, Lev N, Kaushansky N, Eilam R, Rimmerman N, Levy R, et al. Cannabidiol inhibits pathogenic T cells, decreases spinal microglial activation and ameliorates multiple sclerosis-like disease in C57BL/6 mice. Br J Pharmacol. 2011;163(7):1507-19. Epub 2011/04/01.

117. Maresz K, Pryce G, Ponomarev ED, Marsicano G, Croxford JL, Shriver LP, et al. Direct suppression of CNS autoimmune inflammation via the cannabinoid receptor CB1 on neurons and CB2 on autoreactive T cells. Nature medicine. 2007;13(4):492-7. Epub 2007/04/03.

118. Pryce G, Riddall DR, Selwood DL, Giovannoni G, Baker D. Neuroprotection in Experimental Autoimmune Encephalomyelitis and Progressive Multiple Sclerosis by Cannabis-Based Cannabinoids. Journal of neuroimmune pharmacology : the official journal of the Society on NeuroImmune Pharmacology. 2015;10(2):281-92. Epub 2014/12/30.

119. Ahmed Z, Doward AI, Pryce G, Taylor DL, Pocock JM, Leonard JP, et al. A role for caspase-1 and-3 in the pathology of experimental allergic encephalomyelitis - Inflammation versus degeneration. Am J Pathol. 2002;161(5):1577-86.

120. Pryce G, Ahmed Z, Hankey DJR, Jackson SJ, Croxford JL, Pocock JM, et al. Cannabinoids inhibit neurodegeneration in models of multiple sclerosis. Brain. 2003;126:2191-202.

121. Lyman WD, Sonett JR, Brosnan CF, Elkin R, Bornstein MB. Delta 9-tetrahydrocannabinol: a novel treatment for experimental autoimmune encephalomyelitis. J Neuroimmunol. 1989;23(1):73-81. Epub 1989/06/01.

122. Brown P. Lymphatic system: unlocking the drains. Nature. 2005;436(7050):456-8.

123. Swartz MA. The physiology of the lymphatic system. Adv Drug Deliv Rev. 2001;50(1-2):3-20. Epub 2001/08/08.

124. Loukas M, Bellary SS, Kuklinski M, Ferrauiola J, Yadav A, Shoja MM, et al. The lymphatic system: a historical perspective. Clin Anat. 2011;24(7):807-16. Epub 2011/05/06.

125. Saroj P, Verma M, Jha K. An overview on immunomodulation. Journal of Advanced Scientific Research. 2012;3(1).

126. Skobe M, Detmar M. Structure, function, and molecular control of the skin lymphatic system. J Investig Dermatol Symp Proc. 2000;5(1):14-9. Epub 2001/01/09.

127. Saladin KS. Anatomy & Physiology: The Unity of Form and Function: McGraw-Hill; 2012.

128. Jurisic G, Detmar M. Lymphatic endothelium in health and disease. Cell and tissue research. 2009;335(1):97-108. Epub 2008/07/24.

129. Iqbal J, Hussain MM. Intestinal lipid absorption. Am J Physiol Endocrinol Metab. 2009;296(6):E1183-94. Epub 2009/01/23.

130. Black DD. Development and physiological regulation of intestinal lipid absorption. I. Development of intestinal lipid absorption: cellular events in chylomicron assembly and secretion. American journal of physiology Gastrointestinal and liver physiology. 2007;293(3):G519-24. Epub 2007/05/15.

131. Nordskog BK, Phan CT, Nutting DF, Tso P. An examination of the factors affecting intestinal lymphatic transport of dietary lipids. Adv Drug Deliv Rev. 2001;50(1-2):21-44. Epub 2001/08/08.

132. Charman WNA, Stella VJ. Estimating the Maximal Potential for Intestinal Lymphatic Transport of Lipophilic Drug Molecules. Int J Pharm. 1986;34(1-2):175-8.

133. von Andrian UH, Mempel TR. Homing and cellular traffic in lymph nodes. Nature reviews Immunology. 2003;3(11):867-78. Epub 2003/12/12.

134. Trevaskis NL, Charman WN, Porter CJ. Targeted drug delivery to lymphocytes: a route to site-specific immunomodulation? Molecular pharmaceutics. 2010;7(6):2297-309. Epub 2010/10/21.

135. Saladin K. Anatomy & Physiology: The Unity of Form and Function: McGraw-Hill Education; 2011.

136. Clement C, Santambrogio L. The Lymph Proteome, Peptidome, and Degradome. In: Santambrogio L, editor. Immunology of the Lymphatic System: Springer New York; 2013. p. 65-79.

137. Cueni LN, Detmar M. New insights into the molecular control of the lymphatic vascular system and its role in disease. The Journal of investigative dermatology. 2006;126(10):2167-77. Epub 2006/09/20.

138. McAllaster JD, Cohen MS. Role of the lymphatics in cancer metastasis and chemotherapy applications. Advanced drug delivery reviews. 2011;63(10-11):867-75. Epub 2011/06/28.

139. Shields J. Lymph and Lymphatic Capillaries in Cancer. In: Santambrogio L, editor. Immunology of the Lymphatic System: Springer New York; 2013. p. 121-42.

140. Ohl L, Bernhardt G, Pabst O, Förster R, editors. Chemokines as organizers of primary and secondary lymphoid organs. Seminars in immunology; 2003: Elsevier.

141. Fu YX, Chaplin DD. Development and maturation of secondary lymphoid tissues. Annual review of immunology. 1999;17:399-433. Epub 1999/06/08.

142. Pal I, Ramsey JD. The role of the lymphatic system in vaccine trafficking and immune response. Advanced drug delivery reviews. 2011;63(10-11):909-22. Epub 2011/06/21.

143. Cesta MF. Normal structure, function, and histology of mucosa-associated lymphoid tissue. Toxicologic pathology. 2006;34(5):599-608. Epub 2006/10/28.

144. Mowat AM. Anatomical basis of tolerance and immunity to intestinal antigens. Nature reviews Immunology. 2003;3(4):331-41. Epub 2003/04/02.

145. Forchielli ML, Walker WA. The role of gut-associated lymphoid tissues and mucosal defence. The British journal of nutrition. 2005;93 Suppl 1:S41-8. Epub 2005/05/10.

146. Nakajima-Adachi H, Kikuchi A, Fujimura Y, Shibahara K, Makino T, Goseki-Sone M, et al. Peyer's Patches and Mesenteric Lymph Nodes Cooperatively Promote Enteropathy in a Mouse Model of Food Allergy. PloS one. 2014;9(10):e107492. Epub 2014/10/08.

147. Wershil BK, Furuta GT. 4. Gastrointestinal mucosal immunity. The Journal of allergy and clinical immunology. 2008;121(2 Suppl):S380-3; quiz S415. Epub 2008/02/05.

148. Cheroutre H, Lambolez F, Mucida D. The light and dark sides of intestinal intraepithelial lymphocytes. Nature reviews Immunology. 2011;11(7):445-56. Epub 2011/06/18.

149. Miura S, Sekizuka E, Nagata H, Oshio C, Minamitani H, Suematsu M, et al. Increased lymphocyte transport by lipid absorption in rat mesenteric lymphatics. The American journal of physiology. 1987;253(5 Pt 1):G596-600.

150. Hamada H, Hiroi T, Nishiyama Y, Takahashi H, Masunaga Y, Hachimura S, et al. Identification of multiple isolated lymphoid follicles on the antimesenteric wall of the mouse small intestine. J Immunol. 2002;168(1):57-64. Epub 2001/12/26.

151. Varol C, Zigmond E, Jung S. Securing the immune tightrope: mononuclear phagocytes in the intestinal lamina propria. Nature reviews Immunology. 2010;10(6):415-26. Epub 2010/05/26.

152. Watzl B, Girrbach S, Roller M. Inulin, oligofructose and immunomodulation. The British journal of nutrition. 2005;93 Suppl 1:S49-55. Epub 2005/05/10.

153. Miura S, Tsuzuki Y, Hokari R, Ishii H. Modulation of intestinal immune system by dietary fat intake: relevance to Crohn's disease. Journal of gastroenterology and hepatology. 1998;13(12):1183-90. Epub 1999/01/26.

154. Coombes JL, Powrie F. Dendritic cells in intestinal immune regulation. Nature reviews Immunology. 2008;8(6):435-46. Epub 2008/05/27.

155. Spahn TW, Kucharzik T. Modulating the intestinal immune system: the role of lymphotoxin and GALT organs. Gut. 2004;53(3):456-65. Epub 2004/02/13.

156. Porter CJ, Trevaskis NL, Charman WN. Lipids and lipid-based formulations: optimizing the oral delivery of lipophilic drugs. Nat Rev Drug Discov. 2007;6(3):231-48. Epub 2007/03/03.

157. Blanchard DK, Budde JM, Hatch GF, 3rd, Wertheimer-Hatch L, Hatch KF, Davis GB, et al. Tumors of the small intestine. World journal of surgery. 2000;24(4):421-9. Epub 2000/03/09.

158. Porter CJ, Charman WN. Intestinal lymphatic drug transport: an update. Adv Drug Deliv Rev. 2001;50(1-2):61-80. Epub 2001/08/08.

159. Paliwal R, Rai S, Vaidya B, Khatri K, Goyal AK, Mishra N, et al. Effect of lipid core material on characteristics of solid lipid nanoparticles designed for oral lymphatic delivery. Nanomedicine: Nanotechnology, Biology and Medicine. 2009;5(2):184-91.

160. Trevaskis NL, Charman WN, Porter CJ. Lipid-based delivery systems and intestinal lymphatic drug transport: a mechanistic update. Adv Drug Deliv Rev. 2008;60(6):702-16. Epub 2007/12/25.

161. Wasan KM, Cassidy SM. Role of plasma lipoproteins in modifying the biological activity of hydrophobic drugs. Journal of pharmaceutical sciences. 1998;87(4):411-24. Epub 1998/04/21.

162. Caliph SM, Charman WN, Porter CJ. Effect of short-, medium-, and long-chain fatty acid-based vehicles on the absolute oral bioavailability and intestinal lymphatic transport of halofantrine and assessment of mass balance in lymph-cannulated and non-cannulated rats. J Pharm Sci. 2000;89(8):1073-84. Epub 2000/07/25.

163. Gershkovich P, Hoffman A. Effect of a high-fat meal on absorption and disposition of lipophilic compounds: the importance of degree of association with triglyceride-rich lipoproteins. Eur J Pharm Sci. 2007;32(1):24-32. Epub 2007/07/03.

164. Dahan A, Hoffman A. Evaluation of a chylomicron flow blocking approach to investigate the intestinal lymphatic transport of lipophilic drugs. Eur J Pharm Sci. 2005;24(4):381-8. Epub 2005/03/01.

165. Gershkovich P, Qadri B, Yacovan A, Amselem S, Hoffman A. Different impacts of intestinal lymphatic transport on the oral bioavailability of structurally similar synthetic lipophilic cannabinoids: dexanabinol and PRS-211,220. Eur J Pharm Sci. 2007;31(5):298-305. Epub 2007/06/15.

166. Gershkovich P, Hoffman A. Uptake of lipophilic drugs by plasma derived isolated chylomicrons: linear correlation with intestinal lymphatic bioavailability. European journal of pharmaceutical sciences : official journal of the European Federation for Pharmaceutical Sciences. 2005;26(5):394-404. Epub 2005/09/06.

167. Hauss DJ, Mehta SC, Radebaugh GW. Targeted lymphatic transport and modified systemic distribution of CI-976, a lipophilic lipid-regulator drug, via a formulation approach. Int J Pharm. 1994;108(2):85-93.

168. Zgair A LJ, Wong JC, Fischer PM, Barrett DA, Constantinescu CS and Gershkovich P. Effect of Long-Chain Triglyceride Formulation on the Oral Bioavailability of Cannabidiol. AAPS Annual Meeting and Exposition; Oct 2015; Colorado, Denver, USA(2015).

169. Ichihashi T, Nagasaki T, Takagishi Y, Yamada H. A quantitative concept of the mechanism of intestinal lymphatic transfer of lipophilic molecules. Pharmaceutical research. 1994;11(4):508-12.

170. Gupta S, Kesarla R, Omri A. Formulation strategies to improve the bioavailability of poorly absorbed drugs with special emphasis on self-emulsifying systems. ISRN pharmaceutics. 2013;2013:848043. Epub 2014/01/25.

171. Tan A, Rao S, Prestidge CA. Transforming lipid-based oral drug delivery systems into solid dosage forms: an overview of solid carriers, physicochemical properties, and biopharmaceutical performance. Pharm Res. 2013;30(12):2993-3017. Epub 2013/06/19.

172. Holm R, Porter CJ, Edwards GA, Müllertz A, Kristensen HG, Charman WN. Examination of oral absorption and lymphatic transport of halofantrine in a triple-cannulated canine model after administration in self-microemulsifying drug delivery systems (SMEDDS) containing structured triglycerides. Eur J Pharm Sci. 2003;20(1):91-7.

173. Lian T, Ho RJY. Trends and developments in liposome drug delivery systems. Journal of Pharmaceutical Sciences. 2001;90(6):667-80.

174. Gabizon A, Dagan A, Goren D, Barenholz Y, Fuks Z. Liposomes as in Vivo Carriers of Adriamycin: Reduced Cardiac Uptake and Preserved Antitumor Activity in Mice. Cancer Research. 1982;42(11):4734-9.

175. Sheue Nee Ling S, Magosso E, Abdul Karim Khan N, Hay Yuen K, Anne Barker S. Enhanced oral bioavailability and intestinal lymphatic transport of a hydrophilic drug using liposomes. Drug Dev Ind Pharm. 2006;32(3):335-45.

176. Guan P, Lu Y, Qi J, Niu M, Lian R, Hu F, et al. Enhanced oral bioavailability of cyclosporine A by liposomes containing a bile salt. International journal of nanomedicine. 2011;6:965-74. Epub 2011/07/02.

177. Bargoni A, Cavalli R, Caputo O, Fundarò A, Gasco MR, Zara GP. Solid lipid nanoparticles in lymph and plasma after duodenal administration to rats. Pharmaceutical research. 1998;15(5):745-50.

178. Manjunath K, Venkateswarlu V. Pharmacokinetics, tissue distribution and bioavailability of clozapine solid lipid nanoparticles after intravenous and intraduodenal administration. Journal of controlled release : official journal of the Controlled Release Society. 2005;107(2):215-28. Epub 2005/07/15.

179. Chalikwar SS, Belgamwar VS, Talele VR, Surana SJ, Patil MU. Formulation and evaluation of Nimodipine-loaded solid lipid nanoparticles delivered via lymphatic transport system. Colloids and surfaces B, Biointerfaces. 2012;97:109-16. Epub 2012/05/23.

180. Shackleford DM, Porter CJ, Charman WN. Lymphatic absorption of orally administered prodrugs. Prodrugs: Springer; 2007. p. 653-82.

181. Coert A, Geelen J, de Visser J, van der Vies J. The pharmacology and metabolism of testosterone undecanoate (TU), a new orally active androgen. Acta endocrinologica. 1975;79(4):789-800. Epub 1975/08/01.

182. Skakkebaek NE, Bancroft J, Davidson DW, Warner P. Androgen replacement with oral testosterone undecanoate in hypogonadal men: a double blind controlled study. Clinical endocrinology. 1981;14(1):49-61. Epub 1981/01/01.

183. Shackleford DM, Faassen WA, Houwing N, Lass H, Edwards GA, Porter CJ, et al. Contribution of lymphatically transported testosterone undecanoate to the systemic exposure of testosterone after oral administration of two andriol formulations in conscious lymph duct-cannulated dogs. The Journal of pharmacology and experimental therapeutics. 2003;306(3):925-33. Epub 2003/06/17.

184. Katchan V, David P, Shoenfeld Y. Cannabinoids and autoimmune diseases: A systematic review. Autoimmunity reviews. 2016;15(6):513-28. Epub 2016/02/16.

185. Health UDo, Services H. Guidance for industry, bioanalytical method validation. http://www fda gov/cder/guidance/index htm. 2001.

186. Gershkovich P, Ibrahim F, Sivak O, Darlington JW, Wasan KM. A simple and sensitive method for determination of vitamins D3 and K1 in rat plasma: application for an in vivo pharmacokinetic study. Drug Dev Ind Pharm. 2014;40(3):338-44. Epub 2013/02/05.

187. Halabi A, Ferrayoli C, Palacio M, Dabbene V, Palacios S. Validation of a chiral HPLC assay for (R)-salbutamol sulfate. J Pharm Biomed Anal. 2004;34(1):45-51. Epub 2004/01/24.

188. Benito-Gallo P, Marlow M, Zann V, Scholes P, Gershkovich P. Linking in Vitro Lipolysis and Microsomal Metabolism for the Quantitative Prediction of Oral Bioavailability of BCS II Drugs Administered in Lipidic Formulations. Molecular pharmaceutics. 2016;13(10):3526-40. Epub 2016/08/25.

189. Benito-Gallo P, Franceschetto A, Wong JC, Marlow M, Zann V, Scholes P, et al. Chain length affects pancreatic lipase activity and the extent and pH-time profile of triglyceride lipolysis. Eur J Pharm Biopharm. 2015;93:353-62. Epub 2015/05/06.

190. Gershkovich P, Fanous J, Qadri B, Yacovan A, Amselem S, Hoffman A. The role of molecular physicochemical properties and apolipoproteins in association of drugs with triglyceride-rich lipoproteins: in-silico prediction of uptake by chylomicrons. J Pharm Pharmacol. 2009;61(1):31-9.

191. Lu Y, Qiu YT, Qi JP, Feng MQ, Ju DW, Wu W. Biomimetic reassembled chylomicrons as novel association model for the prediction of lymphatic transportation of highly lipophilic drugs via the oral route. Int J Pharm. 2015;483(1-2):69-76.

192. Cohn JS, McNamara JR, Krasinski SD, Russell RM, Schaefer EJ. Role of triglyceride-rich lipoproteins from the liver and intestine in the etiology of postprandial peaks in plasma triglyceride concentration. Metabolism: clinical and experimental. 1989;38(5):484-90. Epub 1989/05/01.

193. Cohn JS, McNamara JR, Cohn SD, Ordovas JM, Schaefer EJ. Postprandial plasma lipoprotein changes in human subjects of different ages. Journal of lipid research. 1988;29(4):469-79. Epub 1988/04/01.

194. Wong JCM. Contribution of Intestinal Lymphatic Transport to the Immunosuppressive Effect of Δ^9-Tetrahydrocannabinol: University of Nattingham; 2017.

195. Parkinson CM, O'Brien A, Albers TM, Simon MA, Clifford CB, Pritchett-Corning KR. Diagnostic necropsy and selected tissue and sample collection in rats and mice. Journal of visualized experiments : JoVE. 2011(54). Epub 2011/08/19.

196. Boyd M, Risovic V, Jull P, Choo E, Wasan KM. A stepwise surgical procedure to investigate the lymphatic transport of lipid-based oral drug formulations: Cannulation of the mesenteric and thoracic lymph ducts within the rat. J Pharmacol Toxicol Methods. 2004;49(2):115-20. Epub 2004/03/03.

197. Ullman AH, Thorpe TM, Boutilier GD. Analytical Problem Solving: Selection of Analytical Methods. Encyclopedia of Analytical Chemistry.

198. Hearn MT, Grego B, Hancock WS. High-performance liquid chromatography of amino acids, peptides and proteins. XX. Investigation of the effects of pH and ion-pair formation on the retention of peptides on chemically-

bonded hydrocarbonaceous stationary phases. J Chromatogr. 1979;185:429-44. Epub 1979/12/20.

199. Ambach L, Penitschka F, Broillet A, König S, Weinmann W, Bernhard W. Simultaneous quantification of delta-9-THC, THC-acid A, CBN and CBD in seized drugs using HPLC-DAD. Forensic Sci Int. 2014;243:107-11.

200. De Backer B, Debrus B, Lebrun P, Theunis L, Dubois N, Decock L, et al. Innovative development and validation of an HPLC/DAD method for the qualitative and quantitative determination of major cannabinoids in cannabis plant material. Journal of chromatography B, Analytical technologies in the biomedical and life sciences. 2009;877(32):4115-24. Epub 2009/11/26.

201. Smith RN. High pressure liquid chromatography on cannabis. Identification of separated constituents. J Chromatogr. 1975;115(1):101-6. Epub 1975/12/10.

202. Aizpurua-Olaizola O, Omar J, Navarro P, Olivares M, Etxebarria N, Usobiaga A. Identification and quantification of cannabinoids in Cannabis sativa L. plants by high performance liquid chromatography-mass spectrometry. Analytical and bioanalytical chemistry. 2014;406(29):7549-60. Epub 2014/10/24.

203. Sanchez-Gonzalez J, Salgueiro-Fernandez R, Cabarcos P, Bermejo AM, Bermejo-Barrera P, Moreda-Pineiro A. Cannabinoids assessment in plasma and urine by high performance liquid chromatography-tandem mass spectrometry after molecularly imprinted polymer microsolid-phase extraction. Analytical and bioanalytical chemistry. 2016. Epub 2016/11/07.

204. Gul W, Gul SW, Radwan MM, Wanas AS, Mehmedic Z, Khan, II, et al. Determination of 11 Cannabinoids in Biomass and Extracts of Different Varieties of Cannabis Using High-Performance Liquid Chromatography. J AOAC Int. 2015;98(6):1523-8. Epub 2015/12/15.

205. Yang R, Xie W. Determination of cannabinoids in biological samples using a new solid phase micro-extraction membrane and liquid chromatography–mass spectrometry. Forensic Sci Int. 2006;162(1):135-9.

206. Nadulski T, Sporkert F, Schnelle M, Stadelmann AM, Roser P, Schefter T, et al. Simultaneous and sensitive analysis of THC, 11-OH-THC, THC-COOH, CBD, and CBN by GC-MS in plasma after oral application of small doses of THC and cannabis extract. J Anal Toxicol. 2005;29(8):782-9.

207. Wall ME, Harvey TM, Bursey JT, Brine DR, Rosenthal D. Analytical methods for the determination of cannabinoids in biological media. NIDA Res Monogr. 1976(7):107-17. Epub 1976/05/01.

208. Want E, Compton BJ, Hollenbeck T, Siuzdak G. The application of mass spectrometry in pharmacokinetics studies. Journal of Spectroscopy. 2003;17(4):681-91.

209. Deiana S, Watanabe A, Yamasaki Y, Amada N, Arthur M, Fleming S, et al. Plasma and brain pharmacokinetic profile of cannabidiol (CBD),

cannabidivarine (CBDV), Delta(9)-tetrahydrocannabivarin (THCV) and cannabigerol (CBG) in rats and mice following oral and intraperitoneal administration and CBD action on obsessive-compulsive behaviour. Psychopharmacology. 2012;219(3):859-73. Epub 2011/07/29.

210. Grauwiler SB, Scholer A, Drewe J. Development of a LC/MS/MS method for the analysis of cannabinoids in human EDTA-plasma and urine after small doses of Cannabis sativa extracts. Journal of chromatography B, Analytical technologies in the biomedical and life sciences. 2007;850(1-2):515-22. Epub 2007/01/24.

211. Samara E, Bialer M. Rapid high-performance liquid chromatographic assay with pharmacokinetic applications for monitoring cannabidiol in plasma. J Chromatogr. 1987;416(2):370-4. Epub 1987/05/15.

212. Grebe SK, Singh RJ. LC-MS/MS in the Clinical Laboratory–Where to From Here? The Clinical Biochemist Reviews. 2011;32(1):5.

213. Smith R, Vaughan C. High-pressure liquid chromatography of cannabis: Quantitative analysis of acidic and neutral cannabinoids. J Chromatogr A. 1976;129:347-54.

214. Polson C, Sarkar P, Incledon B, Raguvaran V, Grant R. Optimization of protein precipitation based upon effectiveness of protein removal and ionization effect in liquid chromatography–tandem mass spectrometry. Journal of Chromatography B. 2003;785(2):263-75.

215. Souverain S, Rudaz S, Veuthey JL. Protein precipitation for the analysis of a drug cocktail in plasma by LC-ESI-MS. J Pharm Biomed Anal. 2004;35(4):913-20. Epub 2004/06/15.

216. Casas ME, Hansen M, Krogh KA, Styrishave B, Björklund E. Analytical sample preparation strategies for the determination of antimalarial drugs in human whole blood, plasma and urine. Journal of Chromatography B. 2014;962(0):109-31.

217. Kole PL, Venkatesh G, Kotecha J, Sheshala R. Recent advances in sample preparation techniques for effective bioanalytical methods. Biomedical Chromatography. 2011;25(1-2):199-217.

218. Iffland K, Grotenhermen F. Safety and Side Effects of Cannabidiol–A review of clinical data and relevant animal studies.

219. Pisanti S, Malfitano AM, Ciaglia E, Lamberti A, Ranieri R, Cuomo G, et al. Cannabidiol: State of the art and new challenges for therapeutic applications. Pharmacol Ther. 2017.

220. Moore C, Rana S, Coulter C. Simultaneous identification of 2-carboxy-tetrahydrocannabinol, tetrahydrocannabinol, cannabinol and cannabidiol in oral fluid. Journal of Chromatography B. 2007;852(1):459-64.

221. Bauer AE. Cannabinoid Extraction from Cannabinoid-Laced Brownies by QuEChERS and Quantification by Gas Chromatography-Mass Spectrometry: University of California, Davis; 2016.

222. Nadulski T, Pragst F. Simple and sensitive determination of Δ 9-tetrahydrocannabinol, cannabidiol and cannabinol in hair by combined silylation, headspace solid phase microextraction and gas chromatography–mass spectrometry. Journal of Chromatography B. 2007;846(1):78-85.

223. Karschner EL, Barnes AJ, Lowe RH, Scheidweiler KB, Huestis MA. Validation of a two-dimensional gas chromatography mass spectrometry method for the simultaneous quantification of cannabidiol, Delta(9)-tetrahydrocannabinol (THC), 11-hydroxy-THC, and 11-nor-9-carboxy-THC in plasma. Analytical and bioanalytical chemistry. 2010;397(2):603-11. Epub 2010/03/23.

224. Zgair A, Wong JC, Sabri A, Fischer PM, Barrett DA, Constantinescu CS, et al. Development of a simple and sensitive HPLC-UV method for the simultaneous determination of cannabidiol and Delta(9)-tetrahydrocannabinol in rat plasma. J Pharm Biomed Anal. 2015;114:145-51. Epub 2015/06/07.

225. Amidon GL, Lennernas H, Shah VP, Crison JR. A theoretical basis for a biopharmaceutic drug classification: the correlation of in vitro drug product dissolution and in vivo bioavailability. Pharm Res. 1995;12(3):413-20. Epub 1995/03/01.

226. Dahan A, Hoffman A. Rationalizing the selection of oral lipid based drug delivery systems by an in vitro dynamic lipolysis model for improved oral bioavailability of poorly water soluble drugs. Journal of controlled release : official journal of the Controlled Release Society. 2008;129(1):1-10.

227. Dahan A, Hoffman A. Enhanced gastrointestinal absorption of lipophilic drugs. Enhancement in drug delivery: CRC Press, Boca Raton, FL; 2006. p. 111-27.

228. Carriere F. Impact of gastrointestinal lipolysis on oral lipid-based formulations and bioavailability of lipophilic drugs. Biochimie. 2016;125:297-305. Epub 2015/11/27.

229. Costanzo LS. Physiology: Saunders Elsevier; 2006.

230. Kossena GA, Charman WN, Wilson CG, O'Mahony B, Lindsay B, Hempenstall JM, et al. Low dose lipid formulations: effects on gastric emptying and biliary secretion. Pharm Res. 2007;24(11):2084-96. Epub 2007/07/28.

231. Dahan A, Hoffman A. The effect of different lipid based formulations on the oral absorption of lipophilic drugs: the ability of in vitro lipolysis and consecutive ex vivo intestinal permeability data to predict in vivo bioavailability in rats. Eur J Pharm Biopharm. 2007;67(1):96-105. Epub 2007/03/03.

232. Sek L, Porter CJ, Kaukonen AM, Charman WN. Evaluation of the in-vitro digestion profiles of long and medium chain glycerides and the phase behaviour

of their lipolytic products. Journal of Pharmacy and Pharmacology. 2002;54(1):29-41.

233. Christensen JO, Schultz K, Mollgaard B, Kristensen HG, Mullertz A. Solubilisation of poorly water-soluble drugs during in vitro lipolysis of medium- and long-chain triacylglycerols. European journal of pharmaceutical sciences : official journal of the European Federation for Pharmaceutical Sciences. 2004;23(3):287-96. Epub 2004/10/19.

234. Williams HD, Sassene P, Kleberg K, Bakala-N'Goma JC, Calderone M, Jannin V, et al. Toward the establishment of standardized in vitro tests for lipid-based formulations, part 1: method parameterization and comparison of in vitro digestion profiles across a range of representative formulations. Journal of pharmaceutical sciences. 2012;101(9):3360-80. Epub 2012/05/31.

235. Dahan A, Hoffman A. Use of a dynamic in vitro lipolysis model to rationalize oral formulation development for poor water soluble drugs: correlation with in vivo data and the relationship to intra-enterocyte processes in rats. Pharm Res. 2006;23(9):2165-74.

236. Larsen AT, Sassene P, Müllertz A. < i> In vitro</i> lipolysis models as a tool for the characterization of oral lipid and surfactant based drug delivery systems. Int J Pharm. 2011;417(1):245-55.

237. Feeney OM, Crum MF, McEvoy CL, Trevaskis NL, Williams HD, Pouton CW, et al. 50years of oral lipid-based formulations: Provenance, progress and future perspectives. Adv Drug Deliv Rev. 2016;101:167-94.

238. Holm R, Hoest J. Successful in silico predicting of intestinal lymphatic transfer. Int J Pharm. 2004;272(1-2):189-93. Epub 2004/03/17.

239. Yanez JA, Wang SW, Knemeyer IW, Wirth MA, Alton KB. Intestinal lymphatic transport for drug delivery. Adv Drug Deliv Rev. 2011;63(10-11):923-42. Epub 2011/06/22.

240. Pouton CW. Lipid formulations for oral administration of drugs: non-emulsifying, self-emulsifying and 'self-microemulsifying'drug delivery systems. Eur J Pharm Sci. 2000;11:S93-S8.

241. Kollipara S, Gandhi RK. Pharmacokinetic aspects and in vitro–in vivo correlation potential for lipid-based formulations. Acta Pharmaceutica Sinica B. 2014;4(5):333-49.

242. Thomas N, Holm R, Rades T, Mullertz A. Characterising Lipid Lipolysis and Its Implication in Lipid-Based Formulation Development. The AAPS journal. 2012;14(4):860-71.

243. Kaukonen AM, Boyd BJ, Porter CJ, Charman WN. Drug solubilization behavior during in vitro digestion of simple triglyceride lipid solution formulations. Pharm Res. 2004;21(2):245-53. Epub 2004/03/23.

244. von Bonsdorff-Nikander A, Christiansen L, Huikko L, Lampi AM, Piironen V, Yliruusi J, et al. A comparison of the effect of medium- vs. long-chain

triglycerides on the in vitro solubilization of cholesterol and/or phytosterol into mixed micelles. Lipids. 2005;40(2):181-90. Epub 2005/05/12.

245. Zangenberg NH, Mullertz A, Kristensen HG, Hovgaard L. A dynamic in vitro lipolysis model. II: Evaluation of the model. Eur J Pharm Sci. 2001;14(3):237-44. Epub 2001/09/29.

246. Porter CJ, Pouton CW, Cuine JF, Charman WN. Enhancing intestinal drug solubilisation using lipid-based delivery systems. Adv Drug Deliv Rev. 2008;60(6):673-91.

247. Carey MC, Small DM, Bliss CM. Lipid digestion and absorption. Annu Rev Physiol. 1983;45(1):651-77.

248. Hall W, Solowij N. Adverse effects of cannabis. Lancet. 1998;352(9140):1611-6. Epub 1998/12/08.

249. Gottlieb A. Cooking with Cannabis: The Most Effective Methods of Preparing Food and Drink with Marijuana, Hashish, and Hash Oil Third E: Ronin Publishing; 2009.

250. Magazine EHT, McDonough E, Remington S. The Official High Times Cannabis Cookbook: More Than 50 Irresistible Recipes That Will Get You High: Chronicle Books LLC; 2012.

251. Orrin Devinsky EM, Daniel Friedman, Elizabeth Thiele, Linda Laux, Joseph Sullivan, Ian Miller, Robert Flamini, Angus Wilfong, Francis Filloux, Matthew Wong, Nicole Tilton, Patricia Bruno, Judith Bluvstein, Julie Hedlund, Rebecca Kamensb, Jane Maclean, Srishti Nangia, Nilika Shah Singhal, Carey A Wilson, Anup Patel, Maria Roberta Cilio. Cannabidiol in patients with treatment-resistant epilepsy: an open-label interventional trial. The Lancet Neurology. 2015.

252. Consroe P, Laguna J, Allender J, Snider S, Stern L, Sandyk R, et al. Controlled clinical trial of cannabidiol in Huntington's disease. Pharmacol Biochem Behav. 1991;40(3):701-8. Epub 1991/11/01.

253. Zajicek J, Fox P, Sanders H, Wright D, Vickery J, Nunn A, et al. Cannabinoids for treatment of spasticity and other symptoms related to multiple sclerosis (CAMS study): multicentre randomised placebo-controlled trial. Lancet. 2003;362(9395):1517-26. Epub 2003/11/15.

254. Holdcroft A, Smith M, Jacklin A, Hodgson H, Smith B, Newton M, et al. Pain relief with oral cannabinoids in familial Mediterranean fever. Anaesthesia. 1997;52(5):483-6. Epub 1997/05/01.

255. Freeman RM, Adekanmi O, Waterfield MR, Waterfield AE, Wright D, Zajicek J. The effect of cannabis on urge incontinence in patients with multiple sclerosis: a multicentre, randomised placebo-controlled trial (CAMS-LUTS). Int Urogynecol J Pelvic Floor Dysfunct. 2006;17(6):636-41. Epub 2006/03/23.

256. Belle-Isle L, Walsh Z, Callaway R, Lucas P, Capler R, Kay R, et al. Barriers to access for Canadians who use cannabis for therapeutic purposes. International Journal of Drug Policy. 2014;25(4):691-9.

257. Lindgren JE, Ohlsson A, Agurell S, Hollister L, Gillespie H. Clinical effects and plasma levels of delta 9-tetrahydrocannabinol (delta 9-THC) in heavy and light users of cannabis. Psychopharmacology (Berl). 1981;74(3):208-12. Epub 1981/01/01.

258. Khoo SM, Shackleford DM, Porter CJ, Edwards GA, Charman WN. Intestinal lymphatic transport of halofantrine occurs after oral administration of a unit-dose lipid-based formulation to fasted dogs. Pharm Res. 2003;20(9):1460-5. Epub 2003/10/22.

259. Joint F. Fats and fatty acids in human nutrition: Karger; 2009.

260. Fan J, de Lannoy IA. Pharmacokinetics. Biochem Pharmacol. 2014;87(1):93-120. Epub 2013/09/24.

261. Willard-Mack CL. Normal structure, function, and histology of lymph nodes. Toxicol Pathol. 2006;34(5):409-24. Epub 2006/10/28.

262. Malfait AM, Gallily R, Sumariwalla PF, Malik AS, Andreakos E, Mechoulam R, et al. The nonpsychoactive cannabis constituent cannabidiol is an oral anti-arthritic therapeutic in murine collagen-induced arthritis. Proc Natl Acad Sci U S A. 2000;97(17):9561-6.

263. Weiss L, Zeira M, Reich S, Slavin S, Raz I, Mechoulam R, et al. Cannabidiol arrests onset of autoimmune diabetes in NOD mice. Neuropharmacology. 2008;54(1):244-9. Epub 2007/08/24.

264. Jan TR, Farraj AK, Harkema JR, Kaminski NE. Attenuation of the ovalbumin-induced allergic airway response by cannabinoid treatment in A/J mice. Toxicol Appl Pharmacol. 2003;188(1):24-35. Epub 2003/04/02.

265. Hegde VL, Nagarkatti PS, Nagarkatti M. Role of myeloid-derived suppressor cells in amelioration of experimental autoimmune hepatitis following activation of TRPV1 receptors by cannabidiol. PLoS One. 2011;6(4):e18281. Epub 2011/04/13.

266. Borrelli F, Aviello G, Romano B, Orlando P, Capasso R, Maiello F, et al. Cannabidiol, a safe and non-psychotropic ingredient of the marijuana plant Cannabis sativa, is protective in a murine model of colitis. J Mol Med (Berl). 2009;87(11):1111-21. Epub 2009/08/20.

267. Lyman W, Sonett J, Brosnan C, Elkin R, Bornstein M. < i> Δ</i>< sup> 9</sup>-Tetrahydrocannabinol: a novel treatment for experimental autoimmune encephalomyelitis. Journal of neuroimmunology. 1989;23(1):73-81.

268. Li X, Kaminski NE, Fischer LJ. Examination of the immunosuppressive effect of delta9-tetrahydrocannabinol in streptozotocin-induced autoimmune diabetes. Int Immunopharmacol. 2001;1(4):699-712. Epub 2001/05/19.

269. Weiss L, Zeira M, Reich S, Har-Noy M, Mechoulam R, Slavin S, et al. Cannabidiol lowers incidence of diabetes in non-obese diabetic mice. Autoimmunity. 2006;39(2):143-51. Epub 2006/05/16.

270. Killestein J, Hoogervorst EL, Reif M, Blauw B, Smits M, Uitdehaag BM, et al. Immunomodulatory effects of orally administered cannabinoids in multiple sclerosis. J Neuroimmunol. 2003;137(1-2):140-3. Epub 2003/04/02.

271. Katona S, Kaminski E, Sanders H, Zajicek J. Cannabinoid influence on cytokine profile in multiple sclerosis. Clin Exp Immunol. 2005;140(3):580-5. Epub 2005/06/04.

272. Ruth MR, Field CJ. The immune modifying effects of amino acids on gut-associated lymphoid tissue. Journal of animal science and biotechnology. 2013;4(1):27. Epub 2013/08/01.

273. de Fries R, Mitsuhashi M. Quantification of mitogen induced human lymphocyte proliferation: comparison of alamarBlue assay to 3H-thymidine incorporation assay. J Clin Lab Anal. 1995;9(2):89-95. Epub 1995/01/01.

274. Zgair A, Wong JCM, Gershkovich P. Targeting Immunomodulatory Agents to the Gut-Associated Lymphoid Tissue. In: Constantinescu C, Arsenescu R, Arsenescu V, editors. Neuro-Immuno-Gastroenterology. Cham: Springer International Publishing; 2016. p. 237-61.

275. Han S, Quach T, Hu L, Wahab A, Charman WN, Stella VJ, et al. Targeted delivery of a model immunomodulator to the lymphatic system: comparison of alkyl ester versus triglyceride mimetic lipid prodrug strategies. Journal of controlled release : official journal of the Controlled Release Society. 2014;177:1-10. Epub 2014/01/09.

276. Moudgil KD, Choubey D. Cytokines in autoimmunity: role in induction, regulation, and treatment. J Interferon Cytokine Res. 2011;31(10):695-703. Epub 2011/09/29.

277. Martin-Santos R, Crippa JA, Batalla A, Bhattacharyya S, Atakan Z, Borgwardt S, et al. Acute effects of a single, oral dose of d9-tetrahydrocannabinol (THC) and cannabidiol (CBD) administration in healthy volunteers. Curr Pharm Des. 2012;18(32):4966-79. Epub 2012/06/22.

278. Zgair A, Wong JC, Lee JB, Mistry J, Sivak O, Wasan KM, et al. Dietary fats and pharmaceutical lipid excipients increase systemic exposure to orally administered cannabis and cannabis-based medicines. American journal of translational research. 2016;8(8):3448-59. Epub 2016/09/21.

279. Sun M, Zhai X, Xue K, Hu L, Yang X, Li G, et al. Intestinal absorption and intestinal lymphatic transport of sirolimus from self-microemulsifying drug delivery systems assessed using the single-pass intestinal perfusion (SPIP) technique and a chylomicron flow blocking approach: linear correlation with oral bioavailabilities in rats. Eur J Pharm Sci. 2011;43(3):132-40. Epub 2011/05/03.

280. Calder PC, Yaqoob P, Newsholme EA. Triacylglycerol metabolism by lymphocytes and the effect of triacylglycerols on lymphocyte proliferation. The Biochemical journal. 1994;298 Pt 3:605-11. Epub 1994/03/15.

281. Jean-Gilles L, Braitch M, Latif ML, Aram J, Fahey AJ, Edwards LJ, et al. Effects of pro-inflammatory cytokines on cannabinoid CB1 and CB2 receptors in immune cells. Acta Physiol (Oxf). 2015;214(1):63-74. Epub 2015/02/24.

282. Maresz K, Pryce G, Ponomarev ED, Marsicano G, Croxford JL, Shriver LP, et al. Direct suppression of CNS autoimmune inflammation via the cannabinoid receptor CB1 on neurons and CB2 on autoreactive T cells. Nat Med. 2007;13(4):492-7. Epub 2007/04/03.

283. Springs AE, Karmaus PW, Crawford RB, Kaplan BL, Kaminski NE. Effects of targeted deletion of cannabinoid receptors CB1 and CB2 on immune competence and sensitivity to immune modulation by Delta9-tetrahydrocannabinol. J Leukoc Biol. 2008;84(6):1574-84. Epub 2008/09/16.

284. Mackall CL, Fleisher TA, Brown MR, Magrath IT, Shad AT, Horowitz ME, et al. Lymphocyte depletion during treatment with intensive chemotherapy for cancer. Blood. 1994;84(7):2221-8. Epub 1994/10/01.

285. O'Shea JJ, Ma A, Lipsky P. Cytokines and autoimmunity. Nature reviews Immunology. 2002;2(1):37-45. Epub 2002/03/22.

286. El-Behi M, Ciric B, Dai H, Yan Y, Cullimore M, Safavi F, et al. The encephalitogenicity of TH17 cells is dependent on IL-1-and IL-23-induced production of the cytokine GM-CSF. Nature immunology. 2011;12(6):568-75.

287. Noster R, Riedel R, Mashreghi MF, Radbruch H, Harms L, Haftmann C, et al. IL-17 and GM-CSF expression are antagonistically regulated by human T helper cells. Science translational medicine. 2014;6(241):241ra80. Epub 2014/06/20.

288. Hemmer B, Kerschensteiner M, Korn T. Role of the innate and adaptive immune responses in the course of multiple sclerosis. The Lancet Neurology. 2015;14(4):406-19. Epub 2015/03/21.

289. Hartmann FJ, Khademi M, Aram J, Ammann S, Kockum I, Constantinescu C, et al. Multiple sclerosis-associated IL2RA polymorphism controls GM-CSF production in human TH cells. Nature communications. 2014;5:5056. Epub 2014/10/04.

290. Watzl B, Scuderi P, Watson RR. Marijuana components stimulate human peripheral blood mononuclear cell secretion of interferon-gamma and suppress interleukin-1 alpha in vitro. Int J Immunopharmacol. 1991;13(8):1091-7. Epub 1991/01/01.

291. Du Pasquier RA, Pinschewer DD, Merkler D. Immunological mechanism of action and clinical profile of disease-modifying treatments in multiple sclerosis. CNS Drugs. 2014;28(6):535-58. Epub 2014/04/12.

292. Bergamaschi MM, Queiroz RH, Zuardi AW, Crippa JA. Safety and side effects of cannabidiol, a Cannabis sativa constituent. Current drug safety. 2011;6(4):237-49. Epub 2011/12/02.

293. Bachmann MF, Oxenius A. Interleukin 2: from immunostimulation to immunoregulation and back again. EMBO reports. 2007;8(12):1142-8. Epub 2007/12/07.

294. Ito T, Connett JM, Kunkel SL, Matsukawa A. The linkage of innate and adaptive immune response during granulomatous development. Frontiers in immunology. 2013;4:10. Epub 2013/02/07.

295. Abrams DI, Guzman M. Cannabis in cancer care. Clinical pharmacology and therapeutics. 2015;97(6):575-86. Epub 2015/03/18.

296. Burt RK, Traynor AE, Pope R, Schroeder J, Cohen B, Karlin KH, et al. Treatment of autoimmune disease by intense immunosuppressive conditioning and autologous hematopoietic stem cell transplantation. Blood. 1998;92(10):3505-14. Epub 1998/11/10.

297. Mix E, Meyer-Rienecker H, Hartung HP, Zettl UK. Animal models of multiple sclerosis--potentials and limitations. Prog Neurobiol. 2010;92(3):386-404. Epub 2010/06/19.

298. Gold R, Linington C, Lassmann H. Understanding pathogenesis and therapy of multiple sclerosis via animal models: 70 years of merits and culprits in experimental autoimmune encephalomyelitis research. Brain. 2006;129(Pt 8):1953-71. Epub 2006/04/25.

299. Green SI, Ajami NJ, Ma L, Poole NM, Price RE, Petrosino JF, et al. Murine model of chemotherapy-induced extraintestinal pathogenic Escherichia coli translocation. Infect Immun. 2015;83(8):3243-56. Epub 2015/06/03.

300. Campos MI, Vieira WD, Campos CN, Aarestrup FM, Aarestrup BJ. Atorvastatin and trans-caryophyllene for the prevention of leukopenia in an experimental chemotherapy model in Wistar rats. Molecular and clinical oncology. 2015;3(4):825-8. Epub 2015/07/15.

301. Sonis ST, Tracey C, Shklar G, Jenson J, Florine D. An animal model for mucositis induced by cancer chemotherapy. Oral Surg Oral Med Oral Pathol. 1990;69(4):437-43. Epub 1990/04/01.

302. de Bruin NM, Schmitz K, Schiffmann S, Tafferner N, Schmidt M, Jordan H, et al. Multiple rodent models and behavioral measures reveal unexpected responses to FTY720 and DMF in experimental autoimmune encephalomyelitis. Behav Brain Res. 2016;300:160-74. Epub 2015/12/23.

303. Croxford AL, Kurschus FC, Waisman A. Mouse models for multiple sclerosis: historical facts and future implications. Biochim Biophys Acta. 2011;1812(2):177-83. Epub 2010/07/06.

304. McRae BL, Kennedy MK, Tan LJ, Dal Canto MC, Picha KS, Miller SD. Induction of active and adoptive relapsing experimental autoimmune

encephalomyelitis (EAE) using an encephalitogenic epitope of proteolipid protein. J Neuroimmunol. 1992;38(3):229-40. Epub 1992/06/01.

305. Palle P, Ferreira FM, Methner A, Buch T. The more the merrier? Scoring, statistics and animal welfare in experimental autoimmune encephalomyelitis. Lab Anim. 2016;50(6):427-32. Epub 2016/12/03.

306. Bittner S, Afzali AM, Wiendl H, Meuth SG. Myelin oligodendrocyte glycoprotein (MOG35-55) induced experimental autoimmune encephalomyelitis (EAE) in C57BL/6 mice. JoVE (Journal of Visualized Experiments). 2014(86):e51275-e.

307. Vento S, Cainelli F. Infections in patients with cancer undergoing chemotherapy: aetiology, prevention, and treatment. The Lancet Oncology. 2003;4(10):595-604. Epub 2003/10/14.

308. Choi TY, Lee MS, Ernst E. Moxibustion for the treatment of chemotherapy-induced leukopenia: a systematic review of randomized clinical trials. Supportive care in cancer : official journal of the Multinational Association of Supportive Care in Cancer. 2015;23(6):1819-26. Epub 2014/12/05.

309. Lalla RV, Sonis ST, Peterson DE. Management of oral mucositis in patients who have cancer. Dental Clinics of North America. 2008;52(1):61-77.

310. Aras MH, Sezer U, Erkilic S, Demir T, Dagli SN. Effect of dietary boron on 5-fluorouracil induced oral mucositis in rats. European journal of dentistry. 2013;7(3):310-4. Epub 2014/06/14.

311. Medeiros CA, Leitao RF, Macedo RN, Barboza DR, Gomes AS, Nogueira NA, et al. Effect of atorvastatin on 5-fluorouracil-induced experimental oral mucositis. Cancer Chemother Pharmacol. 2011;67(5):1085-100. Epub 2010/07/28.